Eye position dependency of nystagmus: performance of the oculomotor velocity-to-position nerual integrator

Bockisch, C J

Klinik für Neurologie
Universitätsspital Zürich
Prof. Dr. med. M. Weller

Habilitationsschrift:

EYE POSITION DEPENDENCY OF NYSTAGMUS: PERFORMACE OF THE OCULOMOTOR VELOCITY-TO-POSITION NEURAL INTEGRATOR

zur Erlangung der Venia legendi der Universität Zürich

vorgelegt von
Christopher J Bockisch, Ph.D.
Zürich, 2013

Klinik für Neurologie
Universitätsspital Zürich
Prof. Dr. med. M. Weller

Zusammenfassung der Habilitationsschrift:

EYE POSITION DEPENDENCY OF NYSTAGMUS: PERFORMACE OF THE OCULOMOTOR VELOCITY-TO-POSITION NEURAL INTEGRATOR

zur Erlangung der Venia legendi der Universität Zürich

vorgelegt von
Christopher J Bockisch, PhD
Zürich, 2013

Zu Grunde liegende Arbeiten:

1. Hegemann S, Straumann D, Bockisch CJ (2007). Alexander's law in patients with acute vestibular tone asymmetry – evidence for multiple horizontal neural integrators. Journal of the Association for Research in Otolaryngology, 8(4), 551-61.
2. Bockisch CJ, Hegemann S (2008). Alexander's law and the oculomotor neural integrator: three-dimensional eye velocity in patients with an acute vestibular asymmetry. Journal of Neurophysiology, 100(6), 3105-16.
3. Bockisch CJ, Khojasteh E, Straumann D, Hegemann SC. (2012). Development of eye position dependency of slow phase velocity during caloric stimulation. PLoS One, 7(12):e51409.
4. Bockisch CJ, Khojasteh E, Straumann D, Hegemann SC. (2013). Eye position dependency of nystagmus during constant vestibular stimulation. Exp Brain Res, 226,2, 175-182.
5. Bertolini, G, Tarnutzer AA, Olasagasti I, Khojasteh E, Weber KP, Bockisch CJ, Straumann D, Marti S. (2013). Gaze holding in healthy subjects. PloS One, 8(4), e61389.
6. Khojasteh E, Bockisch CJ, Straumann D, Hegemann SC. (2013). A dynamic model for eye-position-dependence of spontaneous nystagmus in acute unilateral vestibular deficit (Alexander's Law). European Journal of Neuroscience, 37, 1, 141-9.

Summary

We present a series of studies on the mechanism that allows us to maintain fixation of the eyes and ensure good vision. The muscles and tissues surrounding the eye exert an elastic force that tries to pull the eye back to a central position. To counteract this force, a neural command to the muscles is created within a network of neurons in the brainstem and cerebellum. This command to hold the eye at a constant position is created by integrating the velocity command to move the eye; hence the mechanism is called the oculomotor velocity-to-position neural integrator. If the command to maintain fixation is insufficient, the eye drifts back to a central position with a time course that can be approximated by a decaying exponential, and the rate of the drift indicates the *time constant* of the neural integrator. The time constant is defined as position divided by velocity, so if the drift velocity is small, the time constant is large. If the time constant is small, the integrator is said to be 'leaky', in analogy to water leaky from a bucket with holes. Failure of this neural integrator, by damage to the brainstem or cerebellum or as a side effect of medications or alcohol intoxication, results in gaze evoked nystagmus, a pattern of eye movements where the eye drifts back to a central position, followed by a quick resetting movement to direct the line of sight back to the target.

Patients with peripheral vestibular lesions develop nystagmus that has a gaze evoked component: eye velocity is higher in the direction of the fast phase. This pattern of nystagmus is very familiar to clinicians, and is commonly called "Alexander's Law" (after Gustav Alexander, who described it 1912). Since the early 1980's the gaze-evoked component has been thought to be due to adaptive changes in the velocity-to-position neural integrator, and our first two studies sought to study this gaze-evoked component in more detail then had otherwise been done.

In our first study, we measured how horizontal, vertical, and torsional velocity varied with horizontal position in 17 patients with peripheral vestibular lesions. Neurophysiologic evidence suggests there is one brainstem integrator for horizontal eye movements (in the nucleus prepositus hypoglossi), and a separate integrator for vertical and torsional eye movements (in the interstitial nucleus of Cajal). We were interested if there were interactions between these integrators, because it seems likely that the elasticity in one direction likely varies with orthogonal directions. For example, vertical elasticity might vary with horizontal position. The results confirmed this prediction, as the horizontal, vertical, and torsional components varied proportionately with horizontal position. Unexpectedly, we also found that horizontal eye velocity did not usually vary in a linear fashion with horizontal position, as expected from previous studies. We found a stronger dependence of velocity on horizontal position when subjects looked in the slow phase direction compared to the fast phase direction. We speculated that one reason for this finding could be that the neural integrator has the ability to differentially adapt to gaze directions, suggesting that there are functionally separate integrators for left and right gaze. In a second study, we investigated how eye velocity varied when patients looked in different vertical directions. We measured 11 patients with peripheral vestibular lesions. We replicated the finding from the first study that while velocity decreased in the slow phase direction, it was relatively unchanged > 10° into the fast phase direction. Vertical velocity was highest in the vertical fast phase direction, but was relatively unchanged in the slow phase direction. Torsional velocity varied linearly with horizontal, but not vertical, position. These results showed that the horizontal and vertical oculomotor neural integrators react to altered vestibular input by maintaining different integrating time constants depending on gaze direction.

We investigated Alexander's law further in healthy subjects using a paradigm that simulates a peripheral vestibular disorder. Natural head movements cause excitation in the vestibular system on one side and inhibit a paired-canal on the other side. For example, a leftward head turn excites the left horizontal semi-circular canal, and inhibits the right horizontal semi-circular canal. Thus natural rotations always produce a 'push-pull' stimulation pattern. Caloric stimulation (warm or cold water injected into the ear) can be used to excite (warm) or inhibit (cold) the peripheral vestibular system, and so create an artificial vestibular imbalance. One hypothesis of Alexander's Law was that it is an adaptive response to unnatural vestibular stimulation. We assumed that simultaneous irrigation at 44°C on one side (warm, excitatory) and 30°C (cold, inhibitory) on the contralateral side would produce a stimulation pattern similar to that produced by head rotations. If the intervestibular mismatch of unnatural stimulation would cause Alexander's law, then we would expect that it does not

develop during simultaneous bilateral bithermal stimulation or would at least be weaker compared to unilateral caloric stimulation. Contrary to this expectation, we found that Alexander's law developed with bilateral bithermal caloric stimulation, which does not support the hypothesis that Alexander's law can only be observed with unnatural vestibular stimulation.

While bilateral bithermal caloric stimulation is similar to natural vestibular stimulation, it nonetheless may not be identical. We therefore sought a stronger test of the adaptation hypothesis in an additional experiment that used real head movements to stimulate the vestibular system. We used a long acceleration paradigm, where the subject was rotated about the yaw axis (to stimulate the horizontal vestibular ocular reflex) with a near constant acceleration for over 30 seconds. In contrast to peripheral lesions and caloric stimulation, this vestibular stimulation is the result of real head turns, and has the push-pull characteristics of natural movements. The procedure produced an average velocity of 31°/s that was unchanged over the final 35 seconds of the acceleration period. In all 10 healthy human subjects, we found that horizontal eye velocity began to vary with horizontal position in about 10 seconds, and then was stable for the next 25 seconds. Thus, we found a large and stable Alexander's law with natural vestibular stimulation. Constant acceleration and caloric stimulation protocols that show Alexander's law produce very low frequency stimulation; whereas the vestibular ocular reflex studies that do not show Alexander's law use higher frequency stimuli. Alexander's law thus may be a consequence of the velocity-to-position neural integrator being insensitive to very low frequency signals.

Our studies on patients and healthy subjects led us to some unexpected conclusions about the nature of the eye position dependency of velocity, namely, that it does appear to be an adaptive response to unnatural stimulation that had been assumed for over 20 years. In order to develop further hypotheses about the mechanism underlying Alexander's Law, we began the development of a dynamic model of the velocity-to-position neural integrator that could account for the findings from patients with vestibular lesions. The model is a systems-level account of the oculomotor neural integrator that contains two feedback loops: a positive position feedback loop within the brainstem, and a negative velocity feedback loop through the cerebellum. Single neurons were modelled as units which had different thresholds and different saturating values, and linear responses in-between. The population response constructed as the sum of many such units is a sigmoid, which is close to linear over much of its operating range. All of these features are supported by neurophysiologic evidence. Due to the vestibular lesion and insufficient tonic activity on the ipsilesional primary afferents, responses in the ipsilesional vestibular nucleus approach zero, while the contralesional vestibular nucleus becomes excited. The asymmetry in the response of the bilateral vestibular nuclei reduces the linear operating range of the central vestibular circuits which perform the integration of velocity signals. The gain of the brainstem positive feedback loop thus becomes dependent on the merging neural activity, making the integration process dependent on eye movement signals. Therefore, the integration of eye signals in the side of the lesion becomes insufficient (leaky), while in the fast-phase direction the integrator could become unstable. Thus, the model can successfully account for our findings in patients using a physiologically plausible model.

Our previous studies restricted gaze to the central 50° field of view because measuring larger angles is technically challenging. Nonetheless, such measurements are important to have a full understanding of the performance of the oculomotor neural integrator. So, we performed an additional study in healthy subjects to measure gaze holding, and so the performance of the oculomotor neural integrator, over an 80° range. We found that the amount of drift increased sharply at far eccentric positions, suggesting that the better performance near straight ahead gaze may be the result of a tuning procedure which is optimized in the most commonly used range of gaze.

Contents

1. Introduction

The central fovea of the human eye, where acuity is highest, only covers about 2° of the visual field, or about twice the width of a thumb held at arm's length. Therefore, to see clearly the eye must be turned to direct the fovea towards the object of interest. In addition, much as camera movements blur pictures and remove details, eye movements also can degrade vision. Evolution has provided us with a variety of different types of eye movement to improve vision, including saccades, smooth pursuit, vergence, optokinetic, and the vestibular ocular reflex. These movements normally end with fixation, which is hopefully a stable eye position that allows for the greatest acquisition of visual information.

This work is a collection of papers on studies aimed at understanding the ability to maintain eccentric fixation (the eye rotated away from straight ahead gaze). Such control of eye position would be less interesting if maintaining an eccentric eye position was like moving a cup of coffee to a new position on your desk. In this case, it is only necessary to program the movement of the cup; once there the cup will not move until you reach for it again. Unfortunately, elastic forces (principally from the extraocular muscles, but also other tissues surrounding the eye) pull the eye back to a central position, much as if your desk was tilted and gravity caused your coffee cup to slide. To counteract the elastic forces, the extraocular muscles must contract tonically to keep the eyes from moving. This is illustrated in Figure 1, which show the eye position (Figure 1A) and medial and lateral rectus muscle forces (Figure 1B) from a rhesus macque when the monkey made a saccade from about straight ahead to 10° to the right. The medial rectus contracts and the lateral rectus relaxes to move the eye to the eccentric position. Notice that the total force (medial rectus force –lateral rectus force) is higher when the eye is at 10° compared to straight ahead. This extra force is what is needed to counteract the elastic forces that attempt to move the eye back to a central position.

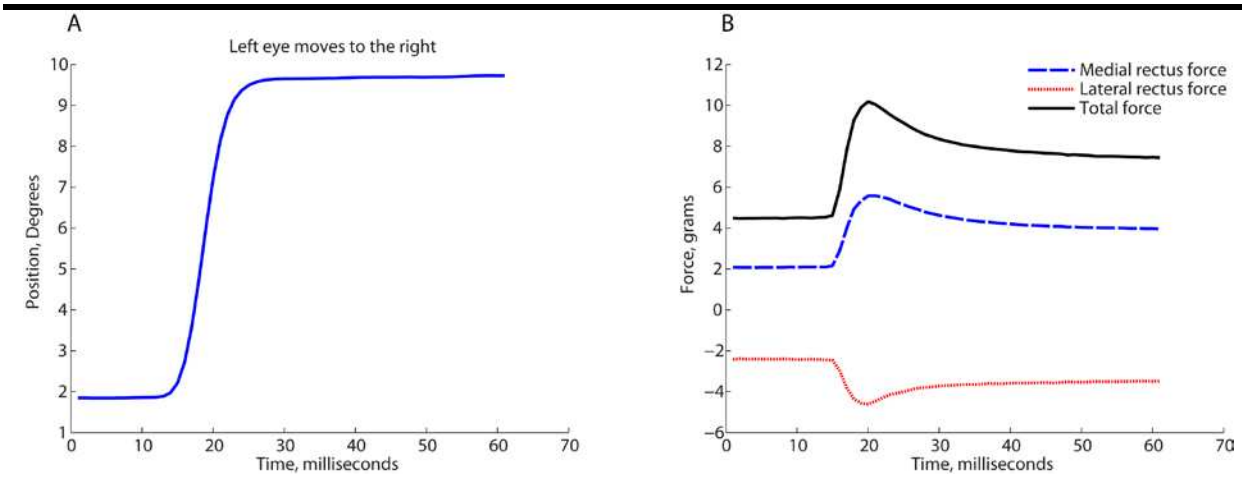

Figure 1. Left eye position (A) and muscle forces (B) in a rhesus macque. Unpublished data.

Ocular motor neurons display firing patterns similar to the force curves shown in Figure 1B, where the firing rate increases when as the eye is in an eccentric position. Interestingly, the pre-motor commands to move the eyes (such as saccades, smooth pursuit, and the vestibular ocular reflex) are for the most part velocity commands to move the eye. Therefore the command to hold the eye at a fixed position must be computed from the velocity input (7). This computation, integration, is now understood to be done by a network of neurons in the brainstem and cerebellum referred to as the 'velocity-to-position neural integrator'. If this integration is diminished (the time constant of the integration is reduced) then the fixation command is insufficient to keep a normal eye from drifting back to a central position, and the neural integrator is said to be 'leaky'. Such patients are said to 'gaze evoked nystagmus', since they need resetting saccades to correct for the drift. This deficit can result from lesions in the brainstem and cerebellum, or from different medications and alcohol consumption. More rarely, the

command from the integrator is too large, and the eye drifts eccentrically, and the neural integrator is said to be 'unstable'.

Hess (8) and Robinson et al (9) proposed that in patients with acute peripheral vestibular lesions the performance of the neural integrator adapts. These patients develop nystagmus, where the velocity of the slow phase is determined mainly by the difference of the tonic vestibular activity between the right and left sides, and the eye drifts towards the side with a lower spontaneous activity. If the tone asymmetry is constant the slow phase velocity should also be constant, and the axis of eye rotation should not depend on gaze position. However, the slow phase velocity in such patients is highest when they look in the direction of fast phase, and is lower when looking in the direction of the slow phase, a behavior commonly called 'Alexander's Law' (10).

Alexander's Law was hypothesized to result from adaptive changes in the velocity-to-position neural integrator (9). If the command from the neural integrator is too small, then gaze evoked nystagmus is created, which, when added to the vestibular component, reduces eye velocity in one direction, but increase velocity in the opposite direction (Figure 2). Robinson et al believed it was an adaptive response, since eye velocity is reduced in some gaze positions, which should help to improve vision.

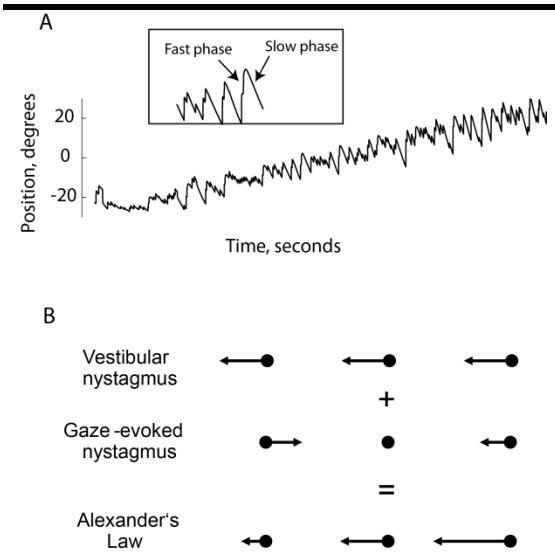

Figure 2. A. An example of the horizontal eye movements in a patient with a peripheral vestibular lesion. Notice that the nystagmus becomes progressively more intense when the patient looks to the right (towards +20°) B. The explanation of Alexander's law proposed by Hess (8) and Robinson et al (9). Top: The vestibular disorder produces eye velocity (arrows pointing to the right) that is the same regardless of the direction the patient is looking (left, middle, right). Middle: The velocity-to-position neural integrator produces a gaze holding command that is insufficient to maintain eccentric eye position, so the eye drifts towards the center. Bottom: When these two drift components are summed, eye velocity varies with position in accordance with Alexander's law. Adapted from (1).

2. Studies in patients with peripheral vestibular disorders

Papers:

Hegemann S, Straumann D, Bockisch CJ (2007). Alexander's law in patients with acute vestibular tone asymmetry – evidence for multiple horizontal neural integrators. Journal of the Association for Research in Otolaryngology, 8(4), 551-61.

Bockisch CJ, Hegemann S (2008). Alexander's law and the oculomotor neural integrator: three-dimensional eye velocity in patients with an acute vestibular asymmetry. Journal of Neurophysiology, 100(6), 3105-16.

While Alexander's law has been known for a century, the measurement of the vertical and torsional components of the eye velocity, rather than just horizontal, had not previously been described. Patients with acute vestibular disorders usually develop nystagmus in the vertical direction in addition to horizontal, so we were interested in whether Alexander's law holds in the vertical direction, as well. (These patients typically also develop torsional nystagmus, but because it is not possible to voluntarily make torsional eye movements, it would be difficult to measure changes in torsional velocity as torsional position changes.) Neurophysiologic studies suggest there are two brainstem neural integrators: one for horizontal gaze, and another for both vertical and torsional eye movements.

Apriori, however, it would seem necessary for there to be some interaction between these integrators, because it is likely the case that the cross-axis elasticity co-varies. For example, the vertical elasticity might vary with horizontal eye position, so the vertical integrator should be able to change performance based on horizontal eye position.

In first study (1), we asked 17 patients with nystagmus to look to a flashing laser spot that moved slowly from -25° left to °25 right, while we measured horizontal, vertical, and torsional eye position with scleral search coils. While there was considerable variation between patients, overall we found that the three components varied proportionately when patients looked from left to right, suggesting there is not complete independence of the horizontal and vertical/torsional neural integrators. An unexpected finding was that horizontal eye velocity did not usually vary in a linear fashion with horizontal position (see Figure 3), as expected from the leaky integrator hypothesis (9). Rather, we found there was a stronger dependence of velocity on horizontal position when subjects looked in the slow phase direction compared to the fast phase direction. We speculated that one reason for this finding could be that the neural integrator has the ability to differentially adapt to gaze directions, suggesting that there are functionally separate integrators for left and right gaze. Conceivably, integrators for positions in the fast-phase direction become leaky, while those in the slow-phase direction can become similarly leaky (Fig. 3A), unchanged (Fig. 3B), or unstable (Fig. 3C). Our results thus support several previous studies that suggested the possibility of multiple integrators (11-13) .

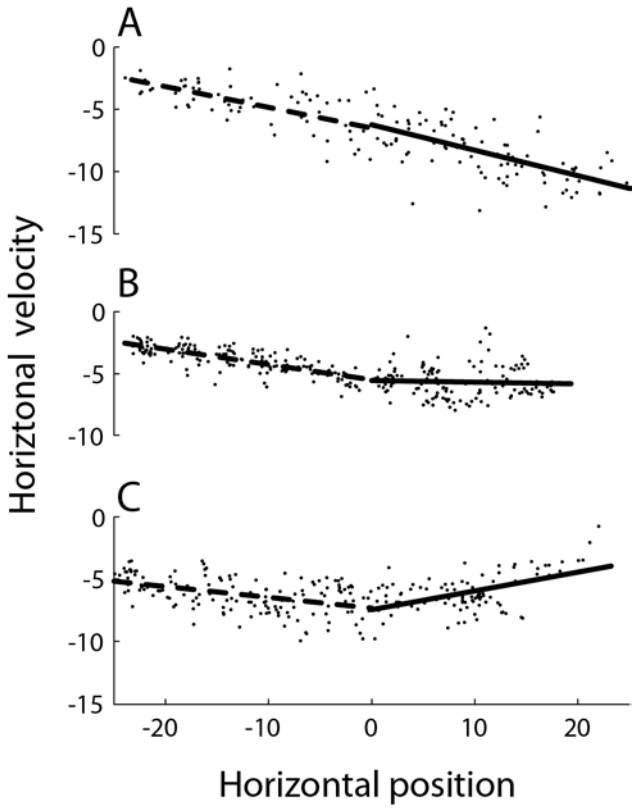

Figure 3. The change in eye velocity with position could be different depending upon whether the subject was looking in the slow-phase direction or the fast-phase direction. A–C Data from three different patients. Solid lines indicate the best-fit lines to the velocity data when subjects looked to the left, dashed lines show the best-fit lines for eye positions to the right. The two slopes for the patient in A show little difference, whereas in B, eye velocity when looking to the right is mostly unchanged, and in C, the slope of the best-fit line changes direction. Adapted from (1).

In a second study (14) we investigated how eye velocity varied when patients looked in different vertical directions. We measured 11 patients with a peripheral vestibular asymmetry. In this study we used second-order equations to describe how velocity varied with position, rather than linear functions, as they provided better fits to the data (See Figure 4). Horizontal velocity changed with horizontal position in accordance with Alexander's law and the second-order term for horizontal position was also significant. Whereas velocity decreased in the slow phase direction, it was relatively unchanged > 10° into the fast phase direction. This confirmed the non-linear finding in our first study (1). Vertical velocity was also highest in the vertical fast phase direction and the second-order term for vertical position was also significant, in that vertical velocity increased in the vertical fast phase

direction, but was unchanging in the slow phase direction. Torsional velocity varied linearly with horizontal, but not vertical, position. These results showed that the horizontal and vertical oculomotor neural integrators react to altered vestibular input by maintaining different integrating time constants depending on gaze direction.

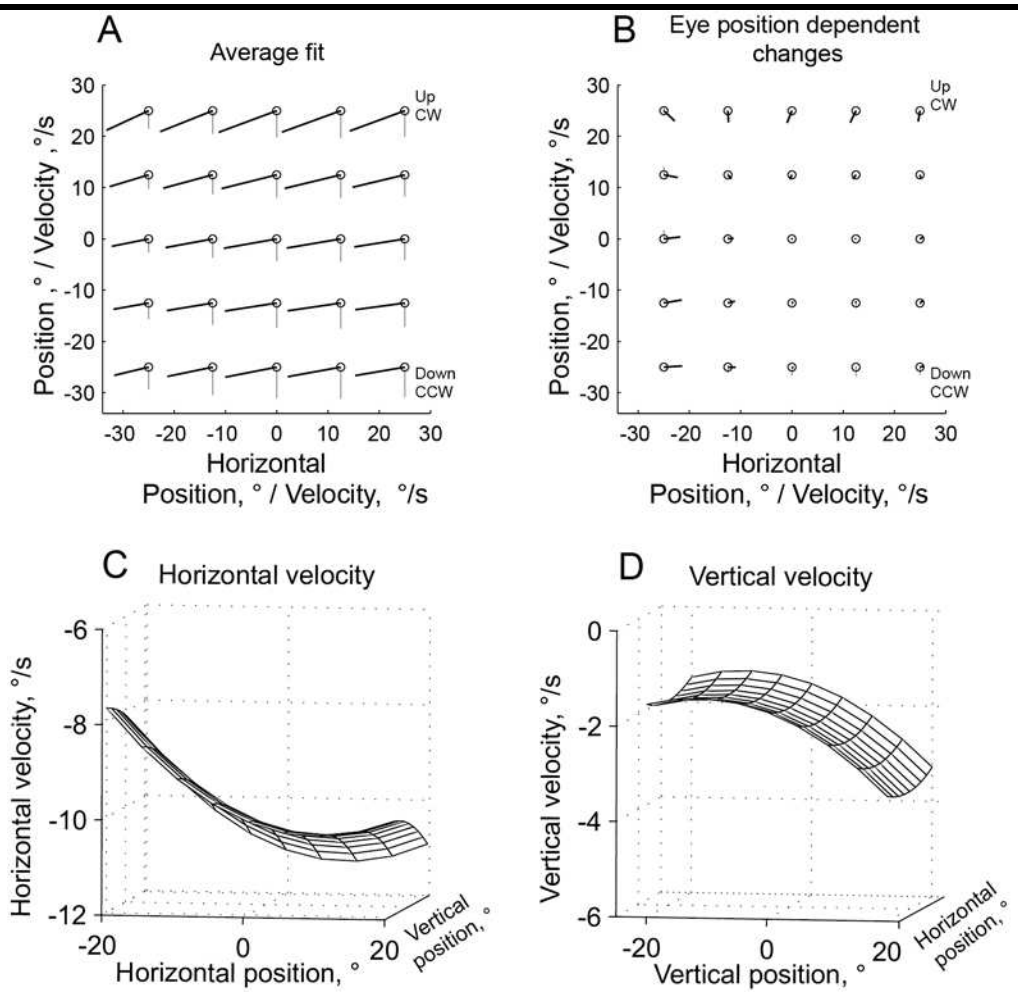

Figure 4. We fit second order equations to describe the change in horizontal, vertical, and torsional velocity with horizontal and vertical position. A: The best 2nd order fit. Each circle indicates horizontal and vertical position for the slow phase eye movements during each fixation period (5 seconds duration). The thick line shows the horizontal and vertical velocity, and so the orientation of the line indicates direction (for example, a line pointing down and to the left shows downward and leftward velocity) and the length represents the speed. Thin lines show torsional velocity, with an upward line indicating clockwise velocity, and a downward line indicating counter-clockwise velocity. B: Gaze dependent changes in drift velocity, which was found by subtracting the fitted drift at straight ahead from fitted drift at all other gaze positions. C-D: The average 2nd order surface fits, shown as surfaces. Adapted from (2).

In summary, the two studies in patients with peripheral vestibular lesions found that all three eye movement components (horizontal, vertical, and torsional), varied with eye position. Further, we found the velocity did not vary linearly with position. These results have two important implications if we can assume that they are due to adaptive changes in the oculomotor velocity-to-position integrators. First, the horizontal and vertical/torsional integrators do not appear to be completely independent. Second, our results also show that the oculomotor neural integrators cannot be characterized by a single time constant, but rather can maintain different integrating time constants depending on gaze direction.

3. Studies in healthy subjects

Papers:

Bockisch CJ, Khojasteh E, Straumann D, Hegemann SC. (2012). Development of eye position dependency of slow phase velocity during caloric stimulation. PLoS One, 7(12):e51409.

Bockisch CJ, Khojasteh E, Straumann D, Hegemann SC. (2013). Eye position dependency of nystagmus during constant vestibular stimulation. Exp Brain Res. 226,2, 175-182.

Bertonlini, G, Tarnutzer AA, Olasagasti I, Khojasteh E, Weber KP, Bockisch CJ, Straumann D, Marti S. (2013). Gaze holding in healthy subjects. PloS One, 8(4): e61389.

Robinson et al. (9) investigated the time course of the development of the eye position dependency in three subjects during caloric induced nystagmus and found that it first occurred 20-46 s after the onset of nystagmus. With natural vestibular stimulation (real movements of the head in space on a turntable), the eye position dependency was small, and did not evolve over time, which led to the proposition that Alexander's law is an adaptive response to unnatural vestibular stimulation. By 'unnatural', Robinson et al meant that a change in vestibular input from one side is not accompanied by the opposite change from the other side for 25 seconds. If Alexander's law is produced by changes in the neural integrator, it could be considered an adaptive response, since eye velocity will be reduced for some eye positions, thus aiding vision. During normal yaw head turns, one horizontal semicircular canal is stimulated while the other is inhibited. During non-physiologic unilateral caloric stimulation, on the other hand, only one canal changes its tonic activity depending on the stimulus (increase with warm and decrease with cold stimulation). This unusual pattern of stimulation might be detected and lead to Alexander's law.

We tested Robinson's hypothesis that only unnatural (or non-physiologic) velocity commands evoke Alexander's law (3). We assumed that simultaneous irrigation at 44°C on one side (warm, excitatory) and 30°C (cold, inhibitory) on the contralateral side would produce a stimulation pattern similar to that produced by head rotations. If the intervestibular mismatch of unnatural stimulation would cause Alexander's law, then we would expect that it does not develop during simultaneous bilateral bithermal stimulation or would at least be weaker compared to unilateral caloric stimulation. Contrary to this expectation, we found that Alexander's law developed similarly in all conditions, and the results do not support the hypothesis that Alexander's law can only be observed with non-physiologic vestibular stimulation. In particular, the finding of a significant eye position effect with bilateral bithermal stimulation is troubling for the Robinson et al hypothesis, since this stimulation has the push-pull pattern of natural vestibular stimulation. Further, we found that the development of the eye position dependency of the velocity of nystagmus evolved at about the same rate as the velocity itself, suggesting little delay. This rapid development of Alexander's law, while possible for an adaptive mechanism, is nonetheless quite fast compared to most other ocular motor adaptations. These results suggest that Alexander's law may not be a consequence of a true adaptive mechanism.

While bilateral bithermal caloric stimulation is similar to natural vestibular stimulation, it nonetheless may not be identical. So, we sought a stronger test of the Robinson et al hypothesis in an additional experiment that used real head movements to stimulate the vestibular system (5). Using the three axis turntable at the Vestibular Laboratory at the University Hospital Zürich (Figure 5), the yaw rotation stimulus consisted of a 1 second acceleration ramp (100°/s^2), followed by a lower acceleration ramp (starting at 7.3°/s^2 and increasing at 0.04 °/s^2/s) until 400°/s was reached after 38 seconds (see Figure 6). This stimulus was designed to offset the ~15 second vestibular ocular reflex time constant (and the 150 second adaptation time constant) and produce constant velocity slow phases. In contrast to peripheral lesions, this vestibular stimulation is the result of real head turns, and has the push-pull characteristics of natural movements. The procedure produced an average velocity of 31°/s that was unchanged over the final 35 seconds of the acceleration period. In all 10 healthy human subjects, we found a large and stable Alexander's law, with an average velocity-versus-position slope of -0.366 in the first half that was not significantly different in the second half, -0.347. An example of the results in one subject is shown in Figure 7.These slopes correspond to integrator time constants of < 3 seconds,

are much less than normal time constants (~25 seconds) (15, 16), and are similar to those observed in patients with peripheral vestibular lesions. Alexander's law also developed, on average, in 10 seconds.

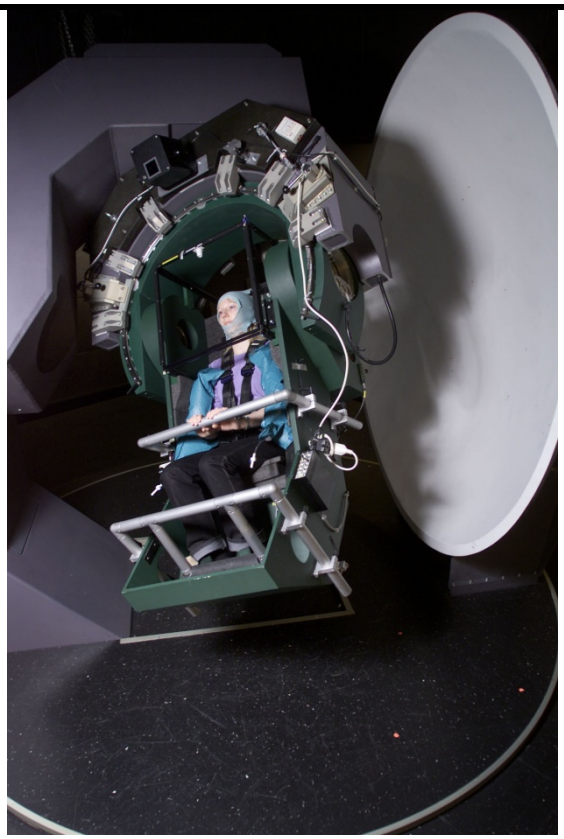

Figure 5. The three axis turntable at the Vestibular Laboratory at the University Hospital Zürich. The turntable consists of three nested axes, all motorized and computer controlled. An outer axis consists of the platform with a fixed, earth-vertical rotation axis; the middle axis is earth horizontal; the inner axis is aligned with the subject's longitudinal axis.

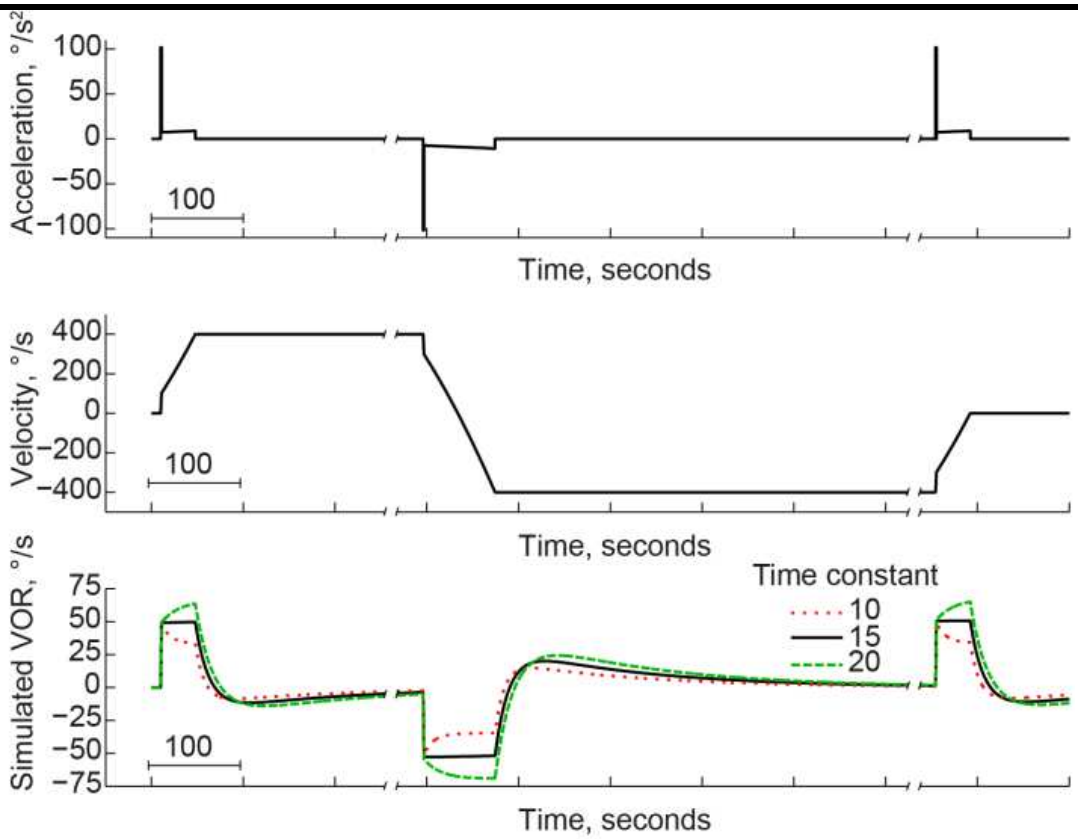

Figure 6. The top and middle panels show the stimulus used in the experiments, with head acceleration in A, and velocity in B. The stimulus was an initial step of velocity to about 100°/s, followed by a slowly increasing acceleration. After the rotation reached 400°/s, the acceleration stopped, and the velocity remained constant until the subject's nystagmus stopped. The acceleration profile was then inverted, so that there was an initial velocity step from 400°/s to 300° /s, followed by a slow change in acceleration until the chair reached -400°/s. In C, the simulated responses to the stimulus from a system consisting of dominant time constants of 10, 15, or 20 seconds, and an adaptation time constant of 150 seconds, and a gain of 0.5 is shown. The velocity response is nearly constant during the acceleration phase and then during the constant velocity phase the response declines and reverses direction, before returning towards zero before the next acceleration phase. Adapted from (5).

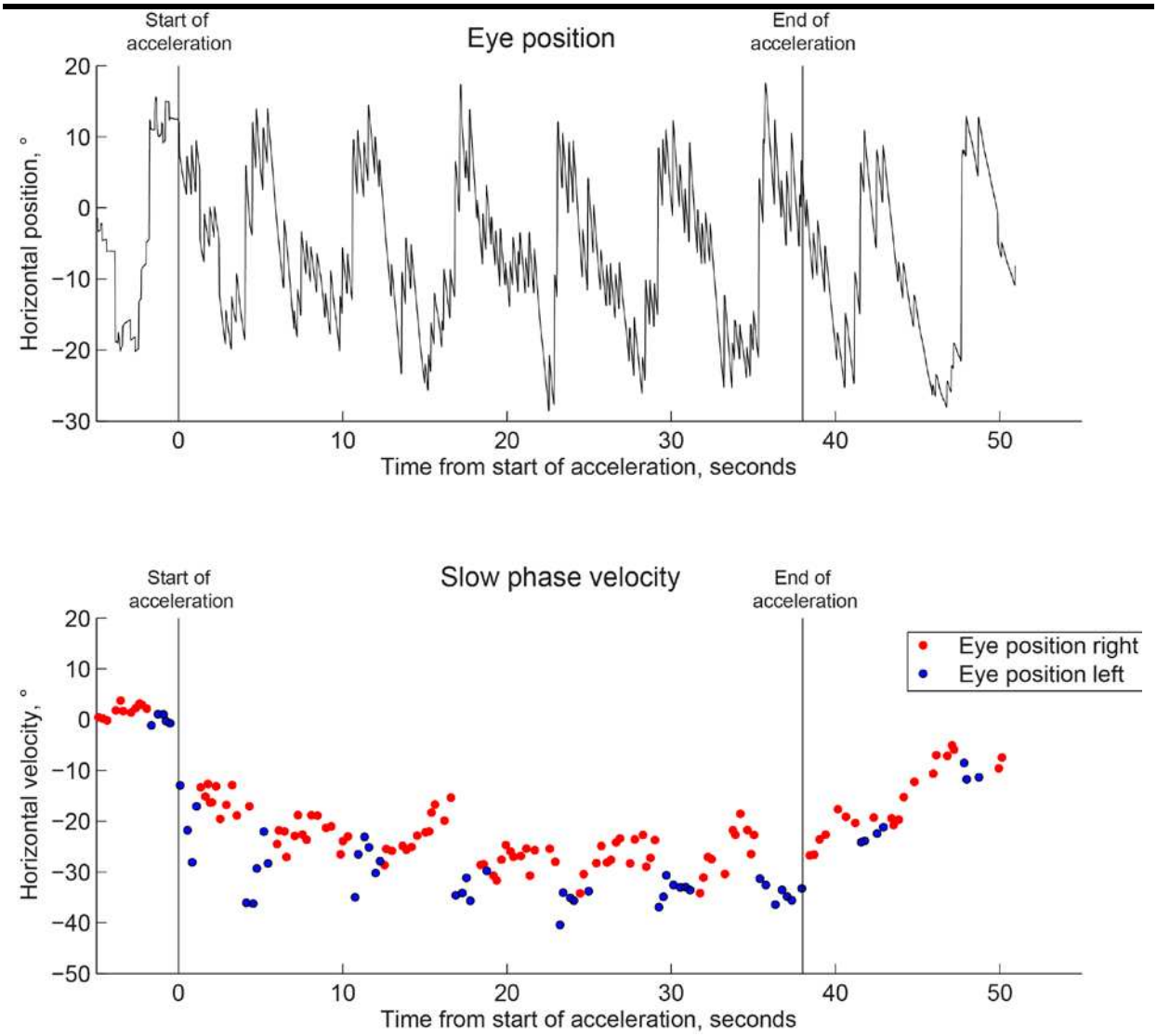

Figure 7. Top: Example horizontal eye position traces are shown. Vertical lines mark the beginning and end of the yaw rotation acceleration period.

Bottom: For the same data shown in the top figure, the velocity of each slow phase is shown, and color-coded to indicate the gaze direction.

Adapted from (5).

Constant acceleration and caloric stimulation protocols that show Alexander's law produce very low frequency stimulation; whereas studies of the vestibular ocular reflex that do not show Alexander's law use higher frequency stimuli. Alexander's law then may be a consequence of the velocity-to-position neural integrator being insensitive to very low frequency signals. One reason for this could be that natural head movements contain mainly high frequency components. Another reason could be to make the integrator insensitive to small imbalances in the tonic stimulation from the left and right vestibular canals. While another mechanism to compensate for such imbalances exists (up-regulation of tonic inputs following peripheral lesion (17), this mechanism operates on a time scale of hours or days (18).

In a final study on normal subjects, we sought a more detailed examination of the gaze evoked nystagmus that healthy people have. In both of our previous studies on normal subjects we had collected similar data to serve as a baseline in order to understand the effects of caloric stimulation or continuous acceleration (5). However, we only measured gaze holding at a few horizontal gaze

positions, and restricted these eye positions to the central field of gaze. In order to support future studies on the performance of the oculomotor neural integrator in patients with cerebellar damage, we measured gaze holding in 20 healthy subjects at positions from -40° left to +40° right in a near continuous fashion. Usually, the observed drift is described using a leaky integrator model, which assumes that eye velocity grows linearly with gaze eccentricity. As expect, since these were healthy subject, drift velocity was weak at all angles tested. We found that, on average, eye velocity grew more rapidly at eye eccentricities > ± 20° than expected from a simple leaky integrator model. We show that a tangent function provides a better fit of the mean of these curves when large eccentricities are considered. This suggests that the linear behavior is the result of a tuning procedure which is optimized in the most commonly used range of gaze. We suggest that the observed non-linearity occurs due to a saturation of the input that each neuron in the integrating network receives from the others as eye eccentricity leaves the central range. As a consequence, gaze-holding performance declines more rapidly at large eccentricities.

4. Dynamic model of Alexander's Law

Paper:

Khojasteh E, Bockisch CJ, Straumann D, Hegemann SC. (2013). A dynamic model for eye-position-dependence of spontaneous nystagmus in acute unilateral vestibular deficit (Alexander's Law). European Journal of Neuroscience, 37,1, 141-9.

Our studies on patients with unilateral vestibular lesions (reviewed in section 2) and in healthy subjects (section 3) led us to some unexpected conclusions about the nature of the eye position dependency of velocity commonly call Alexander's Law. Since Robinson et al's important paper (9), it has been assumed that Alexander's Law results from an adaptive process in response to unnatural stimulation whereby the oculomotor neural integrator reduces it efficiency (becomes 'leaky') in order to reduce eye velocity in some gaze directions. Our results cast doubt on this hypothesis: we found a robust Alexander's law in conditions where the vestibular stimulation was very close to natural (bilateral bithermal caloric stimulation) and real (continuous acceleration). We also found that Alexander's Law developed very quickly, much more rapidly than most other oculomotor adaptations. In order to try to understand if there were other mechanisms that could produce Alexander's law, we began a project to develop a dynamic model of the velocity-to-position neural integrator that could account for the findings from patients with vestibular lesions.

Figure 8 shows the general structure of the model, which simulates the horizontal-canal driven vestibular ocular reflex and is based on known physiology and earlier models (19-21). The model contains a direct pathway from the horizontal canals to the eye plant, and two feedback loops. The first is a positive position feedback loop within the brainstem, and the second is a negative velocity feedback loop through the cerebellum. Critical for the model is describing the transfer function of neurons in the vestibular nucleus, which sum the input from the canals with that of the two feedback loops. Single neurons were modelled as units which had different thresholds and different saturating values, and linear responses in-between. The population response constructed as the sum of many such units is a sigmoid, which is close to linear over much of its operating range (see inset *f(x)* in Figure 8).

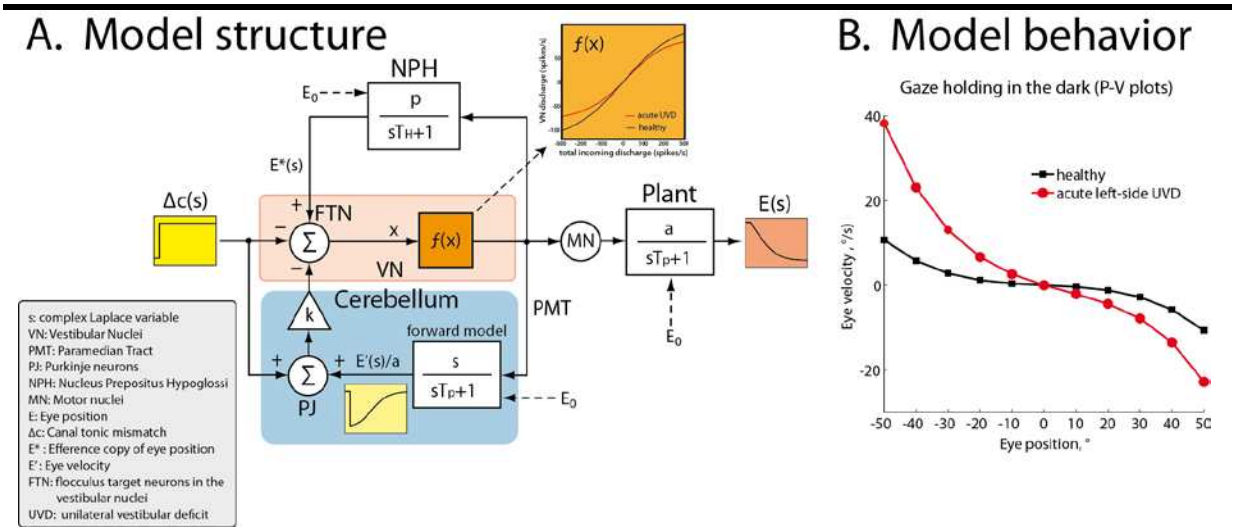

Figure 8. A. The model structure for conjugate horizontal canal-driven vestibular ocular reflex. Canal signals are projected to the vestibular nucleus via primary vestibular afferents. The vestibular nucleus constitute the main vestibular ocular reflex pathway, relaying sensory signals to the motor nuclei. The neural integrator circuit includes the prepositus hypoglossi nuclei, the medial vestibular nucleus and the vestibular cerebellum. The first level of integration is accomplished by the prepositus nucleus in the brainstem (by positive position feedback), which generates and distributes an efference copy of eye position. The second integration is done by the occulus/ventral paraocculus of the cerebellum (by negative velocity feedback). The effect of these feedback loops is to enhance the time constant of the vestibular ocular reflex above the eye plant time constant. B. The model results for stimulated gaze holding in darkness. The black line represents a healthy response, and the red line is the response with a unilateral vestibular deficit. For both cases, the slope increases at far eccentric eye positions, indicating deteriorated integration. Adapted from (4, 22).

With a vestibular lesion, there is insufficient tonic activity on the ipsilesional primary afferents, the ipsilesional vestibular nucleus is silenced, while the contralesional vestibular nucleus becomes hyperactive (17). This asymmetry in the response of the bilateral vestibular nuclei reduces the linear operating range of the central vestibular ocular reflex circuits, which perform the integration of velocity signals. The gain of the brainstem positive feedback loop thus becomes dependent on the merging neural activity, making the integration process dependent on eye movement signals. Hence, integration of eye signals in the slow-phase direction (side of the lesion) is insufficient (leaky). In the fast-phase direction, the integrator can become unstable. Further, the persistent stimulation of the primary vestibular afferents by very low-frequency stimuli could in the same manner saturate the vestibular nucleus on one side, while pushing the other vestibular nucleus into inhibitory cut-off, thus producing eye position–dependent integration similar to unilateral vestibular lesions. The model thus may also account for the findings from our caloric and continuous acceleration experiments, where the stimulus has an extremely low frequency.

5. Conclusions

Constructing short term working memories through persistent neural firing in response to transient stimuli, or neural integration, is a major computational task of neural networks throughout the brain (for example, accumulation of evidence for decision making in parietal cortex (23); development of working memory in prefrontal cortex (24); the head direction cells of the rat limbic system (25); memory in the cerebellar cortex (26)). Integrator circuits also average out the noise that is present in the stimulus or introduced by individual network elements (27). Neural integration is supported by intrinsic biophysical properties of individual neurons as well as interactions between larger populations of neurons at the network level, i.e. positive feedback through recurrent mutual inhibition (28). Among such integrator networks, the neural integrator of the oculomotor system is the most

widely studied, thanks to the unique characteristics of the oculomotor system that make it an excellent model for understanding neural processes involved in motor control (for example, the output of the oculomotor system, eye position, can be measured easily and with high accuracy; the oculomotor system is a single joint motor system; neural centres involved in eye movement are easily accessible for neurophysiological recordings) .

Our research on the eye position dependency of nystagmus in patients with peripheral vestibular deficits as well as in healthy subjects and the accompanying modelling work has added to our knowledge of the workings of the human velocity-to-position neural integrator. In the patient studies, we found that the two principal velocity integrators (horizontal and vertical/torsional) are not completely independent. This should not be too surprising, since the elastic forces in one direction likely vary in orthogonal directions, so, for example, the vertical integrator should be sensitive to horizontal position. Second, our results also show that the oculomotor neural integrators cannot be characterized by a single time constant, but rather can maintain different integrating time constants depending on gaze direction. This could mean, as we originally suggested, that integrators operate as functionally independent integrators for different gaze directions. More recently, however, our modelling work has shown that such behaviour can arise from a single integrator, and so future research will be needed to distinguish between these possibilities.

Our research with healthy subjects was intended to test the hypothesis that Alexander's Law, or the eye position dependent change in velocity during vestibular evoked nystagmus, is an adaptive response to unnatural stimulation. Our results strongly suggest this is not the case. We found that Alexander's Law developed even with natural stimulation, and also developed faster than most other oculomotor adaptive responses. These results were initially disappointing, as one of the initial motivations for these studies was the belief that Alexander's Law was one of the earliest adaptive responses to a vestibular lesion, so if we could understand the mechanism more, we might be able to improve the treatment of patients. However, as our modelling work has revealed, our studies also help us understand how the integrating circuits within the brainstem and cerebellum operate to maintain steady fixation. Temporal integration seems to be a mechanism frequently used throughout the nervous system, so comprehending its usage within the oculomotor system may assist in understanding many other neural functions.

6. References

1. Hegemann S, Straumann D, Bockisch C. Alexander's law in patients with acute vestibular tone asymmetry--evidence for multiple horizontal neural integrators. J Assoc Res Otolaryngol. 2007 Dec;8(4):551-61.
2. Bockisch CJ, Hegemann S. Alexander's law and the oculomotor neural integrator: three-dimensional eye velocity in patients with an acute vestibular asymmetry. Journal of Neurophysiolgy. [90381.2008 pii 10.1152/jn.90381.2008]. 2008;100(6):3105-16.
3. Bockisch CJ, Khojasteh E, Straumann D, Hegemann S. Development of eye position dependency of slow phase velocity during caloric stimulation. PLoS One. 2012;7(12):e51409.
4. Khojasteh E, Bockisch CJ, Straumann D, Hegemann SC. A dynamic model for eye-position-dependence of spontaneous nystagmus in acute unilateral vestibular deficit (Alexander's Law). Eur J Neurosci. 2013 Jan;37(1):141-9.
5. Bockisch CJ, Khojasteh E, Straumann D, Hegemann SCA. Eye position dependency of nystagmus during constant vestibular stimulation. Exp Brain Res. 2013;Epub ahead of print.
6. Bertolini G, Tarnutzer AA, Olasagasti I, Khojasteh E, weber KP, Bockisch CJ. Gaze holding in healthy subjects. PLoS One. 2013;8(4):e61389.
7. Skavenski AA, Robinson DA. Role of abducens neurons in vestibuloocular reflex. J Neurophysiol. 1973 Jul;36(4):724-38.
8. Hess K. Do peripheral-vestibular lesions in man affect the position integrator of the eyes? 1982;Suppl. 10:242-3.
9. Robinson DA, Zee DS, Hain TC, Holmes A, Rosenberg LF. Alexander's law: its behavior and origin in the human vestibulo-ocular reflex. Annals of Neurology. 1984;16(6):714-22.
10. Alexander G. Die Ohrenkrankheiten im Kindesalter. In: Schlossmann A, editor. Handbuch der Kinderheilkunde. Leipzig: Vogel; 1912. p. 84-96.
11. Cannon SC, Robinson DA, Shamma S. A proposed neural network for the integrator of the oculomotor system. 1983;49(2):127-36.
12. Crawford JD, Vilis T. Modularity and parallel processing in the oculomotor integrator. Exp Brain Res. 1993;96(3):443-56.
13. Aksay E, Olasagasti I, Mensh BD, Baker R, Goldman MS, Tank DW. Functional dissection of circuitry in a neural integrator. Nature Neuroscience. 2007;10(4):494-504.
14. Bockisch CJ, Hegemann S. Alexander's law and the oculomotor neural integrator: three-dimensional eye velocity in patients with an acute vestibular asymmetry. [90381.2008 pii 10.1152/jn.90381.2008]. 2008;2008/09/19(6):3105-16.
15. Optican LM, Zee DS. A hypothetical explanation of congenital nystagmus. Biol Cybern. 1984;50(2):119-34.
16. Glasauer S. Cerebellar contribution to saccades and gaze holding: a modeling approach. Ann N Y Acad Sci. 2006;1004:206-19.
17. Smith PF, Curthoys IS. Mechanisms of recovery following unilateral labyrinthectomy: a review. 1989;14(2):155-80.
18. Ris L, Godaux E. Spike discharge regularity of vestibular neurons in labyrinthectomized guinea pigs. Neurosci Lett. 1998 Sep 4;253(2):131-4.
19. Galiana HL, Outerbridge JS. A bilateral model for central neural pathways in vestibuloocular reflex. J Neurophysiol. 1984 Feb;51(2):210-41.
20. Galiana HL, Flohr H, Jones GM. A reevaluation of intervestibular nuclear coupling: its role in vestibular compensation. J Neurophysiol. 1984 Feb;51(2):242-59.
21. Galiana HL. A nystagmus strategy to linearize the vestibulo-ocular reflex. IEEE Trans Biomed Eng. 1991 Jun;38(6):532-43.
22. Khojasteh E, Bockisch CJ, Straumann D, Hegemann SC. A mechanism for eye position effects on spontaneous nystagmus. Conf Proc IEEE Eng Med Biol Soc. 2012;2012:3572-5.
23. Huk AC, Shadlen MN. Neural activity in macaque parietal cortex reflects temporal integration of visual motion signals during perceptual decision making. J Neurosci. 2005 Nov 9;25(45):10420-36.
24. Goldman-Rakic PS. Cellular basis of working memory. Neuron. 1995 Mar;14(3):477-85.

25. Taube JS, Bassett JP. Persistent neural activity in head direction cells. Cereb Cortex. 2003 Nov;13(11):1162-72.
26. Fuster JM, Bressler SL. Cognit activation: a mechanism enabling temporal integration in working memory. Trends Cogn Sci. 2012 Apr;16(4):207-18.
27. Uchida N, Kepecs A, Mainen ZF. Seeing at a glance, smelling in a whiff: rapid forms of perceptual decision making. Nat Rev Neurosci. 2006 Jun;7(6):485-91.
28. Major G, Baker R, Aksay E, Seung HS, Tank DW. Plasticity and tuning of the time course of analog persistent firing in a neural integrator. 2004;101(20):7745-50.

JARO (2007)
DOI: 10.1007/s10162-007-0095-6

JARO
Journal of the Association for Research in Otolaryngology

Alexander's Law in Patients with Acute Vestibular Tone Asymmetry—Evidence for Multiple Horizontal Neural Integrators

S. Hegemann,[1] D. Straumann,[2] and C. Bockisch[1,2,3]

[1]*Department of Otorhinolaryngology, Head and Neck Surgery, Zurich University Hospital, Frauenklinikstr. 24, Ch-8091, Zurich, Switzerland*

[2]*Department of Neurology, Zürich University Hospital, Frauenklinikstr. 26, Ch-8091, Zürich, Switzerland*

[3]*Department of Ophthalmology, Zurich University Hospital, Zurich, Switzerland*

Received: 15 December 2006; Accepted: 30 July 2007

ABSTRACT

Alexander's law (AL) states that the slow-phase velocity of spontaneous nystagmus of peripheral vestibular origin is dependent on horizontal gaze position, with greater velocity when gaze is directed in the fast-phase direction. AL is thought to be a compensatory reaction resulting from adaptive changes in the horizontal ocular motor neural integrator. Until now, only horizontal eye movements have been investigated with respect to AL. Because spontaneous nystagmus usually includes vertical and torsional components, we asked whether horizontal gaze changes would have an effect on the 3D drift of spontaneous nystagmus and, thus, on the vertical/torsional neural integrator. We hypothesized that AL reduces all nystagmus components proportionally. Moreover, we questioned the classical theory of a single bilaterally organized horizontal integrator and searched for nonlinearities of AL implying a network of multiple integrators. Using dual scleral search coils, we measured AL in 17 patients with spontaneous nystagmus. Patients followed a pulsed laser dot at eye level jumping in 5° steps along the horizontal meridian between 25° right and left in otherwise complete darkness. AL was observed in 15 of 17 patients. Whereas individual patients typically showed a change of 3D-drift direction at different horizontal eye positions, the average change in direction was not different from zero. The strength of AL (= rate of change of total velocity with gaze position) correlated with nystagmus slow-phase velocity (Spearman's rho=0.5; $p<0.05$) and, on average, did not change the 3D nystagmus drift direction. In general, eye velocity did not vary linearly with eye position. Rather, there was a stronger dependence of velocity on horizontal position when subjects looked in the slow-phase direction compared to the fast-phase direction. We conclude that the theory of a simple leak of a single horizontal neural integrator is not sufficient to explain all aspects of AL.

Keywords: oculomotor, neural integrator, vestibulo-ocular reflex, nystagmus, adaptation

INTRODUCTION

Patients with an acute vestibular tone asymmetry (AVTA) show spontaneous nystagmus. The velocity of the slow phase of nystagmus is mainly determined by the difference of tonic vestibular activity between the right and left sides, with the eye drifting towards the side with a lower spontaneous activity (Leigh and Zee 2006). When the vestibular tone asymmetry is constant, the slow-phase velocity (SPV) of nystagmus should also be constant and the axis of eye rotation should not change depending on gaze position.

Correspondence to: C. Bockisch • Department of Neurology • Zürich University Hospital • Frauenklinikstr. 26, Ch-8091, Zürich, Switzerland. Telephone: +41-44-2559396; fax: +41-44-2554507; email: chris.bockisch@usz.ch

However, the SPV in ongoing nystagmus varies depending on horizontal gaze position: SPV decreases when looking in the direction of the slow phase (Alexander 1912; Robinson et al. 1984). This behavior is called Alexander's law (AL).

Horizontal position dependency of eye velocity is not a natural feature of the rotational vestibular ocular reflex (VOR) (Robinson et al. 1984), so AL has been presumed to not arise in the peripheral vestibular apparatus, nor is it due to mechanical properties of the orbit. Hess (1982) and Robinson et al. (1984) suggested that AL results from adaptive changes in the neural mechanism that helps to ensure steady fixation at eccentric eye positions, which is necessary to counteract the elastic forces produced by extraocular structures. During eccentric fixation, elastic forces pull the eye back to a central position. A counter-acting force in the muscles is generated by integrating eye velocity commands, and so this mechanism is referred to as a neural integrator (NI) (Robinson 1968, 1975). If this neural integration is diminished, i.e., the time constant of the integrator is reduced, the NI is said to become "leaky" and the fixation command is insufficient to keep a normal eye from drifting back to a central position. This produces gaze-evoked nystagmus whose velocity increases with eccentricity. When combined with vestibular nystagmus, it reduces drift velocity in one direction, but increases velocity in the opposite direction, resulting in AL (Hess 1982; Robinson et al. 1984).

While the NI leak hypothesis is the most widely accepted mechanism for AL, it is not completely consistent with the eye velocity patterns seen in patients. According to the NI leak hypothesis, the change of velocity should be linear over the entire range of eye positions, although Alexander's original report (Alexander 1912), as well that of Hess (1983), describes different nystagmus patterns. Therefore, we sought to clarify these inconsistencies by measuring eye velocity with modern recording techniques in patients over a broad and finely sampled range of horizontal eye positions. Because spontaneous nystagmus of peripheral vestibular origin (SpN) is usually not purely horizontal but also includes vertical and torsional SPV, we further investigated if all nystagmus components are similarly affected, which would imply changes by the vertical/torsional NI. We asked specifically whether horizontal gaze changes would have an effect on the 3D drift of SpN. Finally, Robinson et al. (1984) reported that AL develops within about 25 s in normal people during caloric vestibular stimulation, suggesting a fast-acting adaptive mechanism. Thus, we also tested if the eye position dependency of nystagmus depends on the recent fixation history in patients.

METHOD

Patients

We investigated 17 patients, 10 women and 7 men, aged 21–71 years (mean 52) with an acute spontaneous nystagmus due to peripheral vestibular tone asymmetry (mean onset of vertigo 3.1 days before examination, range 0.25–13 days). All patients underwent a microscopic otoscopy and clinical neuro-otological examination. The clinical diagnosis of a peripheral vestibular tone asymmetry was made when a mixed horizontal torsional nystagmus was observed, no other acute neurological deficits could be detected, and the clinical head impulse test showed a hypofunction of the horizontal VOR with head rotations towards the direction of the slow phase of nystagmus. If no cause of the AVTA could be found, the diagnosis of idiopathic vestibulopathy was made (Table 1). Patients with Meniere's disease and spontaneous nystagmus due to vestibular migraine and patients with any acute neurological deficits other than cochleo-vestibular symptoms were excluded. The characteristics of the peripheral deficit (i.e., which canals were affected) were assessed by quantitative head impulse testing and caloric irrigation. The study adheres to the principles of the Declaration of Helsinki and was approved by the local ethics committee. Accordingly, all subjects gave their written informed consent after the experimental procedure had been explained. Inclusion criteria were an acute onset of vertigo within 14 days and a direction-specific spontaneous nystagmus.

Equipment

Eye and head movements were recorded in a magnetic frame (Remmel-type system, modified by A. Lasker, Baltimore, MD, USA) using dual scleral search coils (Skalar, Delft, the Netherlands) (Robinson 1963; Remmel 1984; Ferman et al. 1987). One search coil was placed on the right eye around the cornea after anesthetizing the conjunctiva with oxybuprocaine 0.4%; a second was tightly fixed on the forehead. Data was sampled at 1 kHz with 16-bit precision. Visual targets were produced by a laser, directed by a two-axis mirror galvanometer, which projected a 0.25°-diameter target on a tangent screen, 1.25 m from the subject. For measurements of nystagmus, the laser was pulsed (20 ms every 2 s) so that we could control the patient's gaze direction without visually suppressing nystagmus.

Procedure

Head impulse testing (Halmagyi and Curthoys 1988) was performed to determine the VOR gain in all

TABLE 1

Results of vestibular function tests: gain values for the VOR test as measured by head impulse testing in the SCC planes

Patient #	*Horizontal R/L*	*RALP/LARP down*	*RALP/LARP up*	*Caloric CP*	*Caloric DP*	*Clinical diagnosis*
1	*0.61*/**0.29**	0.78/**0.18**	*0.58*/**0.47**	**−37**	−16	IVP
2	NA	NA	NA	**50***	4*	Hemorrhagic otitis media
3	0.71/**0.46**	0.87/**0.38**	*0.64*/**0.47**	NA	NA	Hemorrhagic otitis media
4	0.79/**0.55**	NA	NA	−16	**−100**	IVP
5	**0.65**/0.83	**0.47**/0.71	0.92/0.88	**71**	−6	IVP
6	*0.60*/**0.43**	*0.58*/**0.52**	0.86/0.79	**−54**	**−38**	IVP
7	0.75/**0.44**	0.68/**0.31**	0.88/0.72	**−41**	**−46**	IVP
8	0.82/**0.28**	0.70/**0.28**	0.77/**0.44**	**−70**	**−49**	Temporal bone fracture
9	**0.33**/*0.49*	**0.20**/*0.47*	**0.60/0.53**	**53**	**77**	IVP
10	0.73/**0.35**	0.76/**0.17**	**0.47**/0.59	**−47**	**−100**	IVP
11	**0.41**/*0.56*	**0.35**/0.64	**0.64/0.54**	NA	NA	Traumatic perilymphatic fistula
12	0.99/**0.56**	0.89/**0.42**	1.01/0.76	**−55**	**−51**	IVP
13	1.04/**0.42**	1.05/0.65	0.86/0.84	NA	NA	IVP
14	0.77/**0.54**	*0.51*/**0.21**	0.87/0.91	NA	NA	IVP
15	0.74/**0.60**	0.89/0.68	0.70/0.79	**−51**	**−55**	IVP
16	0.88/**0.27**	0.77/**0.23**	0.66/0.82	**−63**	**−59**	IVP
17	**0.35**/*0.69*	**0.18**/*0.40*	**0.34**/*0.52*	**54**	**100**	IVP
Normal	≥0.71/0.70	≥0.69/0.54	≥0.67/0.68	≤+/−25	≤+/−30	IVP

Results of caloric tests are provided as canal paresis factor and directional preponderance according to the Jongkees formulas. Negative values represent hypofunction on the left horizontal SCC relative to the right horizontal SCC and preponderance of right beating nystagmus, respectively. Pathologic values are bold, and reduced gain values of the supposed intact side are in italics. Data with an asterisk are from a measurement 4 weeks after the onset of symptoms because initial testing was not possible due to acute otitis media

Horizontal R/L = horizontal plane, head movement towards right/left, respectively; RALP/LARP = plane of right anterior and left posterior SCC; down = head movement downwards in the respective plane testing mainly for anterior SCC function and up testing mainly for posterior SCC function; RALP = right-anterior left-posterior; LARP left-anterior right-posterior; CP = canal paresis factor; DP = directional preponderance; IVP = idiopathic vestibulopathy; NA = not available

canal planes (horizontal, right-anterior left-posterior, left-anterior right-posterior plane) and for both directions of each plane (Schmid-Priscoveanu et al. 1999). Briefly, patients fixated a target straight ahead, and the examiner stood behind the patient and manually induced short head movements with an amplitude of 10–20°. The mean peak velocities and accelerations were 342°/s and 12,442°/s^2 for horizontal movements, 214°/s and 7,118°/s^2 for movements in the on-directions of the anterior semicircular canals (SCCs), and 200°/s and 6,961°/s^2 for on-directions for the posterior SCCs. Gain was calculated as $\frac{1-\Delta\text{gaze}}{\Delta\text{head}(3°-7°)}$, where gaze (eye-in-space) and head were evaluated when the head had turned from 3° to 7°. A gain of +1 indicates perfect compensation (Palla and Straumann 2004).

Nystagmus was measured by instructing subjects to look in darkness at a pulsed target that moved every 5 s in steps of 5° from 25° right to 25° left and back. In a second trial – the jump paradigm – the flashing laser dot alternated between +/−25° eccentric positions every 20 s. This paradigm was performed in the first eight subjects to test for hysteresis, i.e., whether the previous position would influence the nystagmus velocity. Bithermal caloric vestibular testing was performed using a commercial caloric irrigator (Variotherm, Atmos MedizinTechnik GmbH & Co. KG, Lenzkirch, Germany). Both ears were irrigated for 30 s with 30 ml of water at temperatures of 44 and 30°C, respectively. For eye movement recording, we used a 50-Hz video-oculography system (VisualEyes, Micromedical™ Technologies, Chatham, IL, USA). Canal paresis factor and direction preponderance were calculated as relative differences in percentages in slow-phase eye velocity using the Jongkees formulas (Jongkees 1996). A canal paresis factor of 25% or more and a directional preponderance of 30% or more were regarded as pathologic.

Data analysis

Data were calibrated and processed using interactive programs written in MATLAB© (MathWorks, Natick, MA, USA). We computed rotation vectors and angular velocity as described previously (Hepp 1990; Tweed et al. 1990). We present data in the coordinates of the earth fixed coil frame with the z-axis aligned with gravity. Because the head of the subject was restrained with a chin rest, which kept Reid's line approximately parallel to the earth horizontal, the data represent a head fixed coordinate system, with positive rotations being clockwise, right, and up. We mirrored the horizontal and torsional data of the patients with right-side lesions, so all patients appear to have a left-side AVTA. There was no need to mirror the vertical data because the vertical components of the right and left anterior and right and left posterior SCCs are identical. All patients except one showed a downward drift.

Slow-phase eye velocity was found with an interactive computer program that first automatically detected saccades based on velocity and noise criteria (Holden et al. 1992) and then allowed the user to adjust the automatically marked saccades and to remove blink artifacts. Individual nystagmus slow phases were included in later analysis provided they were at least 100 ms in duration. For each slow phase, we calculated the median position and velocity for each component (horizontal, vertical, and torsional). For some graphs, we then averaged the slow-phase velocities and/or positions for each target direction, though all quantitative analysis was made without averaging over target positions.

We determined the linear change in eye velocity with horizontal gaze position with least-squares fits to the torsional, vertical, and horizontal eye velocity components, as well as to the total velocity (the length of the 3D eye velocity vector). Rank-order correlations were tested with Spearman's rho.

We analyzed the direction of nystagmus by decomposing the 3D eye velocity vector into two angles. We first projected the 3D velocity vector onto the plane defined by the horizontal and vertical components and calculated the angle of the projection in this plane. This angle varies from 0° (upward vertical velocity, with no horizontal component), to 90° (leftward, with no vertical component), to 180° (downward), to 270° (rightward). Likewise, we projected the vector on to the plane defined by the horizontal and torsional components, which gives an angle related to the horizontal/torsional direction: 0° is clockwise torsion, 90° is leftward, 180° is counterclockwise, and 270° is rightward. (The remaining direction in the torsional–vertical plane was ignored because subjects did not voluntarily change eye position in the vertical or torsional direction and the position change induced by the nystagmus was small.) When analyzed as a function of horizontal gaze position, this analysis provides us with information about how the direction of nystagmus, independent of the speed, varies with horizontal gaze position.

RESULTS

SCC lesion patterns

Table 1 shows the results of head impulse and caloric testing for each patient. One patient (#2) opted not to receive head impulse testing because of severe neck pain. In the remaining 16 patients, quantitative head impulse testing showed reduced gains for at least one horizontal canal (HC). Seven patients (44%) showed the pattern of a so-called superior vestibular neuropathy, with the HC and anterior canal (AC) affected but the posterior canal spared, and seven (44%) had a complete vestibulopathy with all SCCs affected. Two patients (13%) had an isolated HC defect only. The vertical canals were not tested in one patient (#4). In 11 patients, the gain reduction of the HC was unilateral. In five patients, HC gain reduction was bilateral, but in all patients the HC gains were reduced asymmetrically with the gain on the weaker side at least 20% decreased relative to the other side. Spontaneous nystagmus was consistently beating towards the side with the higher gain.

Caloric irrigation revealed a vestibular tone asymmetry in all patients tested. Five patients could not be tested in the initial phase, two (#2 and #3) because of an acute hemorrhagic otitis media and one (#11) because of a traumatic perilymphatic fistula. The latter was asymptomatic the day after closure of the perilymphatic fistula on the side with the weaker gain. Patient 2 had neither an initial head impulse nor caloric testing but was tested 4 weeks later by caloric irrigation showing a canal paresis factor of 50%. Two patients refused caloric testing.

In summary, 12 patients had an AVTA with a relative hypofunction on the left and 5 on the right side. Seven patients had a vestibular loss with affection of all three SCCs, seven showed the pattern of a superior vestibular neuritis (HC and AC affected), and two patients had a lesion of the lateral SCC canal only.

Drift direction of nystagmus slow phase in relation to the lesion pattern

The horizontal drift component (the slow-phase direction) was always towards the weaker HC according to head impulse and caloric testing, as expected. Horizontal drift velocity at gaze straight ahead ranged from −1 to −14°/s with a mean of −6.5°/s. All patients except one had a downward slow-phase drift. Vertical drift velocities ranged from 0.2 to −6°/s (mean: −2.2°/s). The patient with the upward slow-phase drift (#8) had the weakest vertical drift velocity. Torsional SPV was between 0.5 and 20°/s, and the direction was always counter-clockwise. Figure 1 shows the axis of rotation of the nystagmus slow phase for straight-ahead gaze for each patient normalized by the velocity magnitude. The axes thus show nystagmus direction. Also shown are the ocular motor rotation axes associated with excitatory stimulation of each SCC, which were derived according to the anatomical measurements of Della Santina et al. (2005). The nystagmus rotation axes cluster near the excitatory direction of the right horizontal SCC or opposite the direction of the weaker, left horizontal SCC. The axes also deviate slightly to oppose the left anterior SCC.

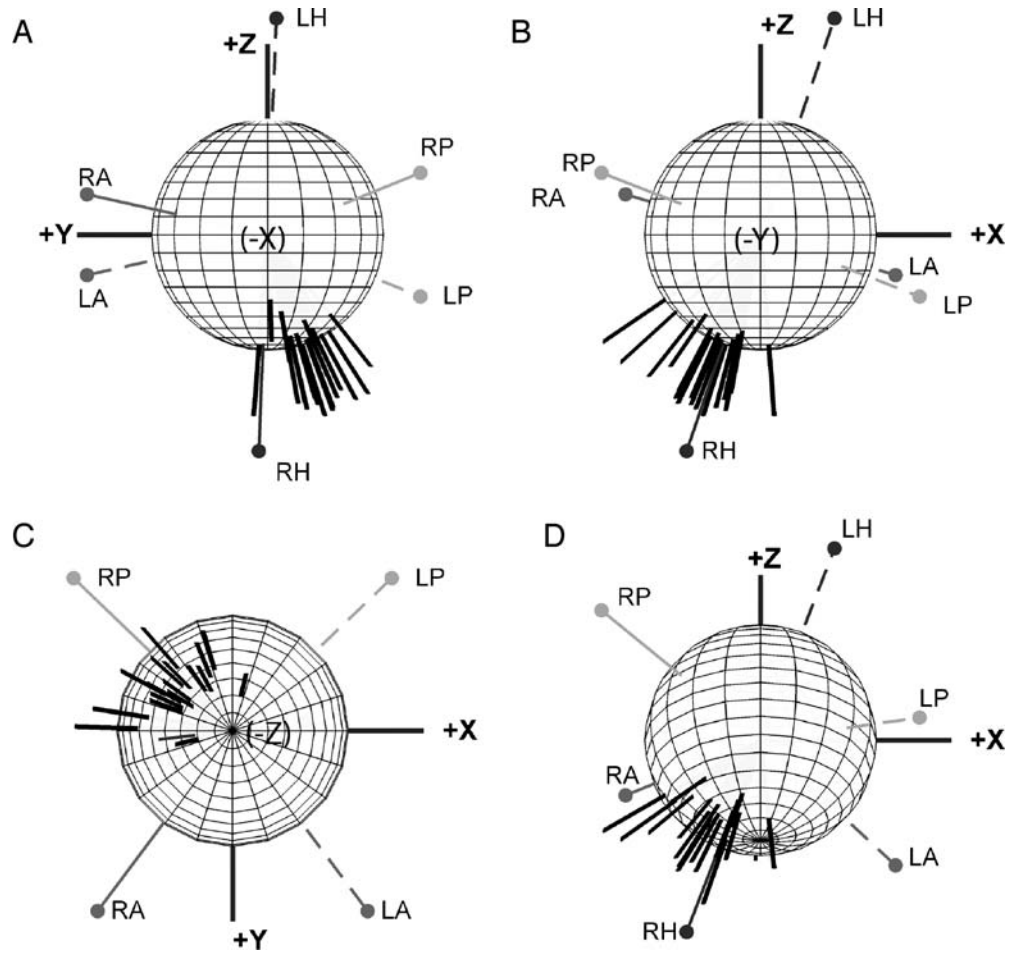

FIG. 1. The axes of eye velocity (*black lines*) are shown for each patient at straight-ahead gaze (intercept of linear fits to the velocity vs. position data), normalized by the velocity magnitude. The orientations of the axes thus show drift direction. Also shown are the oculomotor rotation axes associated with excitatory stimulation of each SCC [*L*(*R*)*H* = left (right) horizontal, *LP* = left posterior, *LA* = left anterior]. The Y-axis is aligned with Reid's line with a positive direction to the right, X and Z are normal to Reid's line with forward and upward directions positive. Each plot, **A**–**D**, shows the same data from different viewpoints: **A** view from behind (−X); **B** view from the left (−Y); **C** view from below (−Z); **D** view from a left-low-posterior position.

Dependence of slow-phase drift velocity on gaze position

Figure 2 shows representative data from three patients. The top panel shows eye position as a patient (#9) followed the flashing target from 25° left to 25° right. The right-beating nystagmus when looking left is weaker then when looking to the right, that is, the nystagmus is stronger in the direction of the fast phase in accord with AL. Figure 2A also shows nystagmus in both vertical and torsional eye position. In Figure 2B, the median eye velocity of each slow phase is shown, as a function of horizontal eye position, for the same patient. This patient shows a linear dependence of horizontal velocity on horizontal gaze position, with a peak velocity of about −12°/s when looking 25° right, which declined to about −2°/s when looking 25° left. In our patients, we never observed a reversal of the direction of horizontal eye velocity, as reported by Hess (1983), although this might be because we only measured to 25° eccentricity. In addition, Figure 2B shows the vertical and torsional velocity of the slow phases, which also show a clear linear dependence of eye velocity on horizontal gaze position. Figure 2C and D show different patterns of results from two different patients. In Figure 2C (#6), while eye velocity is apparent in all three directions, there is very little change in velocity with horizontal gaze position. The patient in Figure 2D (#15) showed a constant change in eye velocity when looking left, although in rightward gaze there is less of a change in eye velocity.

As represented in Figure 2, the patients typically showed downward and counterclockwise drift (upper pole rolls towards patients left side), in addition to the leftward horizontal component. These components are expected from a vestibular disturbance from the left HC with or without involvement of the anterior SCC as explained above. We used linear

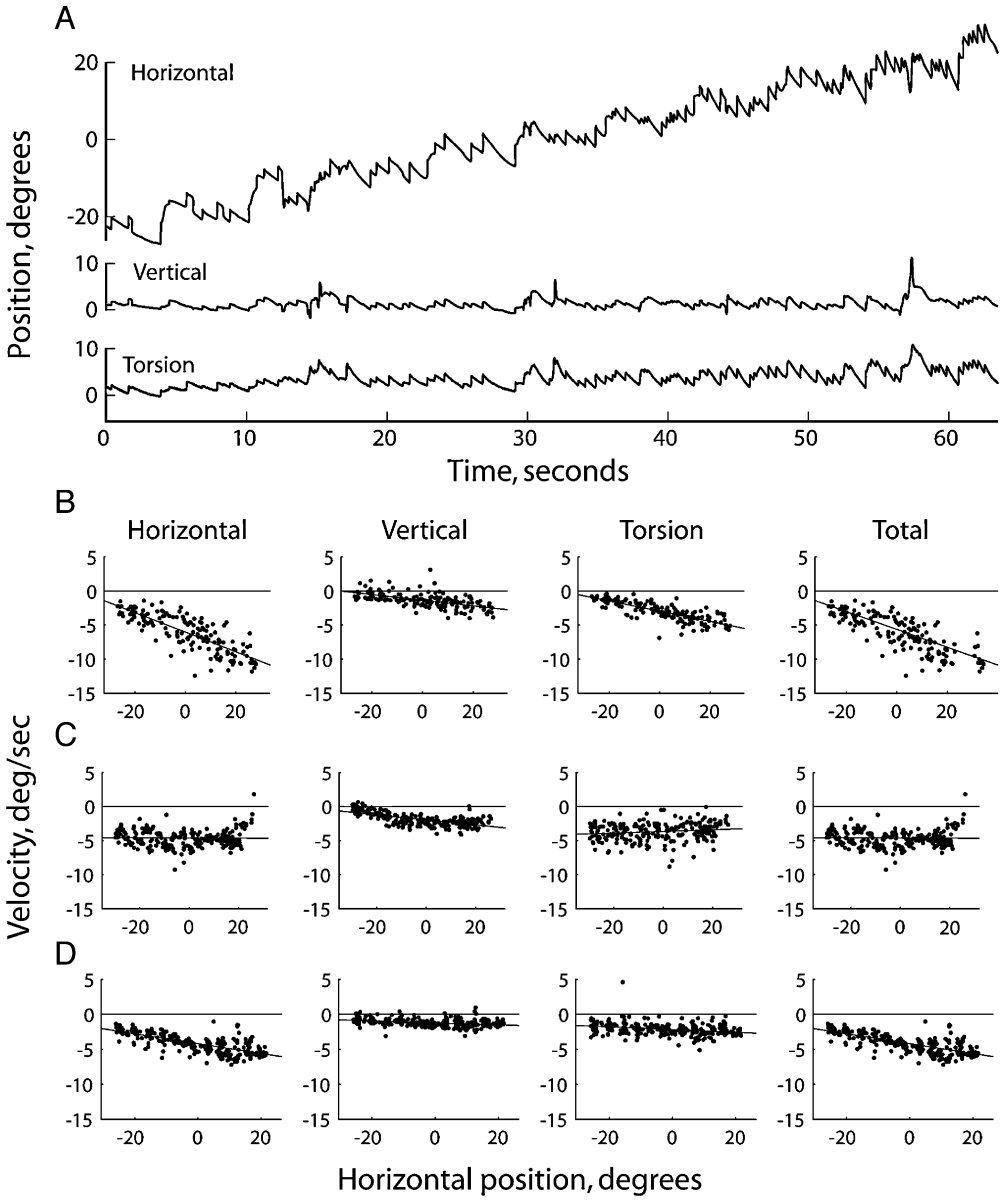

FIG. 2. **A** Horizontal, vertical, and torsional eye position as a patient (#9) followed a flashing target that moved from 25° left to 25° right. For horizontal position, the eye drifts slowly to the left, and a saccade redirects gaze to the right. **B** The median eye velocities for each slow phase are shown from the same patient as in **A**, including an additional "sweep" as the target moved right-to-left that is not shown in **A**. Horizontal, vertical, and torsional eye velocity are all greatest for rightward gaze. The best-fit regression lines are also shown. **C** A second patient (#6), where horizontal eye velocity is constant with horizontal gaze position but vertical eye velocity shows a small change with velocity being greatest for gaze to the right. **D** A third patient (#15), where horizontal eye velocity is linearly increasing from 25 degrees left to about 5 degrees right gaze, but on further right gaze one gets the impression that velocity change is reduced.

regression to characterize the change in horizontal, vertical, torsional, and total velocity on horizontal eye position (see Fig. 2). Fifteen of 17 patients showed a significant change in horizontal velocity with horizontal position that was consistent with AL (all ps<0.05). The average slope of the linear fits was −0.1°/s per degree of horizontal position, and the average bias (intercept), which indicates horizontal eye velocity at gaze straight ahead, was −6.5°/s. Both the average slope and bias were significantly different from zero (*t* tests: slope t=7.8, p<0.01; bias t=4.8°/s, p<0.01). The average slope of −0.1 corresponds to a NI time constant of 10 s (time constant=1/slope), whereas normal values are measured between 15 and 70 s (Becker and Klein 1973; Hess et al. 1985). Most patients also showed significant changes in vertical (16 of 17) and torsional (13 of 17) velocity with horizontal position. For vertical velocity, the average bias was −2.2 (t=5.2, p<0.01) and the average slope was −0.043 (t=3.0; p<0.01). For torsional velocity, the average bias was −3.5 (t=3.0, p<0.01) and the average slope was −0.034 (t=2.3; p<0.05). The average slopes

of the change in torsional, vertical, and horizontal eye velocity were such that, in general, eye velocity in all components decreased when the patients looked to the left.

If the change in eye velocity with gaze position is an adaptive response to the vestibular induced nystagmus, one would expect the strength of the effect to depend on the magnitude of the nystagmus. Figure 3 shows these relationships, taking the bias of the fits of total velocity vs. gaze position (the "total bias") as an estimate of the vestibular contribution to the nystagmus. The correlation between the horizontal slope and the bias was significant (Spearman's rho=0.5; t=2.3; p<0.05). The correlation between vertical slope and total bias was also significant, (rho=0.57; t=2.7; p<0.05), whereas the torsional slope was not (rho=0.16; t=0.62; p>0.5). The slope for total eye velocity was significantly correlated with the total bias (rho=0.53; t=2.4; p<0.05).

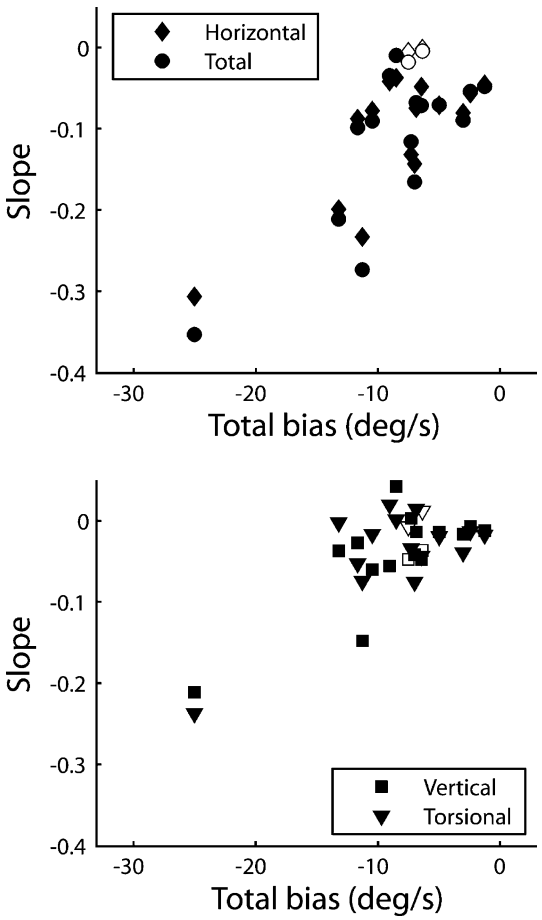

FIG. 3. The strength of AL varies with nystagmus intensity. *Top*: The slopes of the best-fit lines of horizontal and total eye velocity vs. the horizontal position are plotted vs. the total eye velocity bias. The sign of the total bias, and the slope for total velocity, have been inverted to facilitate comparison with the horizontal data. The total bias is the total 3D velocity at gaze straight ahead. Each *symbol* represents a single patient, and *filled symbols* indicate those patients who showed a statistically significant AL. *Bottom*: The slopes of the best-fit lines of vertical and torsional eye velocity vs. the horizontal position are plotted vs. the total eye velocity.

No hysteresis

The "jump" paradigm was designed to find hysteresis in eye velocity by having the patients alternate gaze between +25° and −25°. We performed this analysis on the first eight patients and found no difference in either the slope or bias for horizontal, vertical, torsional, or total eye velocity compared to our standard protocol. (Horizontal differences: bias=0.05°/s, paired t=0.1, p=0.9; slope=−0.02, t=0.88; p<0.5; all other components showed similarly small, statistically insignificant differences.) Because we did not find any hysteresis, we stopped testing for hysteresis to reduce the test duration.

Drift direction

For our patients with a relative left-hypofunction, eye drift for gaze straight ahead was left, down, and counterclockwise. However, the direction could change depending upon horizontal gaze position. Figure 4A, B shows an example of the direction of drift in the horizontal/vertical and horizontal/torsional planes. In this patient (#11), the downward component seen in right gaze (the fast-phase direction) disappears (and may even change to an upward component) in left gaze (Fig. 4A). Figure 4C shows the drift orientation in the same patient as a function of horizontal eye position. Zero-orientation indicates up (for the horizontal/vertical plane) and clockwise (for the horizontal/torsional plane), respectively, and 90° indicates left. Best fit lines to this data are shown. The vertical component becomes relatively smaller in the slow-phase direction (positive slope), or, in other words, the dependence of velocity on horizontal eye position is relatively stronger for vertical compared to horizontal velocity. The torsional component tends to be relatively larger in left gaze, and thus, the slope of the orientation vs. horizontal position is negative. The histograms in Figure 4D show the change in orientation of the slow-phase drift, that is, the slopes of the best fit lines of orientation vs. horizontal position such as those in Figure 4C. The maximum slope was about 1.4, which means that the nystagmus of this patient changed its direction by 14 degrees when the patient changed horizontal gaze position by 10 degrees.

In most patients, drift direction varied significantly with horizontal gaze position. We computed linear fits of the drift direction orientation vs. horizontal eye position, and in the horizontal–vertical plane, 14 of 17 (82%) patients showed a significant change in

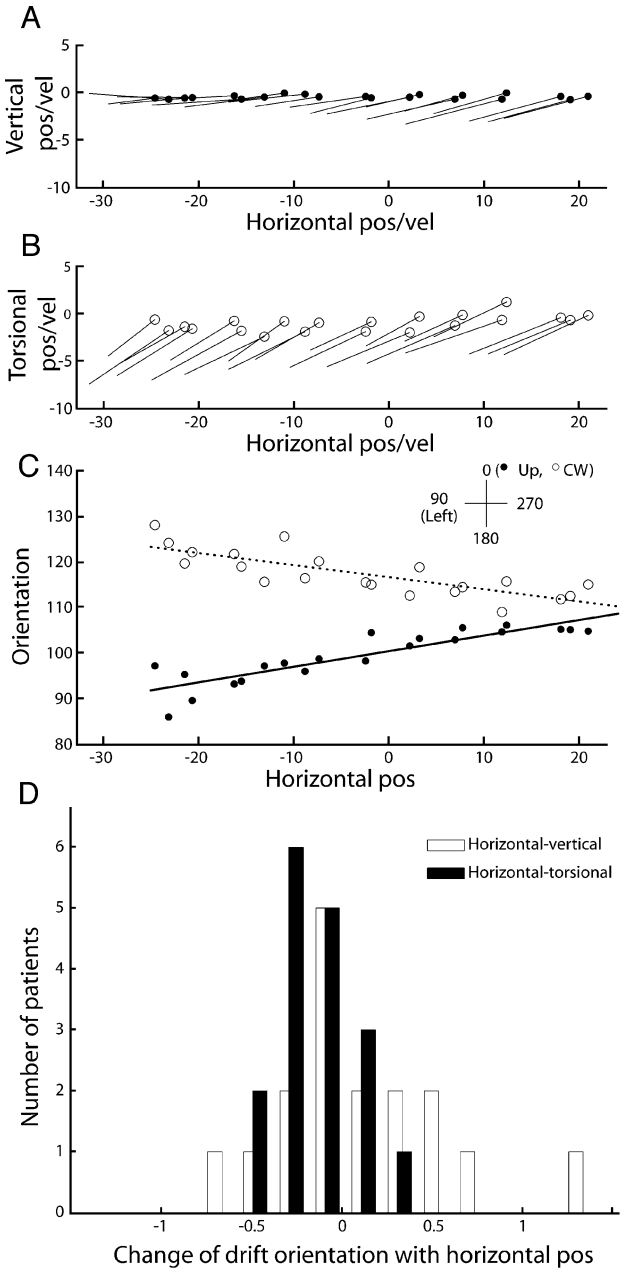

FIG. 4. Slow-phase drift direction could change with horizontal eye velocity. **A–C** Data from patient #11. **A** Each point shows the average horizontal and vertical eye position during each fixation period. The line extending from each point indicates the average horizontal and vertical velocity for that fixation period. Thus, the orientation of the line gives the direction of nystagmus in the horizontal/vertical plane, and the length is the magnitude. **B** Torsional and horizontal position and velocity. **C** The direction of nystagmus in the horizontal–torsional direction (*solid symbols*) and horizontal–vertical direction (*open*) is shown relative to horizontal position for the same patient, along with the best-fit lines. **D** Histograms showing the change in orientation of the slow-phase drift for the horizontal–vertical direction (*open bars*) and horizontal–torsional direction (*solid bars*) for all patients. These are the slopes from linear fits, such as in **C**.

drift direction. In the horizontal–torsional plane, 10 of 17 patients (59%) showed a significant change in drift direction with horizontal eye position. Only two patients (12%) showed no change in drift direction in both planes. Note that these were not identical with the two patients who showed no AL in the horizontal velocity component.

If AL modulates drift velocity, the direction of drift will remain constant if and only if the change in velocity is proportional in all components. In Figure 4A, the vertical component changes more, proportionally, than the horizontal component, leading to a change in drift direction. In Figure 4B, the changes in horizontal and torsional component are closer, so a change in the horizontal–torsional difference is less obvious. This is clearer in Figure 4C, where the slope of the best-fit horizontal–vertical line is greater than the horizontal–torsional line.

Despite significant changes of drift direction in individual patients, there was no consistent pattern of direction change. Thus, for the whole group, the average change in direction (the slope of best fit line for direction and gaze position) was not significantly different from zero for both the horizontal–vertical plane (mean=0.075; t=0.6; p=0.5) and the horizontal–torsional plane (mean=−0.1; t=1.9; p<0.08) (Fig. 4D).

Gaze dependent changes in the slope of velocity vs. position

We frequently observed that the change of eye velocity with eye position was not constant but could be different depending upon whether the patient was looking to the left or to the right. Figure 5B and C provide two such examples. We fit separate lines to eye velocity depending upon whether the patient was looking to the left or right of straight ahead. Figure 5A (#9) shows an example where the slopes of the two lines were very similar. In Figure 5B (#2), when the patient looked in the positive direction, where eye velocity was higher, there was little change in velocity with position, in contrast to the negative direction. Figure 5C (#6) shows a more extreme example, where the change in velocity reverses direction. Averaged over all patients, the slope for gaze in the slow-phase direction was −0.14, whereas the slope for gaze in the fast-phase direction was −0.04, a difference that was significant (paired t=2.6, p<0.05). We found that 15 of 17 patients (88%) showed a significant decrease in horizontal velocity with horizontal position when looking in the slow-phase direction. In the fast-phase direction, nine patients showed a significant negative slope, three (numbers 4, 6, and 13) showed a significant positive slope, and five (numbers 2, 3, 12, 15, and 16) showed a slope that was not significantly different from 0. Figure 5D shows the parameters of the linear fits of the horizontal

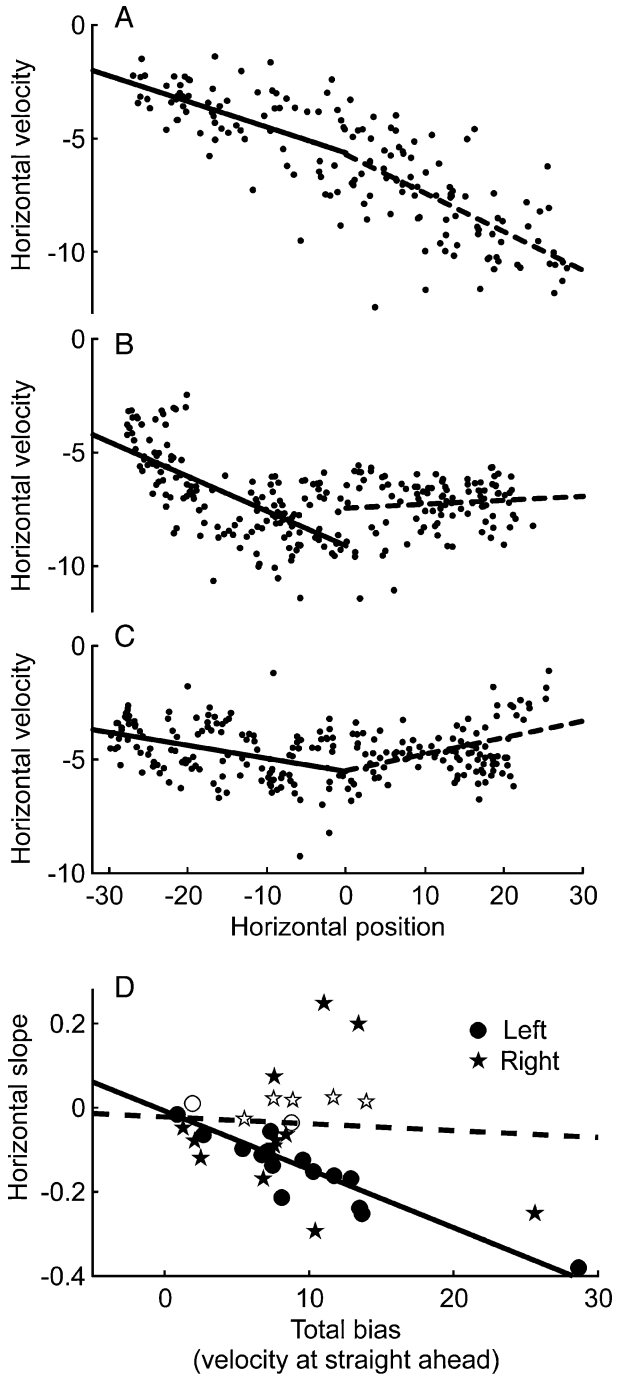

FIG. 5. The change in eye velocity with position could be different depending upon whether the subject was looking in the slow-phase direction or the fast-phase direction. **A–C** Data from different patients. *Solid lines* indicate the best-fit lines to the velocity data when subjects looked to the left, *dashed lines* show the best-fit lines for eye positions to the right. The two slopes for the patient in **A** (#9) show little difference, whereas in **B** (#2), eye velocity when looking to the right is mostly unchanged, and in **C** (#6), the slope of the best-fit line changes direction. **D** The slope-values of each best-fit line to horizontal velocity for the left and right hemifield for all patients are plotted against the total eye velocity, showing that, in left gaze, the slope of AL increases with the total eye velocity, but not in right gaze. *Circles* indicate data when patients looked to the left and *stars* indicate data when they looked to the right. *Solid symbols* indicate slopes that were significantly different from zero.

slopes vs. the total eye velocity. When looking left (in the slow-phase direction), the slope of the best-fit line increases with the total bias (slope=0.014; R^2=0.8; p<0.01), whereas when looking to the right, the slope does not consistently vary with the total bias (slope=−0.002, R^2=0.004, p>0.7). We also calculated Spearman's rho, a nonparametric correlation measure, for velocity axes vs. the total eye velocity. When looking in the slow-phase direction, horizontal, vertical, and total velocity components showed significant correlations with the total bias (all ps<0.01), but the change in torsional velocity with horizontal eye position was not correlated with the total bias (p>0.3). When looking in the fast-phase direction, all correlations were not significant (all p values>0.18).

Finally, we analyzed whether the direction of the slow phase varied with eye position, similar to the analysis in Figure 4, when looking to the left, where we observed stronger AL. The average change in direction (the slope of best fit line for direction and gaze position) was not significantly different from zero for both the horizontal–vertical direction (mean=−0.08; t=0.5; p>0.6) and the horizontal–torsional direction (mean=−0.1; t=1.3; p>0.1).

DISCUSSION

We measured the effect of horizontal gaze position on eye velocity and drift direction in patients with AVTA, as determined by head impulse testing and bithermal caloric testing. For the first time, we described the effects of horizontal eye position changes on 3D velocity and drift direction changes. We found that the strength of AL, the gaze-dependent change of eye velocity, increased in patients with higher nystagmus velocity. This is consistent with the view that AL is a compensatory reaction that reduces nystagmus SPV in one direction of gaze so that retinal image slip is minimized. Since the studies by Hess (1982) and Robinson et al. (1984), it has been assumed that AL is a consequence of a single horizontal NI becoming leaky, that is, the normal force command needed to maintain an eccentric horizontal eye position is reduced. Below, we consider how our results require modification of this view.

Unilateral vestibular deficit vs. asymmetric bilateral hypofunction

We found bilateral – although asymmetric – VOR gain reductions during head impulse testing in 7 of 17 patients. Although concomitant VOR gain reduction with head impulses towards the supposed healthy side is known in patients with acute unilateral peripheral vestibulopathy (Aw et al. 2001; Halmagyi

et al. 1990; Palla and Straumann 2004), we cannot exclude a bilateral asymmetric affection in these patients. AL was observed in all of these patients, and a difference between unilateral and asymmetric bilateral hypofunction has never been made in the literature with respect to AL. Thus, we think it is reasonable to not distinguish between pure unilateral hypofunction and asymmetric bilateral hypofunction here.

No hysteresis

By comparing small, stepwise position changes with large gaze jumps, we tested the hypothesis that AL is dependent on the eye position immediately preceding the new position. Robinson et al. (1984) reported that, in normal subjects with nystagmus induced with calorics, AL can develop in ~25 s with the sudden onset of nystagmus. We found no hysteresis, i.e., no evidence for any fast-acting adaptation process, perhaps because the response to calorics is different or the adaptation process in patients that have experienced an abnormal vestibular stimulus for at least many hours is different from the initial adaptive response.

Dependence of vertical and torsional eye velocity and nystagmus direction on horizontal eye position

Studies of AL have typically been limited to descriptions of horizontal eye velocity, although nystagmus resulting from vestibular lesions is more complex, usually containing vertical and torsional components, as well. An unexpected finding was that, in our AVTA patients, the vertical and torsional nystagmus decreased when they looked in the direction of the horizontal slow phase. This could occur if the vertical–torsional NI was sensitive to horizontal eye position, and adapted as well. Static torsional position does vary with horizontal position when the head is pitched forward or backward (Haslwanter et al. 1992; Bockisch et al. 2001; Furman and Schor 2003); if this torsional command passes through the common torsional–vertical NI, then the torsional–vertical NI must be sensitive to horizontal gaze position.

Our patients typically had downward and counterclockwise drift in addition to the dominant horizontal component, and all three typically modulated with horizontal gaze position. In 82% of patients, the direction of nystagmus varied significantly with eye position, but the changes were not consistently in the same direction, and so across patients the average change in direction was not different from zero. An explanation of this finding might be that changes in the horizontal and vertical/torsional NI are not rigidly coupled but show individual variations, and in general, both integrators work together to reduce the horizontal, vertical, and torsional nystagmus components in approximately equal proportions.

Multiple horizontal NIs

Superimposing a gaze-evoked nystagmus (where the eye drifts back towards a central orbital position) on to the vestibular evoked nystagmus decreases eye velocity in the slow-phase direction but has the unfortunate consequence of increasing eye velocity in the fast-phase direction. A more adaptive response, in terms of reducing the vestibular nystagmus, would be for the NI to become unstable in the fast-phase direction, that is, to produce a gaze-evoked nystagmus that would normally push the eye to eccentric positions. Indeed, we observed this behavior in three patients (Fig. 5C). In general, we found that eye velocity varied more with gaze position when patients looked in the fast-phase direction compared to when they looked in the slow-phase direction. This means that the NI has the ability to differentially adapt to gaze directions, suggesting that there are functionally separate integrators for left and right gaze. The diverse patterns of behavior seen in Figure 5 can be explained as arising from the relative amounts of adaptation for left and right gaze: the integrators for positions in the phase-fast direction become leaky, while those in the slow-phase direction can become similarly leaky (Fig. 5A), unchanged (Fig. 5B), or unstable (Fig. 5C). Cannon et al. (1983) introduced the concept of multiple integrators in their neural network model of the NI to improve the network's stability. Crawford and Vilis (1993) provided evidence for multiple vertical/torsional integrators when they pharmacologically inhibited the integrator and found that the eye did not drift to a single resting position, but rather, multiple resting positions were possible. Recent experimental findings in goldfish also support the hypothesis of separate integrators for horizontal gaze (Aksay et al. 2007).

CONCLUSION

AL is frequently observed in AVTA patients and has traditionally been explained as a simple change in the horizontal NI. Our measurements of the 3D eye movements in AVTA patients suggest the mechanism of AL, while still perhaps based on brainstem and cerebellar NIs, might not be as simple as originally thought. Our data lend support to the idea of multiple horizontal NIs adapting differentially to the vestibular tone asymmetry. Furthermore, we showed that horizontal eye position influences both the horizontal and vertical/torsional NI.

ACKNOWLEDGEMENTS

We would like to thank Itsaso Olasagasti for insightful discussions, Jean Laurens and Aasef G. Shaik for proofreading the manuscript; Tanja Schmückle Meier, Elisabeth Schafflützel, and Elena Buffone for assistance with patient evaluation and data collection; and Albert Züger for technical help. This study was supported by the Swiss National Science Foundation (#3200B0-105434) and the Betty and David Koetser Foundation for Brain Research, Zurich, Switzerland.

REFERENCES

AKSAY E, OLASAGASTI I, MENSH BD, BAKER R, GOLDMAN MS, TANK DW. Functional dissection of circuitry in a neural integrator. Nat. Neurosci. 10(4):494–504, 2007.

ALEXANDER G. Die Ohrenkrankheiten im Kindesalter. In: Schlossmann A (ed) Handbuch der Kinderheilkunde. Leipzig, Verlag von F.C.W. Vogel, pp. 84–96, 1912.

AW ST, FETTER M, CREMER PD, KARLBERG M, HALMAGYI GM. Individual semicircular canal function in superior and inferior vestibular neuritis. Neurology 57:768–774, 2001.

BECKER W, KLEIN HM. Accuracy of saccadic eye movements and maintenance of eccentric eye position in the dark. Vis. Res. 13:1021–1034, 1973.

BOCKISCH CJ, HASLWANTER T. Three-dimensional eye position during static roll and pitch in humans. Vis. Res. 41:2127–2137, 2001.

CANNON SC, ROBINSON DA, SHAMMA S. A proposed neural network for the integrator of the oculomotor system. Biol. Cybern. 49:127–136, 1983.

CRAWFORD JD, VILIS T. Modularity and parallel processing in the oculomotor integrator. Exp. Brain Res. 96:443–456, 1993.

DELLA SANTINA CC, POTYAGAYLO V, MIGLIACCIO AA, MINOR LB, CAREY JP. Orientation of human semicircular canals measured by three-dimensional multiplanar CT reconstruction. J. Assoc. Res. Otolaryngol. 6:191–206, 2005.

FERMAN L, COLLEWIJN H, JANSEN TC, VAN DEN BERG AV. Human gaze stability in the horizontal, vertical and torsional direction during voluntary head movements, evaluated with a three-dimensional scleral induction coil technique. Vis. Res. 27:811–828, 1987.

FURMAN JM, SCHOR RH. Orientation of Listing's plane during static tilt in young and older human subjects. Vis. Res. 43:67–76, 2003.

HALMAGYI GM, CURTHOYS IS. A clinical sign of canal paresis. Arch. Neurol. 45(7):737–739, 1988.

HALMAGYI GM, CURTHOYS IS, CREMER PD, HENDERSON CJ, STAPLES M. Head impulses after unilateral vestibular deafferentation validate Ewald's second law. J. Vestib. Res. 1:187–197, 1990.

HASLWANTER T, STRAUMANN D, HESS BJ, HENN V. Static roll and pitch in the monkey: shift and rotation of Listing's plane. Vis. Res. 32:1341–1348, 1992.

HEPP K. On Listing's law. Commun. Math. Phys. 132:285–292, 1990.

HESS K. Do peripheral-vestibular lesions in man affect the position integrator of the eyes? Neurosci. Lett. Suppl. 10:242–243, 1982.

HESS K. Counterdrifting of the eyes following unilateral labyrinthine disorders. Adv. Otorhinolaryngol. 30:46–49, 1983.

HESS K, REISINE H, DÜRSTELER M. Normal eye drift and saccadic drift correction in darkness. Neuroophthalmology 5:247–252, 1985.

HOLDEN JR, WEARNE SL, CURTHOYS IS. A fast, portable desaccading program. J. Vestib. Res. 2:175–179, 1992.

JONGKEES LBW. The Evaluation of the Vestibular Caloric Test. Philadelphia, University of Pennsylvania Press, 1996.

LEIGH RJ, ZEE DS. The Neurology of Eye Movements. Fourth Edition. London: Oxford University Press, 2006.

PALLA A, STRAUMANN D. Recovery of the high-acceleration vestibulo-ocular reflex after vestibular neuritis. J. Assoc. Res. Otolaryngol. 5:427–435, 2004.

REMMEL RS. An inexpensive eye movement monitor using the scleral search coil technique. IEEE Trans. Biomed. Eng. 31:388–390, 1984.

ROBINSON DA. A method of measuring eye movements using a scleral search coil in a magnetic field. IEEE Trans. Biomed. Eng. 10:137–145, 1963.

ROBINSON DA. Eye movement control in primates. The oculomotor system contains specialized subsystems for acquiring and tracking visual targets. Science 161:1219–1224, 1968.

ROBINSON DA. Oculomotor control signals. In: Lennerstrand G and Bach-y-Rita P (eds) Basic Mechanisms of Ocular Motility and their Clinical Implications. Oxford: Pergamon, pp. 337–378, 1975.

ROBINSON DA, ZEE DS, HAIN TC, HOLMES A, ROSENBERG LF. Alexander's law: its behavior and origin in the human vestibulo-ocular reflex. Ann. Neurol. 16:714–722, 1984.

SCHMID-PRISCOVEANU A, STRAUMANN D, BOHMER A, OBZINA H. Vestibulo-ocular responses during static head roll and three-dimensional head impulses after vestibular neuritis. Acta Otolaryngol. 119:750–757, 1999.

TWEED D, CADERA W, VILIS T. Computing three-dimensional eye position quaternions and eye velocity from search coil signals. Vis. Res. 30:97–110, 1990.

J Neurophysiol 100: 3105–3116, 2008.
First published September 17, 2008; doi:10.1152/jn.90381.2008.

Alexander's Law and the Oculomotor Neural Integrator: Three-Dimensional Eye Velocity in Patients With an Acute Vestibular Asymmetry

Christopher J. Bockisch[1,2,3,4] and Stefan Hegemann[1,4]

[1]*Department of Otorhinolaryngology, Head and Neck Surgery,* [2]*Department of Neurology, and* [3]*Department of Ophthalmology, Zürich University Hospital; and* [4]*Zürich Center for Integrative Human Physiology, University of Zürich, Zurich, Switzerland*

Submitted 20 March 2008; accepted in final form 14 September 2008

Bockisch CJ, Hegemann S. Alexander's law and the oculomotor neural integrator: three-dimensional eye velocity in patients with an acute vestibular asymmetry. *J Neurophysiol* 100: 3105–3116, 2008. First published September 17, 2008; doi:10.1152/jn.90381.2008. According to Alexander's law (AL), the slow phase velocity of nystagmus of vestibular origin is dependent on horizontal position, with lower velocity when gaze is directed in the slow compared with the fast phase direction. Adaptive changes in the velocity-to-position neural integrator are thought to cause AL. Although these changes have been described for the horizontal neural integrator, nystagmus often includes vertical and torsional components, but the adaptive abilities of the vertical and torsional integrators have not been investigated. We measured 11 patients with a peripheral vestibular asymmetry and used second-order equations to describe how velocity varied with position. Horizontal velocity changed with horizontal position in accordance with AL and the second-order term for horizontal position was also significant. Whereas velocity decreased in the slow phase direction, it was relatively unchanged >10° into the fast phase direction. Vertical velocity was also highest in the vertical fast phase direction and the second-order term for vertical position was also significant, in that vertical velocity increased in the vertical fast phase direction, but was unchanging in the slow phase direction. Torsional velocity varied linearly with horizontal, but not vertical, position. These results show that the horizontal and vertical oculomotor neural integrators react to altered vestibular input by maintaining different integrating time constants depending on gaze direction.

INTRODUCTION

Alexander (1912) observed that in patients with spontaneous nystagmus due to an acute vestibular asymmetry, the slow phase velocity, or drift, of nystagmus is lower when the subject looks toward the side of the slow component of nystagmus compared with the fast phase direction. This observation is so frequently observed that it is referred to as "Alexander's Law."

Hess (Hess et al. 1984) and Robinson (Robinson et al. 1984) proposed that Alexander's Law (AL) results from changes in the neural mechanism that helps maintain steady eye position at eccentric positions. Without such a mechanism, elastic forces produced by the extraocular tissues would pull the eye back to a central position. Robinson (1968, 1975) proposed that the counteracting force is produced by integrating eye velocity commands, so this gaze-holding mechanism is referred to as a neural integrator (NI). If the NI produces a command that is too small to maintain fixation, the eye will drift back to an elastic equilibrium position and the NI is said to be "leaky," whereas a command from the NI that is too large and causes the eye to drift eccentrically is termed "unstable." Normally, the NI is slightly leaky, showing integrating time constants of ≥20 s (Cannon and Robinson 1987; Goltz et al. 1997). The NI explanation of AL is that the NI becomes leaky and, when combined with the constant velocity vestibular nystagmus, reduces drift velocity in one direction, increases velocity in the opposite direction. This mechanism is thought to be adaptive in the sense that it reduces drift velocity for some gaze positions, thus improving vision, albeit eye drift is higher in the opposite direction.

Figure 1*A* shows a simple, hypothetical drift pattern expected with a left vestibular lesion that produces only horizontal nystagmus. Velocity is the same for all horizontal and vertical positions. In Fig. 1*B*, the drift pattern that occurs with a leaky horizontal NI is shown, in which centrifugal drift increases with horizontal eccentricity, but does not vary with vertical position. The combination of the vestibular-evoked drift in Fig. 1*A* and the gaze evoke drift in Fig. 1*B* is shown in Fig. 1*C*, illustrating the pattern of AL where velocity is highest in the fast phase direction. Figure 1*D* shows a more realistic example of vestibular nystagmus, which has horizontal, vertical, and torsional components, and the patterns of drift that result from combining this with a leaky horizontal NI (Fig. 1*E*) and both a leaky horizontal and vertical NI (Fig. 1*F*) are also shown.

Recently, we showed that in most patients with nystagmus due to an acute vestibular asymmetry, AL does not change drift velocity linearly with horizontal gaze position (Hegemann et al. 2007), as would be predicted by the traditional leaky integrator model proposed by Robinson et al. (1984). Instead, drift velocity was reduced proportional to position in the slow phase direction but was not significantly increased in the fast phase direction, showing differential NI adaptation for right and left gazes. We suggested the differential adaptation was due to functionally separate NIs for left and right gaze, a hypothesis that originates in the modeling study of Cannon et al. (1983), and was suggested by physiologic work in monkey (Crawford and Vilis 1993) and goldfish (Aksay et al. 2007). Chan and Galiana (2005, 2007) also proposed that the NI can maintain different integrating time constants, depending on gaze direction.

Although AL is a frequent clinical observation, the few detailed studies of AL are limited to horizontal movements (Doslak et al. 1979, 1982; Hegemann et al. 2007; Hess et al. 1984; Jeffcoat et al. 2008; Robinson et al. 1984). AL has been

Address for reprint requests and other correspondence: C. J. Bockisch, Neurology Department, Zürich University Hospital, Frauenklinikstrasse 26, 8091 Zurich, Switzerland (E-mail: chris.bockisch@usz.ch).

The costs of publication of this article were defrayed in part by the payment of page charges. The article must therefore be hereby marked "*advertisement*" in accordance with 18 U.S.C. Section 1734 solely to indicate this fact.

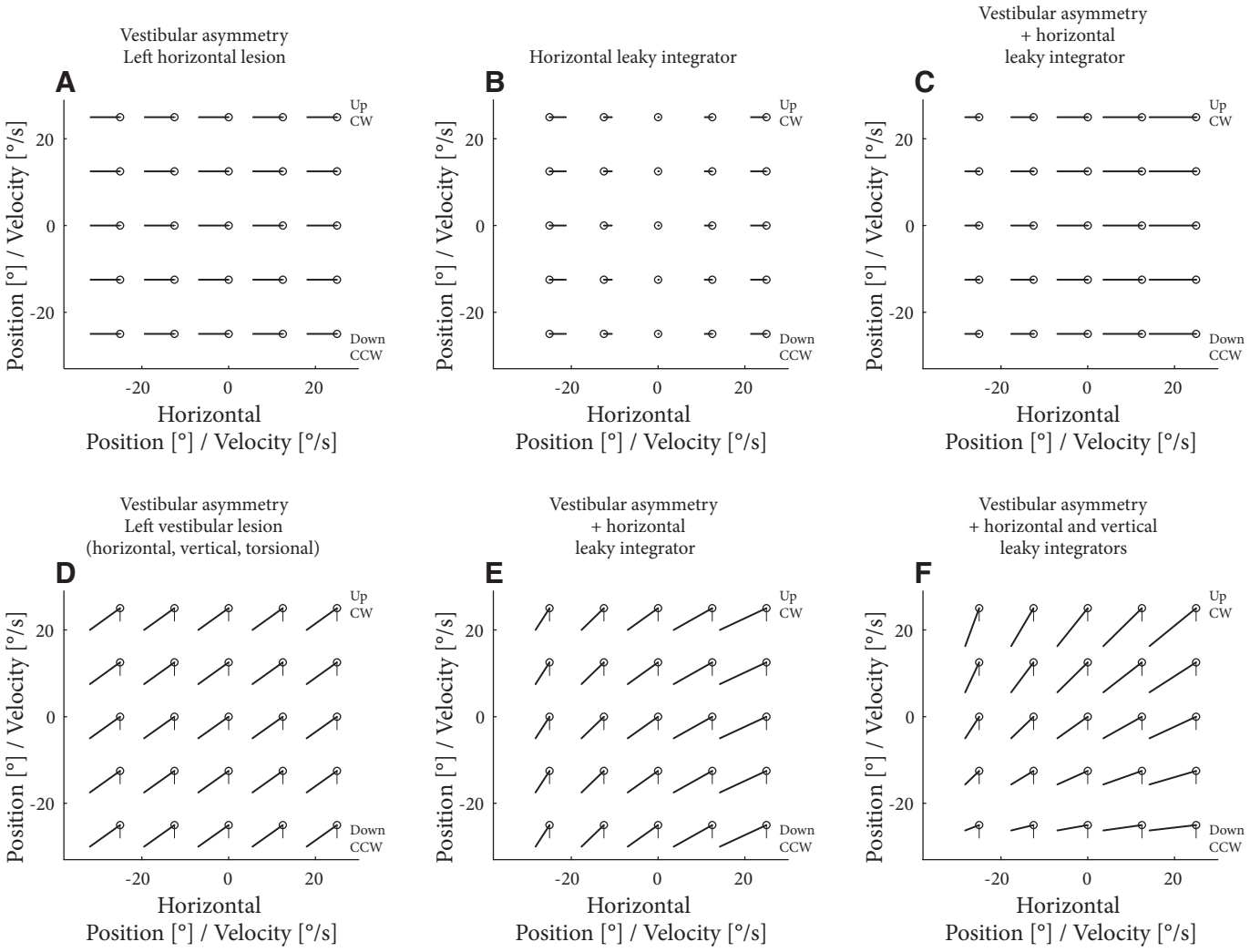

FIG. 1. Hypothetical combinations of vestibular and gaze-evoked nystagmus. *A*: the drift pattern associated with a left vestibular lesion that evokes only horizontal nystagmus. Each circle indicates horizontal and vertical positions and the thick line shows the horizontal and vertical velocities, and so the orientation of the line indicates direction and the length represents the speed. Drift velocity is to the left and does not vary with horizontal or vertical position. *B*: drift pattern associated with a gaze-evoked nystagmus caused by a leaky horizontal neural integrator (NI) (time constant = 6.7 s). For eccentric horizontal gaze positions, the eye moves back to the center with a velocity that increases with eccentricity. Velocity does not vary with vertical position. *C*: the combination of *A* and *B*. The nystagmus velocity changes linearly with horizontal but not vertical eye position. *D*: vestibular nystagmus, which has horizontal, vertical, and torsional components. Thin lines show torsional velocity, with an upward line indicating clockwise velocity and a downward line indicating counterclockwise velocity. *E*: the pattern of drift that occurs when combining the vestibular nystagmus of *D* with a leaky horizontal NI (*B*). *F*: the pattern of drift that occurs when combining the vestibular nystagmus of *D* with both a leaky horizontal NI and a leaky vertical NI. All simulations ignore other possible gaze-dependent changes in velocity, such as the half- or quarter-angle rules (Crane et al. 2006; Misslisch et al. 1994; Palla et al. 1999; Tweed et al. 1990).

observed for vertical eye movements in patients with cerebellar disease (Glasauer et al. 2003; Straumann et al. 2000) and in healthy people with pursuit-afternystagmus (Marti et al. 2005). Here we investigate the characteristics of AL by having patients with a peripheral vestibular asymmetry look in different horizontal and vertical directions. Since vestibular nystagmus usually consists of horizontal, vertical, and torsional components, we asked whether AL is also valid for the vertical and torsional components and whether we would find asymmetries similar to those in horizontal gaze holding.

METHODS

Patients and equipment

We investigated 11 patients, 5 women and 6 men, ages 21–67 yr (mean 51 yr), with an acute spontaneous nystagmus due to a peripheral vestibular asymmetry (mean onset of vertigo 2.5 days before examination, range 0.25–6.5 days). Data from horizontal gaze changes without variation in vertical position from patients 1 through 6 (Table 1) were also used in our previous study (Hegemann et al. 2007). Patients had an onset of vertigo ≤7 days before measurements, a clinical diagnosis of a peripheral vestibular asymmetry, and no other acute neurological deficits. Patients with Ménière's disease, spontaneous nystagmus due to vestibular migraine, or any other cochleovestibular symptoms were excluded. The affected canals were identified with quantitative head impulse testing and caloric irrigation. The study adhered to the principles of the Declaration of Helsinki and was approved by the local ethics committee. All patients gave their written informed consent after the experimental procedure had been explained.

Three-dimensional (3D) movements of the head and the right eye were recorded in a magnetic frame (Remmel-type system, modified by A. Lasker, Baltimore, MD) using dual scleral search coils (Skalar

TABLE 1. *Results of vestibular function tests*

Patient	Horizontal Right/Left	RALP/LARP Down	RALP/LARP Up	Caloric CP	Caloric DP	Clinical Diagnosis
1	**0.41**/*0.56*	**0.35**/0.64	**0.64/0.54**	NA	NA	Traumatic PLF
2	1.04/**0.42**	1.05/0.65	0.86/0.84	NA	NA	IVP
3	0.77/**0.54**	*0.51*/**0.21**	0.87/0.91	NA	NA	IVP
4	0.74/**0.60**	0.89/0.68	0.70/0.79	**−51**	**−55**	IVP
5	0.88/**0.27**	0.77/**0.23**	0.66/0.82	**−63**	**−59**	IVP
6	**0.35**/*0.69*	**0.18**/*0.40*	**0.34**/*0.52*	**54**	**−100**	IVP
7	**0.31**/*0.63*	**0.68**/0.79	**0.60**/0.81	**24**	**91**	IVP
8	*0.60*/**0.55**	0.70/0.87	0.94/**0.61**	NA	NA	IVP
9	0.56/0.41	0.72/0.40	0.75/0.18	**76.5**	**57**	IVP
10	*0.62*/**0.27**	*0.60*/**0.31**	0.88/**0.52**	**−67**	**−100**	IVP
11	**NA**	**NA**	**NA**	**52**	**42**	IVP
Normal	≥0.71/0.70	≥0.69/0.54	≥0.67/0.68	≤ ±25	≤ ±30	

Gain values for the vestibuloocular reflex test as measured by head impulse testing in the SCC planes, horizontal right/left = horizontal plane, head movement toward right/left, respectively; RALP/LARP = plane of right anterior and left posterior SCC, down = head movement downward in the respective plane testing mainly for anterior SCC function and up testing mainly for posterior SCC function. Results of caloric tests are provided as CP (canal paresis factor) and DP (directional preponderance) according to the Jongkees formulas. Negative values represent hypofunction on the left horizontal SCC relative to the right horizontal SCC and preponderance of right beating nystagmus, respectively. Pathologic values are in bold and reduced gain values of the supposed intact side are in italic. NA, not available; PLF, perilymphatic fistula; IVP, idiopathic vestibulopathy.

Instruments, Delft, The Netherlands) (Ferman et al. 1987; Remmel 1984; Robinson 1963). The calibration procedure was described by Bergamin et al. (2001). Data were sampled at 1 kHz with 16-bit precision and peak-to-peak noise in the system was <0.2°, in all directions. Visual targets were produced by a laser and directed by a two-axis mirror galvanometer, which produced a 0.25° diameter target on a tangent screen, 1.25 m from the subject.

Procedure

We performed head impulse testing (Halmagyi et al. 1990) to determine the vestibuloocular reflex gain in all canal planes (horizontal, right-anterior left-posterior, left-anterior right-posterior) and for both directions of each plane (Hegemann et al. 2007; Schmid-Priscoveanu et al. 1999). Bithermal caloric vestibular testing with water at 44 and 30°C, respectively, was performed using a commercial caloric irrigator (Variotherm, ATMOS MedizinTechnik, Lenzkirch, Germany) and eye movements were recorded using a 50-Hz videooculography system (VisualEyes, Micromedical Technologies). Canal paresis factor and direction preponderance were calculated as relative differences in percentages in slow phase eye velocity using the Jongkees formulas (Jongkees et al. 1962). The canal paresis factor, the difference between left and right sides relative to the total response is defined as $100 \times [(W_L + C_L) - (W_R + C_R)]/(W_L + C_L + W_R + C_R)$, where W is warm, C is cold, and the subscripts refer to the side of stimulation. The directional preponderance, the relative difference between rightward and leftward nystagmus, is $100 \times [(W_R + C_L) - (W_L + C_R)]/(W_L + C_L + W_R + C_R)$. A canal paresis factor of ≥25% and a directional preponderance of ≥30% were regarded as pathologic.

Gaze-dependent changes in nystagmus were measured by instructing patients to look in darkness at a pulsed target that moved every 5 s in steps of 5 from 25° right to 25° left and back. The laser was pulsed (20 ms every 2 s) so that we could direct the patient's gaze direction without visually suppressing nystagmus. This was repeated at vertical elevations of 20° up and down.

Data analysis

Data were analyzed using programs written in MATLAB (The MathWorks, Natick, MA). Eye movements are described by rotation vectors and component velocity (Hepp 1990; Tweed et al. 1990) and we report the results in degrees and degrees per second. Component velocity, the derivative of position, is not the same as angular velocity (Haslwanter 1995; Hepp 1990). Data are presented in a head-fixed coordinate system, with positive rotations being clockwise, right, and up. We mirrored the horizontal and torsional data of the patients with right-side lesions, so all patients appear to have a left-side lesion (slow phase drift to the left). Saccades were identified and removed with an interactive computer program that first automatically detected saccades based on velocity and noise criteria (Holden et al. 1992) and then allowed the user to adjust the automatically marked saccades and to remove blink artifacts. Individual nystagmus slow phases were included in later analysis if they were ≥100 ms in duration. Short phases >200 ms were split into two or more shorter parts of ≥100 ms. We calculated for each slow phase the median position and velocity for each component (horizontal, vertical, and torsional). For some graphs we then averaged the slow phase properties for each target direction, although all quantitative analysis was made without averaging.

To characterize how velocity varied with horizontal and vertical eye position, we fit two equations to horizontal, vertical, and torsional velocities. First we fit a simple plane to the data

$$Vel_{(hvt)} = \beta_{0(hvt)} + \beta_{1(hvt)}H + \beta_{2(hvt)}V \quad (1)$$

where *Vel* is velocity and the subscripts refer to horizontal (*h*), vertical (*v*), and torsional (*t*) components; *H* is horizontal position; and *V* is vertical position. The bias component β_0 indicates the velocity at straight-ahead gaze ($V = H = 0°$). β_1 and β_2 (with units of 1/s) indicate the proportional change of velocity with horizontal and vertical eye position and, together, represent a plane. This fit is the two-dimensional extension of the traditional method of analyzing AL in one dimension with a straight line. In a second analysis, we fit the following second-order equation to horizontal, vertical, and torsional velocities

$$Vel_{(hvt)} = \beta_{0(hvt)} + \beta_{1(hvt)}H + \beta_{2(hvt)}V + \beta_{3(hvt)}HV + \beta_{4(hvt)}H^2 + \beta_{5(hvt)}V^2 \quad (2)$$

The equation can be visualized as representing a 3D, parabolic surface (see Figs. 3 and 4 for examples). The bias term β_0 indicates the velocity at straight-ahead gaze ($V = H = 0°$) and the terms β_1 and β_2 (with units of 1/s) indicate the proportional change of velocity with horizontal and vertical eye positions. An interaction between horizontal and vertical positions is represented by the β_3 term (units of 1/°s) and permits the plane to twist. The squared terms, β_4 and β_5 (1/°s), permit the surface to have a parabolic shape as a function of horizontal and vertical eye positions.

Both the plane and the second-order equations were fit to the velocity of each subject individually using standard multiple regression techniques, the 10% of the individual data points with the largest residual error were classified as outliers and removed, and the fitting procedure was repeated. The overall fit was evaluated with an F-test and we then tested for significant differences from 0 of the average parameters, across subjects, with *t*-test. Correlations between parameters were performed with Pearson's product-moment correlation coefficient.

To validate each fit, we performed a split-sample analysis. We randomly assigned each slow phase to one of two groups, performed the same fitting procedures described earlier to the first group, and computed the sample squared correlation (R^2). Next, we used the fitted equation to predict the values from the second group and computed the squared correlation between the predicted and the observed data. The difference between these R^2 values, called *shrinkage*, will be small for reliable fits, with a shrinkage value of ≤ 0.1 generally indicating a reliable model (Kleinbaum et al. 1988).

An integrator time constant can be inferred from the fitted equations by -1/slope. For the plane fits, the slope is given directly as the fitted parameters (see *Eq. 1*). For the second-order fits, the slope can be found with the partial derivatives of *Eq. 2*

$$\frac{\partial Vel_{(hvt)}}{\partial H} = \beta_{1(hvt)} + \beta_{3(hvt)}V + 2\beta_{4(hvt)}H \quad (3)$$

$$\frac{\partial Vel_{(hvt)}}{\partial V} = \beta_{2(hvt)} + \beta_{3(hvt)}H + 2\beta_{5(hvt)}V \quad (4)$$

which describe how velocity varies with horizontal (*Eq. 3*) and vertical (*Eq. 4*) eye positions. A positive time constant indicates a leaky integrator and a negative time constant an unstable integrator. To provide additional statistical support for these results, we split the data into halves (left and right for horizontal velocity and up and down for vertical velocity), fit separate planes to each half, and evaluated weather the slopes were different from zero for each subject with *t*-tests.

We analyzed the direction of nystagmus by decomposing the 3D eye velocity vector into two angles. We first projected the 3D velocity vector onto the plane defined by the horizontal and vertical components and calculated the angle of the projection in this plane. This angle varies from 0° (upward vertical velocity, with no horizontal component), to 90° (leftward, with no vertical component), to 180° (downward), and to 270° (rightward). Likewise, we projected the vector onto the plane defined by the horizontal and torsional components, which gives an angle related to the horizontal/torsional direction: 0° is clockwise torsion, 90° is leftward, 180° is counterclockwise, and 270° is rightward. When analyzed as a function of gaze position, this analysis shows how the direction of nystagmus, independent of the speed, varies with gaze position. We fit the same plane and second-order functions described earlier to characterize how the direction of nystagmus varied with eye position.

RESULTS

Patient characteristics

Table 1 shows the results of head impulse and caloric testing for each patient. In patient 11 the tape that fixed the coil to the forehead loosened due to severe sweating of the patient, which makes his head impulse results unreliable. In four patients, caloric vestibular testing could not be performed because of a perilymphatic fistula (patient 1) or severe nausea (patients 2, 3, and 8). Patient 7 showed a right beating nystagmus but had reduced right vestibular function during both head impulse and caloric testing, the latter being performed 1 day after the head impulse test. A central lesion was excluded by magnetic resonance imaging. The patient recovered completely from nystagmus as well as vertigo and unsteadiness within 3 days. We interpret this "paradox" nystagmus as a so-called recovery nystagmus. Since the nystagmus was right beating as in left-sided unilateral vestibular deafferentation (UVD), however, we analyzed it as a left UVD.

Example nystagmus patterns

Patients typically had nystagmus with slow phases directed to the left, down, and counterclockwise when looking straight ahead. As exceptions, two patients had upward drift. Figure 2 shows example eye position traces in one patient (4) who followed the flashing laser spot as it moved from left to right with gaze at zero elevation (*A*), 20° up (*B*), and 20° down (*C*). The *inset* in Fig. 2*A* magnifies the horizontal component when the patient looked left, straight ahead, and to the right, which more clearly shows the greater nystagmus when the patient was looking to the right.

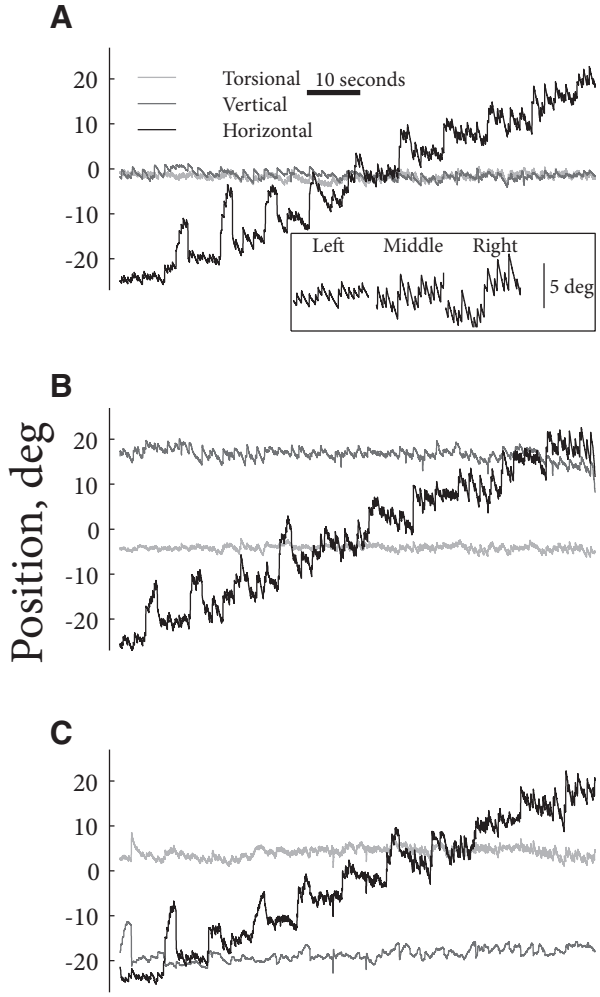

FIG. 2. *A*: example eye-position traces from patient 4. Each panel shows horizontal (bold), vertical (medium), and torsional (light) eye positions as the patient tracked a flashing laser spot (not shown) that moved from left to right in 5° steps. In *A*, gaze elevation was about straight ahead, whereas in *B* gaze was about 20° down and in *C* about 20° up. The *inset* in *A* shows horizontal eye position, magnified, when gaze was left, straight ahead, and to the right.

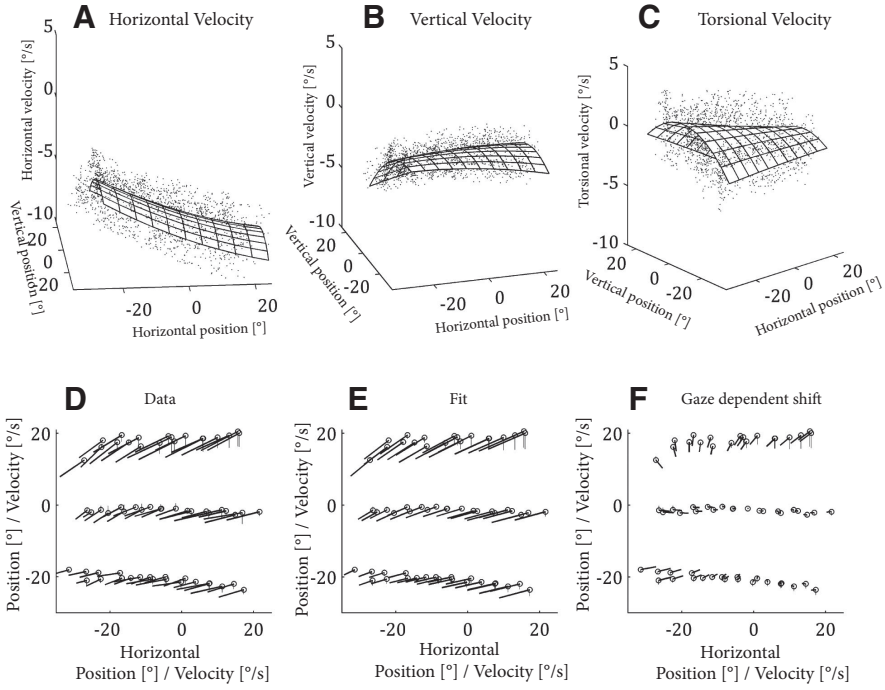

FIG. 3. Example eye velocity in patient 6. The median horizontal (*A*), vertical (*B*), and torsional (*C*) velocities of individual slow phases (●) is plotted against horizontal and vertical eye positions. The best-fit 2nd-order surface is also shown. *D*: a summary of the 3-dimensional (3D) drift is shown for the same subject. Each circle indicates the average horizontal and vertical positions for the slow phase eye movements during each fixation period (5-s duration). The thick line shows the horizontal and vertical velocities, and so the orientation of the line indicates direction (e.g., a line pointing down and to the left shows downward and leftward velocity) and the length represents the speed. Thin lines show torsional velocity, with an upward line indicating clockwise velocity and a downward line indicating counterclockwise velocity. *E*: the fitted values of the best-fit 2nd-order surface. *F*: gaze-dependent changes in drift velocity, which was found by subtracting the fitted drift at straight ahead from fitted drift at all other gaze positions.

Figure 3 shows a summary of the results of another patient (6). Figure 3, *A–C* shows median eye velocity of individual slow phases as a function of horizontal and vertical eye positions, along with the best-fit second-order equation (*Eq. 2*). Figure 3*D* combines the 3D velocity components into a single figure. In this plot, we averaged the eye movement data in each 5-s period where the flashing fixation light was in the same position. Each circle indicates the average horizontal and vertical positions. The thick line shows the horizontal and vertical velocities, and so the orientation of the line indicates direction and the length represents the speed. Thin lines show torsional velocity, with an upward line indicating clockwise velocity and a downward line indicating counterclockwise velocity. Here the overall pattern of the change in nystagmus is more evident than that in the plots in Fig. 3, *A–C*, although these provide a more intuitive view of the fitted surface.

In Fig. 3, *A* and *D*, a change in horizontal eye velocity with horizontal eye position is seen that is consistent with AL, with velocity increasing when the subject looked in the fast phase direction (to the right). The best-fit planes to the data are

$$Vel_h = -7.5 - 0.095H - 0.058V$$

$$Vel_v = -2.9 - 0.0015H - 0.077V$$

$$Vel_t = -1.5 - 0.045H - 0.014V$$

Thus horizontal velocity varies more with horizontal than with vertical position, vertical velocity varies more with vertical than with horizontal position, and torsional velocity varies more with horizontal than with vertical position.

The second-order fits provide a more detailed analysis of how velocity changes with position. The best-fit second-order surface for horizontal velocity for this patient, shown in Fig. 3*A*, is

$$Vel_h = -7.2 - 0.087H - 0.058V + 0.00044HV + 0.00094H^2 - 0.0023V^2$$

All the fitted parameters were significantly different from 0 with all P values <0.01. Horizontal velocity was $-7.2°/s$ at straight ahead. The change in velocity with horizontal position was determined mainly by the linear component, with a value of $-0.087°\cdot s^{-1}\cdot deg^{-1}$. Nonetheless, the second-order term, H^2, was still significant. This indicates that the rate of change in velocity changes at different gaze positions, which is more obvious when considering the partial derivative of the fitted function with respect to horizontal position

$$\frac{\partial Vel_h}{\partial H} = -0.087 + 0.00044V + 0.0019H$$

With gaze straight ahead ($H = V = 0°$), the change of horizontal eye velocity is $-0.087°\cdot s^{-1}\cdot deg^{-1}$, and with $V = 0°$, at 20° left and right, the change is -0.12 and $-0.049°\cdot s^{-1}\cdot deg^{-1}$, respectively. Thus velocity changed the most in left gaze (the slow phase direction). Horizontal velocity also changed with vertical eye position in this patient. In particular, the V^2 term (-0.0023) shows that horizontal velocity increased when this patient looked up and down. The partial derivative with respect to vertical position is

$$\frac{\partial Vel_h}{\partial V} = -0.058 + 0.0004H - 0.0045V$$

so the rate of change of horizontal eye velocity with $H = 0°$ and with vertical positions of 20, 0, and $-20°$ was -0.15, -0.058, and $0.033°\cdot s^{-1}\cdot deg^{-1}$, respectively.

Figure 3*B* shows how vertical velocity varied with eye position in the same patient. Vertical eye velocity increased when the patient looked up, but velocity for down gaze was similar to that at gaze straight ahead. This is consistent with AL, with velocity being highest in the fast phase direction (up). The best-fit function was

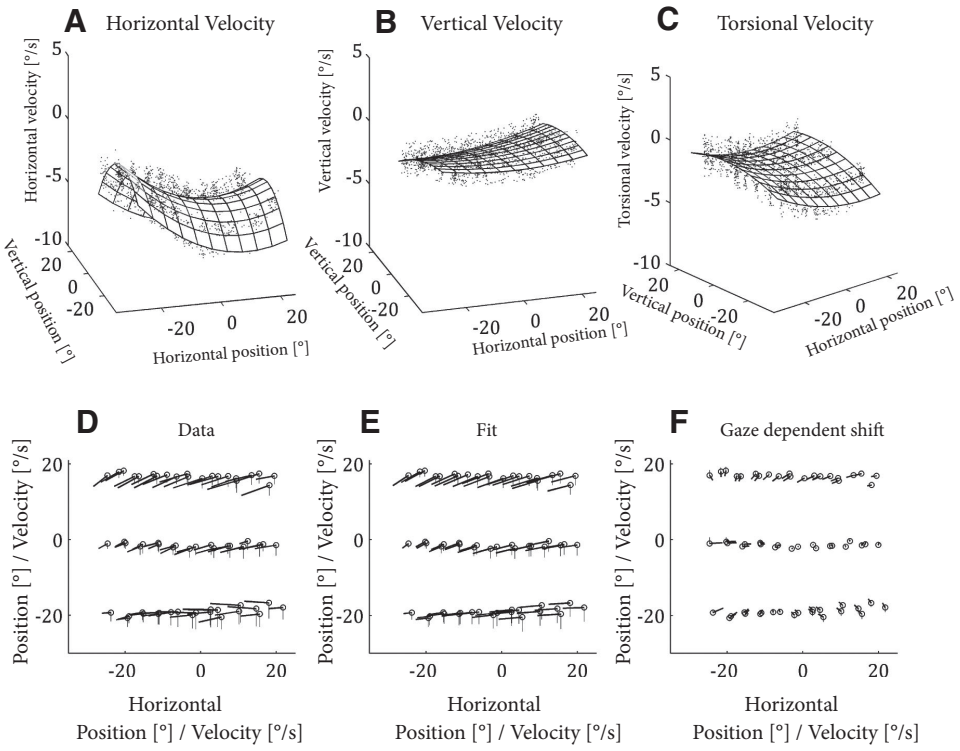

FIG. 4. Example eye velocity in patient 4. The median horizontal (*A*), vertical (*B*), and torsional (*C*) velocities of individual slow phases (●) is plotted against horizontal and vertical eye positions. The best-fit 2nd-order surface is also shown. *D*: a summary of the 3D drift is shown for the same subject. Each circle indicates the average horizontal and vertical positions for the slow phase eye movements during each fixation period (5-s duration). The thick line shows the horizontal and vertical velocities, and so the orientation of the line indicates direction (e.g., a line pointing down and to the left shows downward and leftward velocity) and the length represents the speed. Thin lines show torsional velocity, with an upward line indicating clockwise velocity and a downward line indicating counterclockwise velocity. *E*: the fitted values of the best-fit 2nd-order surface. *F*: gaze-dependent changes in drift velocity, which was found by subtracting the fitted drift at straight ahead from fitted drift at all other gaze positions.

$$Vel_v = -2.2 + 0.0016H - 0.080V + 0.0012HV - 0.00055H^2 - 0.0024V^2$$

and all parameters except the H term were significantly different from 0 (all P values <0.01). Note that the small change in vertical velocity in down gaze, compared with the much larger change in up gaze, is captured in the equation with a combination of the V and V^2 terms. The rate changes in vertical velocity with vertical and horizontal positions are

$$\frac{\partial Vel_v}{\partial V} = -0.080 + 0.0012H - 0.0048V$$

and

$$\frac{\partial Vel_v}{\partial H} = 0.0016 + 0.0012V - 0.0011H$$

Thus in this patient, vertical velocity varies more with vertical than with horizontal position. Figure 3*C* shows torsional velocity in this patient, which followed a similar pattern to the changes in vertical velocity in that velocity increased considerably in up gaze but was relatively unchanged in down gaze. Torsional velocity at straight ahead gaze and in down gaze was about zero, but increased to around −5°/s in up gaze. The best-fit equation is

$$Vel_t = -0.3 - 0.053H - 0.039V - 0.0024HV - 0.00012H^2 - 0.0043V^2$$

and all parameters were significantly different from zero (all P values <0.01), except the H^2 term. Torsional velocity varies slightly with both horizontal and vertical positions and this is reflected in the changes in velocity with vertical and horizontal gaze positions

$$\frac{\partial Vel_t}{\partial V} = -0.04 - 0.0024H - 0.0086V$$

and

$$\frac{\partial Vel_t}{\partial H} = -0.053 + 0.0024V - 0.0002H$$

Figure 3*E* shows the fitted velocity values at the same eye positions, as in Fig. 3*D*. In Fig. 3*F*, we subtracted the velocity at gaze straight ahead (the biases in the best-fit equations) from the fitted values in Fig. 3*E*, which more clearly shows how eye velocity changes with gaze position. There is considerable gaze-evoked nystagmus in left and up gaze, but less of a change down and to the right.

Figure 4 shows an example from a different patient (4), where the horizontal velocity decreases both to the left and right of gaze straight ahead, but increases in up and down gaze. The best-fit plane equations for this patient's data are

$$Vel_h = -5.3 - 0.071H - 0.0041V$$

$$Vel_v = -1.4 + 0.012H - 0.054V$$

$$Vel_t = -2.6 - 0.035H + 0.025V$$

and the best-fit second-order equations are

$$Vel_h = -4.9 - 0.052H - 0.0043V + 0.0010HV + 0.0033H^2 - 0.0046V^2$$

$$Vel_v = -1.4 + 0.016H - 0.053V + 0.00067HV + 0.00085H^2 - 0.00073V^2$$

$$Vel_t = -2.6 - 0.031H + 0.024V + 0.00052HV + 0.0013H^2 - 0.0013V^2$$

Quality of the fitted surfaces

The plane surface fits were highly significant for all patients (overall F-test, all P values $\ll 0.001$). A substantial amount of variation was nonetheless not accounted for by the regression. The mean R^2 values were 0.43, 0.39, and 0.25 for horizontal, vertical, and torsional velocities, respectively. Shrinkage values were low, averaging 0.02, or about 6% of the mean R^2, indicating reliable fits.

Likewise, the fitted second-order surfaces were also highly significant in all cases (F-test, all P values $\ll 0.001$), although again much of the variation in the data was not accounted for by the regression. The second-order fits accounted for about 28% more of the variance than the plane fits. For horizontal velocity, R^2 varied from 0.22 to 0.86, with a mean of 0.56. The mean R^2 for the fits to vertical velocity was 0.48, ranging from 0.15 to 0.77, and the mean torsional R^2 was 0.42 and varied from 0.15 to 0.64. Shrinkage values were also low, indicating reliable fits, averaging 0.03, or about 5% of the mean R^2.

Dependence of horizontal velocity on gaze position

All patients showed significant horizontal drift to the left at straight ahead gaze. The average plane and second-order fits are shown in Table 2. The plane fits indicated an average velocity at straight ahead gaze of −10.04°/s. Ten of 11 patients had a negative slope relating horizontal velocity to horizontal gaze position, which is in accord with AL, and indicates that velocity was higher in the fast phase direction. The average slope of −0.088 corresponds to an integrating time constant of 11 s. There was no consistent change of horizontal velocity with vertical eye position.

For the second-order fits, which provide a more detailed examination of the change of velocity with position, the average bias was −10.35°/s (Table 2; see also Fig. 5). Ten of 11 patients had a negative slope relating horizontal velocity to horizontal gaze position. Eight of the 11 patients also showed a significant, positive H^2 term, with a mean value of 0.003. Positive H^2 indicates a concave up surface that, when combined with the negative H term, reduces horizontal velocity in the fast phase direction compared with that if the term is 0. The average HV, V, and V^2 terms were not significantly different from zero, indicating that, across patients, horizontal velocity did not depend on vertical eye position. Note, however, that for individual patients these parameters were usually significantly different from zero, although the signs were not consistent.

Differentiating the average second-order function fitted to the horizontal eye velocity with respect to horizontal position gives

$$\frac{\partial Vel_h}{\partial H} = -0.054 + 0.00018V - 0.0059H$$

Thus at gaze straight ahead ($V = H = 0°$), the change of horizontal velocity with horizontal position (or slope of the fitted function) is $-0.054°\cdot s^{-1}\cdot deg^{-1}$; at 20° left (the slow phase direction), the slope is $-0.17°\cdot s^{-1}\cdot deg^{-1}$ and at 20° right (the fast phase direction), the slope is $0.064°\cdot s^{-1}\cdot deg^{-1}$. These slopes correspond to time constants of 6, 18, and −16 s for 20° in the slow phase direction, straight ahead, and 20° in the fast phase direction, respectively. The position at which the slope changes sign is 9.2° to the right. So, on average, the gaze-dependent drifts suggest the NI is leaky in the slow phase direction, but becomes unstable at >9° in the fast phase direction. Separate plane fits to horizontal velocity in left and right gaze provide statistical support for these changes in the time constant. In left gaze, all 11 patients showed a significant ($P < 0.05$) negative slope of velocity versus position. In right gaze, 5 patients had a significant negative slope, 4 had significant positive slopes, and 2 showed slopes that were not significantly different from zero.

TABLE 2. *Average best-fit parameters across all subjects*

Parameter	Horizontal Velocity	Vertical Velocity	Torsional Velocity
	A. Plane fits		
Bias	−10.04** (+0/−11)	−2.06** (+2/−9)	−4.40* (+0/−11)
H	−0.088** (+1/−10)	−0.0074** (+3/−4)	−0.042** (+0/−11)
V	−0.027 (+4/−7)	−0.037** (+1/−9)	0.014† (+6/−2)
R^2	0.43	0.39	0.25
	B. Second-order fits		
Bias	−10.35** (+0/−11)	−1.82** (+2/−9)	−4.31* (+0/−11)
H	−0.054* (+1/−10)	−0.0020 (+4/−5)	−0.030** (+2/−9)
V	−0.026 (+3/−8)	−0.046* (+1/−9)	0.016 (+7/−3)
HV	0.00018 (+7/−4)	−0.00003 (+5/−5)	−0.00005 (+6/−5)
H^2	0.0030* (+8/−0)	0.00051† (+8/−3)	0.0015 (+7/−3)
V^2	−0.00054 (+5/−6)	−0.0020* (+1/−9)	−0.0021 (+3/−8)
R^2	0.56	0.48	0.42

The numbers in parentheses indicate the number of patients for which that parameter was significantly different from 0 ($P > 0.05$) in the position and negative directions. For example, for plane fits, all 11 patients had a significant horizontal bias <0. **$P < 0.01$, *$P < 0.05$, †$P < 0.1$.

Dependence of vertical velocity on gaze position

At straight ahead gaze, 9 of the 11 patients showed downward drift and 2 showed upward drift. From the best-fit plane (Table 2), 9 patients showed a negative change in vertical velocity with vertical eye position, with an average slope of −0.037 (time constant = 27 s). This indicates that velocity increased in the fast phase direction of nystagmus, in accord with AL, although the long time constant is in the normal range (>20 s; Cannon and Robinson 1987; Goltz et al. 1997). There was not a consistent change of vertical velocity with horizontal position.

For the second-order fits, 9 of the 11 patients showed a significant negative relationship between vertical velocity and position. Nine of the patients also showed a significant negative V^2 term. As shown in Fig. 5*B*, this is concave down, meaning that, when combined with the negative V-term, vertical velocity increases in the fast phase direction compared with that if the term is 0. Eight patients also showed a significant dependence of vertical velocity on H^2, with an average value of 0.00051, which was not quite significantly different from zero ($P < 0.1$).

Differentiating the average function fit to the vertical eye velocity with respect to vertical position gives

$$\frac{\partial Vel_v}{\partial V} = -0.046 + 0.00003H - 0.0040V$$

Thus at gaze straight ahead, the rate of change of vertical velocity with vertical position is $-0.046°\cdot s^{-1}\cdot deg^{-1}$ (time

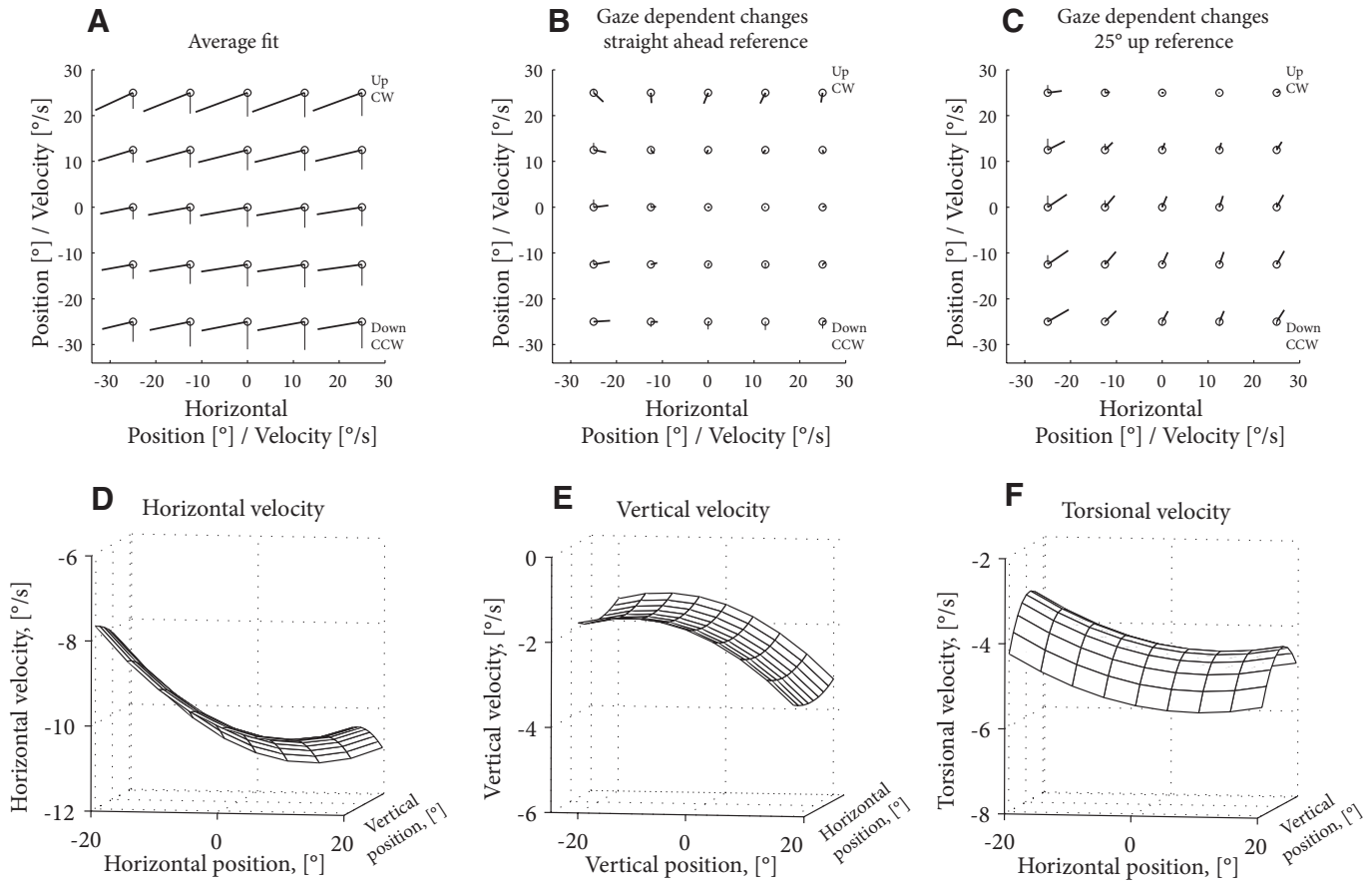

FIG. 5. *A*: the average 2nd-order surface fits, with the same format as that of Fig. 3*D*. *B*: gaze-dependent changes in drift velocity, which was found by subtracting the fitted drift at straight ahead from fitted drift at all other gaze positions. *C*: gaze-dependent changes in drift velocity, which was found by subtracting the fitted drift at 25° up from all other gaze positions. See DISCUSSION for details. *D–F*: the average 2nd-order surface fits, shown as surfaces.

constant = 22 s); at 20° in the slow phase direction the slope is $0.035°\cdot s^{-1}\cdot deg^{-1}$ (time constant = −29 s) and at 20° in the fast phase direction the slope is $-0.12°\cdot s^{-1}\cdot deg^{-1}$ (time constant = 8 s). The position where the partial derivative changes sign is −11° into the slow phase direction. So, on average, the NI is leaky in the fast phase direction, but is unstable in the slow phase direction. Note that this is the opposite of the pattern seen for horizontal velocity.

Separate plane fits to vertical velocity in down and up gaze also provide support for these findings of a change in the NI time constant. In up gaze, 10 of 11 patients showed a significant ($P < 0.05$) negative slope of velocity versus position and one had a significant positive slope. In down gaze, 6 patients had a significant negative slope and 5 had significant positive slopes.

Dependence of torsional velocity on gaze position

According to the average plane fits, all 11 patients had counterclockwise torsion at gaze straight ahead, with a mean of −4.4°/s (Table 2). Plane fits also revealed a highly significant dependence of torsional velocity on horizontal position, with an average slope of −0.042 (Table 2). A marginally significant dependence on vertical position was also found (slope = 0.014, $P < 0.1$).

Second-order fits found an average torsional velocity at gaze straight ahead of −4.31°/s and all 11 patients showed a statistically significant torsional bias (Table 2; see also Fig. 5). Torsional velocity was significantly dependent on horizontal position, with 9 of the 11 patients showing a significant negative slope, with a grand mean of $-0.03°\cdot s^{-1}\cdot deg^{-1}$. Torsional velocity did not consistently depend on any of the other parameters.

Summary of changes in 3D nystagmus

Figure 5*A* shows the average second-order fits and Fig. 5, *D–F* shows the same fits as in Fig. 5*A* plotted as 3D surfaces. Velocity was predominately to the left with smaller downward and counterclockwise components. Figure 5*B* shows the gaze-dependent changes in velocity. Most of the gaze-dependent changes occur in left and up gaze, whereas in right gaze there is not much of a gaze-evoked component.

We tested whether the change of eye velocity was related to the magnitude of the vestibular nystagmus. We used the bias of the second-order fit as an estimate of the vestibular contribution to the nystagmus and computed the slope of the second-order fitted equation for each subject at straight ahead and ±20° in the fast and slow phase directions of the horizontal and vertical nystagmus. The horizontal slope of the function at −20° left (slow phase direction) was significantly correlated with the horizontal bias (correlation = 0.82, $P < 0.01$), whereas there was a significant negative correlation at 20° right gaze (correlation = −0.74, $P < 0.01$); the correlation at

straight ahead was not significant (correlation = 0.11, $P > 0.5$) (Fig. 6). The slope in the slow phase direction was less than the slope in the fast phase direction in all but two patients and in seven patients the slope became positive. We did not find significant correlations between the vertical bias and the vertical or torsional slopes, nor between the horizontal bias and the torsional slopes.

Nystagmus direction changed as a function of gaze direction, as indicated in the average fit in Fig. 5*B*, as well as the examples in Figs. 3*D* and 4*D*. We analyzed the direction change by decomposing the 3D eye velocity vector into two angles. We first projected the 3D velocity vector onto the planes defined by the horizontal and vertical components, and the planes defined by the horizontal and torsional components, and calculated the angles of the projections onto these planes (see METHODS). We then fit *Eqs. 1* and *2* to these angles for each patient, the average fits of which are shown in Table 3. (For the second- order fit, the horizontal–vertical angle is shown directly in Fig. 5*B* in the lines showing the horizontal and vertical velocities.) The bias indicates the slow phase direction at straight ahead gaze. The plane and second-order fits give similar results, with both angles depending mainly on vertical position (only marginally significant in the case of the horizontal–torsional angle). For the horizontal–vertical angle, the V^2 term was also marginally different from zero.

TABLE 3. *Average best-fit parameters to nystagmus direction*

Parameter	HV Angle	HT Angle
	A. Plane fits	
Bias	103°** (+11/−0)	112°** (+11/−0)
H	−0.063 (+4/−7)	0.041 (+8/−2)
V	0.21** (+9/−1)	−0.14† (+3/−7)
R^2	0.33	0.27
	B. Second-order fits	
Bias	101°** (+11/−0)	110°** (+11/−0)
H	−0.069 (+4/−7)	0.056 (+8/−3)
V	0.25** (+10/−1)	−0.13† (+3/−7)
HV	−0.00048 (+5/−5)	0.0036 (+8/−2)
H^2	0.00015 (+6/−4)	0.00097 (+4/−3)
V^2	0.012† (+8/−3)	0.012 (+5/−5)
R^2	0.44	0.41

Nystagmus direction is characterized by two angles. The 3D velocity vector was projected on the planes defined by the horizontal and vertical components, and the plane defined by the horizontal and torsional components and the angles in the planes were calculated. For the horizontal–vertical (HV) angle, the nystagmus direction angle varies from 0° (upward vertical velocity, with no horizontal component), to 90° (leftward, with no vertical component), to 180° (downward), and to 270° (rightward). Likewise, for the horizontal–torsional (HT) angle, 0° is clockwise torsion, 90° is leftward, 180° is counterclockwise, and 270° is rightward. The numbers in parentheses indicate the number of patients for which that parameter was significantly different from 0 ($P > 0.05$) in the position and negative directions. **$P < 0.01$, *$P < 0.05$, †$P < 0.1$.

DISCUSSION

We measured the effect of horizontal and vertical gaze shifts on the 3D velocity of nystagmus in patients with an acute vestibular asymmetry and we characterized the change of velocity with eye position with plane and second-order functions. In all patients the fits were highly significant. All patients showed AL for horizontal velocity, with velocity being higher in the fast phase compared with that in the slow phase direction. In addition, the second-order term for horizontal position was significant in most (8/11) patients, with the result that velocity did not increase in the fast phase direction as rapidly as expected from a linear relationship.

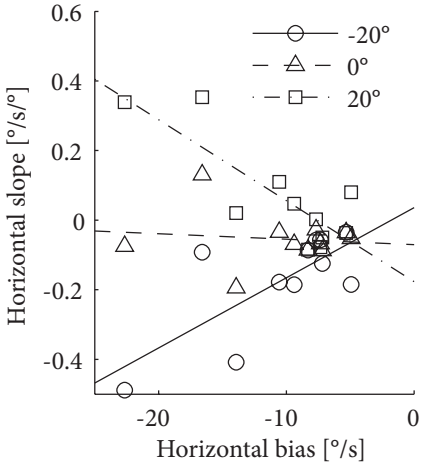

FIG. 6. Correlations between horizontal nystagmus at straight ahead gaze and the change of horizontal eye velocity with eye position. The change of horizontal velocity with horizontal position was computed for left (−20°), right (20°), and straight ahead gaze. Each symbol indicates a single patient and the lines are the best linear fits for each direction.

If we assume that the elastic equilibrium point of the eye in the orbit (null point of the eye) is near straight ahead, the gaze-dependent drifts suggest the horizontal NI is leaky in the slow phase direction; beyond 10° in the fast phase direction, however, the NI is on average unchanged. Some patients even showed an unstable NI in the fast phase direction. Although individual patients usually had a significant dependence of horizontal velocity on vertical position, the direction of the dependence was not consistent.

Vertical velocity also depended on both vertical position and its square. Overall, vertical velocity varied in accord with AL, with velocity being higher in the fast phase direction. Torsional velocity depended mostly on horizontal position.

The change of horizontal velocity with horizontal position was correlated with the horizontal bias (Fig. 6*A*), which could be expected if AL is an adaptive mechanism sensitive to the magnitude of nystagmus. Similar correlations were not found for vertical and torsional velocities, although the velocity of these components is small, making detection of any correlation difficult.

The direction of nystagmus, independent of the speed, changes as a function of vertical eye position. If AL in 3D was due to a single mechanism operating on the magnitude of the nystagmus, we would expect proportional changes in velocity in all components and no change in nystagmus direction. The fact that nystagmus direction changes suggests that the changes in slow phase velocity are not due to a single mechanism, but rather, that the horizontal, vertical, and torsional NIs operate separately to modify the different 3D components.

A comparison of the plane and second-order fits shows that the second-order fits account for about 28% more of the variance in the data (since the plane fits are nested within the higher-order fits, the higher-order fits must account for at least as much of the variance). Clearly, though, the linear compo-

nents are important contributors to the change of velocity, as expected from AL.

Our paradigm is not capable of determining the neural locus of the changes in the oculomotor system, although cerebellar structures known to be important for NI performance (flocculus and paraflocculus; Zee et al. 1981) are likely candidates. It is also possible that other neural structures, particularly those that receive inputs for the NIs, might also be changing as a result of the altered vestibular input.

Vertical Alexander's law

In our patients, vertical eye velocity varied with vertical position in a manner similar to the classically defined Alexander's law for horizontal nystagmus, that is, velocity was highest in the fast phase direction. Vertical AL has been described for patients with downbeat nystagmus resulting from cerebellar lesions (Glasauer et al. 2003; Straumann et al. 2000), as well as in normal subjects with pursuit afternystagmus (Marti et al. 2005). In our patients, vertical velocity was lowest in down gaze, where reducing nystagmus may improve vision during walking and reading.

If we take drift velocity at straight ahead gaze as a reference, vertical eye velocity in the fast phase direction increased, whereas velocity in the slow phase direction was unchanged. This is different from what occurs for horizontal velocity, where velocity decreases in the slow phase direction and is relatively unchanged in the fast phase direction (compare Fig. 5, *D* and *E*). Assuming the NI is responsible for the gaze-dependent changes, and that the elastic equilibrium point is near straight ahead, this suggests the vertical NI changes are maladaptive. However, shifting the equilibrium point upward (~25°) would result in a drift pattern more consistent with an adaptive mechanism—i.e., the NI becomes leaky in down gaze to reduce drift velocity (see Fig. 5*C*). Thus changing the reference position causes the gaze-dependent drift patterns for horizontal and vertical to become more similar, suggesting the horizontal and vertical NIs react similarly to altered vestibular input. Although there have been a few studies of the viscoelastic properties of the orbit in the horizontal (Robinson 1964; Sklavos et al. 2005, 2006) and torsional (Seidman et al. 1995) directions, little is known for vertical movements, and the actual location of equilibrium point is unknown. Shifting the null point, however, does not account for why the shape of the fitted velocity function was concave down, whereas the surface for horizontal was concave up. One possibility is that the velocity when looking down (<2°/s) is low enough to be compensated by visually guided eye movements, and so there was no pressure for adaptive NI changes. Also, although the reactions of the horizontal and vertical NIs appear different, their velocity inputs due to the vestibular lesions in our patients also differ. A left-sided lesion will reduce the input for head turns to the left due to the reduced input from the left horizontal canal, but because both the posterior and anterior canal inputs could be affected, the velocity inputs for both upward and downward movements could also be influenced. Whether the vertical and horizontal NIs respond in a similar fashion in patients with nystagmus therefore remains an open question.

Torsion

Torsional velocity could be expected to vary in a manner similar to that of vertical velocity, since the vertical and torsional NIs share a common neurological location. However, we found that torsional velocity varied mostly with horizontal position, with the lowest velocity being in the horizontal slow phase direction. This implies an independence of the vertical and torsional NIs.

The reason torsion varied with horizontal position is not clear; conceivably, the torsional NI could be sensitive to horizontal position and thus the torsional velocity is modified with horizontal position. Static torsional position varies with horizontal position when the head is pitched backward and forward (Bockisch and Haslwanter 2001; Furman and Schor 2003; Haslwanter et al. 1992) and, if this torsional command passes through the torsional NI, then this NI must therefore be sensitive to horizontal position.

We did not compare torsional velocity with torsional position because of the technical difficulties in measuring small changes of torsional position (coil slippage; Bergamin et al. 2004; Bockisch and Haslwanter 2001). It is thus possible that the torsional modulation we see is actually due to a correlation with torsional position that varies with horizontal position.

Neural integrator time constant depends on gaze direction

The prominent second-order components for horizontal and vertical velocities show that velocity was not proportional to gaze position. Robinson's classic explanation of AL in the horizontal direction was that the NI became "leaky," thereby producing a centripetal nystagmus that superimposed with the vestibular-evoked nystagmus. This would reduce gaze velocity in one direction, but increase velocity in the opposite. Although some of our patients did show the increase in velocity, others showed a prominent decrease and, on average, there was little change in velocity in the horizontal nystagmus fast phase direction. These results suggest that the NI becomes leaky in the slow phase direction, but can be leaky, unchanged, or unstable in the fast phase direction. Becoming unstable in the fast phase direction is the most adaptive response in terms of reducing slow phase velocity.

Differential adaptation can be explained if the NI can maintain different integrating time constants depending on gaze direction, as suggested by Chan and Galiana (2005, 2007) in humans and Mensh et al. (2004) in goldfish. Cannon et al. (1983) originally proposed a related idea, of functionally independent NIs that are sensitive to different gaze directions, and Crawford and Vilis (1993) proposed multiple vertical–torsional NIs based on pharmacological inactivation studies. More recently, Aksay et al. (2007) provided evidence for separate horizontal NIs in goldfish when they pharmacologically lesioned the NI unilaterally and found impaired fixation over only half the oculomotor range.

Null point of the NI

We have interpreted the gaze-dependent changes in velocity in terms of the NI time constant, although changes in the NI null point (the NI's representation of the eye position where the elastic forces of the plant pull the eye) could contribute to the results. Glasauer et al. (2003) concluded that the NI null point

could shift, in addition to changes in the time constant, in patients with downbeat nystagmus. This was predicated on the assumption, based on Crawford et al. (1994), that the NI null point coincides with primary position. Our patients had torsional nystagmus and their eye movements violated Listing's law, and so primary position could not be reliably determined.

Shifting the null point will result in a force command that is insufficient to maintain gaze position in the direction of the null point shift and will produce a command too large in the opposite direction. Thus the NI would appear leaky in the direction of the null point shift and unstable in the opposite direction. To explain our horizontal data, the NI null point shift would have to be to the left, into the slow phase direction. A shift in the null point would result in a change of the constant background activity of the NI that, in our patients with vestibular lesions, would shift the position where the rate of change of eye velocity changes sign. This eye position was about 9° into the fast phase direction for horizontal velocity and about 11° into the slow phase direction for vertical velocity.

Conclusion

We have shown that patients with 3D nystagmus caused by a peripheral vestibular lesion develop eye-position–dependent drift that affects horizontal, vertical, and torsional velocity components. Regression analysis found that horizontal velocity varied with horizontal, but not vertical, position. The significant second-order term indicates that the time constant of the horizontal NI can decrease in one gaze direction, while increasing or remaining unchanged in a different gaze direction. Vertical velocity also varied with vertical position and the results suggest the vertical NI also appears able to adapt differentially to gaze direction. Torsional velocity varied with horizontal position, an effect that we cannot explain. Our results also show that the oculomotor NIs cannot be characterized by a single time constant, but rather can maintain different integrating time constants depending on gaze direction.

ACKNOWLEDGMENTS

We thank I. Olasagasti for insightful discussions; T. Haslwanter for programming assistance; T. Schmückle Meier, E. Schafflützel, and E. Buffone for assistance with patient evaluation and data collection; and A. Züger for technical help.

GRANTS

This work was supported by the Betty and David Koetser Foundation for Brain Research (Zurich, Switzerland) and the Swiss National Science Foundation.

REFERENCES

Aksay E, Olasagasti I, Mensh BD, Baker R, Goldman MS, Tank DW. Functional dissection of circuitry in a neural integrator. *Nat Neurosci* 10: 494–504, 2007.

Alexander G. Die Ohrenkrankheiten im Kindesalter. In: *Handbuch der Kinderheilkunde*, edited by Schlossmann A. Leipzig, Germany: Vogel, 1912, p. 84–96.

Bergamin O, Ramat S, Straumann D, Zee DS. Influence of orientation of exiting wire of search coil annulus on torsion after saccades. *Invest Ophthalmol Vis Sci* 45: 131–137, 2004.

Bergamin O, Zee DS, Roberts DC, Landau K, Lasker AG, Straumann D. Three-dimensional Hess screen test with binocular dual search coils in a three-field magnetic system. *Invest Ophthalmol Vis Sci* 42: 660–667, 2001.

Bockisch CJ, Haslwanter T. Three-dimensional eye position during static roll and pitch in humans. *Vision Res* 41: 2127–2137, 2001.

Cannon SC, Robinson DA. Loss of the neural integrator of the oculomotor system from brain stem lesions in monkey. *J Neurophysiol* 57: 1383–1409, 1987.

Cannon SC, Robinson DA, Shamma S. A proposed neural network for the integrator of the oculomotor system. *Biol Cybern* 49: 127–136, 1983.

Chan WW, Galiana HL. Integrator function in the oculomotor system is dependent on sensory context. *J Neurophysiol* 93: 3709–3717, 2005.

Chan WW, Galiana HL. A non-linear model of the neural integrator in oculomotor control. *Proc IEEE Eng Med Biol Soc* 1: 1156–1159, 2007.

Crane BT, Tian J, Demer JL. Temporal dynamics of ocular position dependence of the initial human vestibulo-ocular reflex. *Invest Ophthalmol Vis Sci* 47: 1426–1438, 2006.

Crawford JD. The oculomotor neural integrator uses a behavior-related coordinate system. *J Neurosci* 14: 6911–6923, 1994.

Crawford JD, Vilis T. Modularity and parallel processing in the oculomotor integrator. *Exp Brain Res* 96: 443–456, 1993.

Doslak MJ, Dell'Osso LF, Daroff RB. A model of Alexander's law of vestibular nystagmus. *Biol Cybern* 34: 181–186, 1979.

Doslak MJ, Dell'Osso LF, Daroff RB. Alexander's law: a model and resulting study. *Ann Otol Rhinol Laryngol* 91: 316–322, 1982.

Ferman L, Collewijn H, Jansen TC, Van den Berg AV. Human gaze stability in the horizontal, vertical and torsional direction during voluntary head movements, evaluated with a three-dimensional scleral induction coil technique. *Vision Res* 27: 811–828, 1987.

Furman JM, Schor RH. Orientation of Listing's plane during static tilt in young and older human subjects. *Vision Res* 43: 67–76, 2003.

Glasauer S, Hoshi M, Kempermann U, Eggert T, Buttner U. Three-dimensional eye position and slow phase velocity in humans with downbeat nystagmus. *J Neurophysiol* 89: 338–354, 2003.

Goltz HC, Irving EL, Steinbach MJ, Eizenman M. Vertical eye position control in darkness: orbital position and body orientation interact to modulate drift velocity. *Vision Res* 37: 789–798, 1997.

Halmagyi GM, Curthoys IS, Cremer PD, Henderson CJ, Staples M. Head impulses after unilateral vestibular deafferentation validate Ewald's second law. *J Vestib Res* 1: 187–197, 1990.

Haslwanter T. Mathematics of three-dimensional eye rotations. *Vision Res* 35: 1727–1739, 1995.

Haslwanter T, Straumann D, Hess BJ, Henn V. Static roll and pitch in the monkey: shift and rotation of Listing's plane. *Vision Res* 32: 1341–1348, 1992.

Hegemann S, Straumann D, Bockisch C. Alexander's Law in patients with acute vestibular tone asymmetry—evidence for multiple horizontal neural integrators (Abstract). *J Assoc Res Otolaryngol* 8: 551, 2007.

Hepp K. On Listing's law. *Commun Math Phys* 132: 285–292, 1990.

Hess K, Dursteler MR, Reisine H. Analysis of slow phase eye velocity during the course of an acute vestibulopathy. *Acta Oto-Laryngol Suppl* 406: 227–230, 1984.

Holden JR, Wearne SL, Curthoys IS. A fast, portable desaccading program. *J Vestib Res* 2: 175–179, 1992.

Jeffcoat B, Shelukhin A, Fong A, Mustain W, Zhou W. Alexander's Law revisited. *J Neurophysiol* 100: 154–159, 2008.

Jongkees LB, Maas JP, Philipszoon AJ. Clinical nystagmography. A detailed study of electro-nystagmography in 341 patients with vertigo. *Pract Otorhinolaryngol* 24: 65–93, 1962.

Kleinbaum DG, Kupper LL, Muller KE. *Applied Regression Analysis and Other Multivariable Methods.* Boston, MA: PWS–Kent, 1988.

Marti S, Bockisch CJ, Straumann D. Prolonged asymmetric smooth-pursuit stimulation leads to downbeat nystagmus in healthy human subjects. *Invest Ophthalmol Vis Sci* 46: 143–149, 2005.

Mensh BD, Aksay E, Lee DD, Seung HS, Tank DW. Spontaneous eye movements in goldfish: oculomotor integrator performance, plasticity, and dependence on visual feedback. *Vision Res* 44: 711–726, 2004.

Misslisch H, Tweed D, Fetter M, Sievering D, Koenig E. Rotational kinematics of the human vestibuloocular reflex. III. Listing's law. *J Neurophysiol* 72: 2490–2502, 1994.

Palla A, Straumann D, Obzina H. Eye-position dependence of three-dimensional ocular rotation-axis orientation during head impulses in humans. *Exp Brain Res* 129: 127–133, 1999.

Remmel RS. An inexpensive eye movement monitor using the scleral search coil technique. *IEEE Trans Biomed Eng* 31: 388–390, 1984.

Robinson DA. A method of measuring eye movements using a scleral search coil in a magnetic field. *IEEE Trans Biomed Eng* 10: 137–145, 1963.

Robinson DA. The mechanics of human saccadic eye movement. *J Physiol* 174: 245–264, 1964.

Robinson DA, Zee DS, Hain TC, Holmes A, Rosenberg LF. Alexander's law: its behavior and origin in the human vestibulo-ocular reflex. *Ann Neurol* 16: 714–722, 1984.

Schmid-Priscoveanu A, Straumann D, Bohmer A, Obzina H. Vestibulo-ocular responses during static head roll and three-dimensional head impulses after vestibular neuritis. *Acta Otolaryngol* 119: 750–757, 1999.

Seidman SH, Leigh RJ, Tomsak RL, Grant MP, Dell'Osso LF. Dynamic properties of the human vestibulo-ocular reflex during head rotations in roll. *Vision Res* 35: 679–689, 1995.

Sklavos S, Dimitrova DM, Goldberg SJ, Porrill J, Dean P. Long time-constant behavior of the oculomotor plant in barbiturate-anesthetized primate. *J Neurophysiol* 95: 774–782, 2006.

Sklavos S, Porrill J, Kaneko CR, Dean P. Evidence for wide range of time scales in oculomotor plant dynamics: implications for models of eye-movement control. *Vision Res* 45: 1525–1542, 2005.

Straumann D, Zee DS, Solomon D. Three-dimensional kinematics of ocular drift in humans with cerebellar atrophy. *J Neurophysiol* 83: 1125–1140, 2000.

Tweed D, Cadera W, Vilis T. Computing three-dimensional eye position quaternions and eye velocity from search coil signals. *Vision Res* 30: 97–110, 1990.

Zee DS, Yamazaki A, Butler PH, Gucer G. Effects of ablation of flocculus and paraflocculus of eye movements in primate. *J Neurophysiol* 46: 878–899, 1981.

OPEN ACCESS Freely available online

PLOS ONE

Development of Eye Position Dependency of Slow Phase Velocity during Caloric Stimulation

Christopher J. Bockisch[1,2,3,4]*, Elham Khojasteh[1], Dominik Straumann[2,4], Stefan C. A. Hegemann[1,4]

1 Department of Otorhinolaryngology, Head & Neck Surgery, University Hospital Zürich, Zürich, Switzerland, **2** Department of Neurology, University Hospital Zürich, Zürich, Switzerland, **3** Department of Ophthalmology, University Hospital Zürich, Zürich, Switzerland, **4** Zürich Centre for Integrative Human Physiology (ZIHP), University of Zürich, Zürich, Switzerland

Abstract

The nystagmus in patients with vestibular disorders often has an eye position dependency, called Alexander's law, where the slow phase velocity is higher with gaze in the fast phase direction compared with gaze in the slow phase direction. Alexander's law has been hypothesized to arise either due to adaptive changes in the velocity-to-position neural integrator, or as a consequence of processing of the vestibular-ocular reflex. We tested whether Alexander's law arises only as a consequence of non-physiologic vestibular stimulation. We measured the time course of the development of Alexander's law in healthy humans with nystagmus caused by three types of caloric vestibular stimulation: cold (unilateral inhibition), warm (unilateral excitation), and simultaneous bilateral bithermal (one side cold, the other warm) stimulation, mimicking the normal push-pull pattern of vestibular stimulation. Alexander's law, measured as a negative slope of the velocity versus position curve, was observed in all conditions. A reversed pattern of eye position dependency (positive slope) was found $<$10% of the time. The slope often changed with nystagmus velocity (cross-correlation of nystagmus speed and slope was significant in 50% of cases), and the average lag of the slope with the speed was not significantly different from zero. Our results do not support the hypothesis that Alexander's law can only be observed with non-physiologic vestibular stimulation. Further, the rapid development of Alexander's law, while possible for an adaptive mechanism, is nonetheless quite fast compared to most other ocular motor adaptations. These results suggest that Alexander's law may not be a consequence of a true adaptive mechanism.

Citation: Bockisch CJ, Khojasteh E, Straumann D, Hegemann SCA (2012) Development of Eye Position Dependency of Slow Phase Velocity during Caloric Stimulation. PLoS ONE 7(12): e51409. doi:10.1371/journal.pone.0051409

Editor: Ramesh Balasubramaniam, McMaster University, Canada

Received August 21, 2012; **Accepted** November 2, 2012; **Published** December 12, 2012

Funding: This study was supported by the Swiss National Science Foundation grant (number 320000_122535/1) and the Betty and David Koetser Foundation for Brain Research, Zurich, Switzerland. E. Khojasteh receives the FQRNT (Fonds de Rescherch du Quebec) post-doctoral scholarship from Quebec, Canada. None of individuals employed or contracted by the funders (other than the named authors) played any role in the study design, data collection and analysis, decision to publish, or preparation of the manuscript.

Competing Interests: The authors have declared that no competing interests exist.

* E-mail: chris.bockisch@usz.ch

Introduction

Alexander's law describes how the slow phase velocity of nystagmus varies with eye position [1], where the slow phase velocity is faster when looking in the direction of the fast phase of nystagmus than in the slow phase direction. This behaviour can be observed in most patients with an acute unilateral vestibular deficit.

Robinson et al [2] and Hess [3] proposed that changes in the velocity-to-position neural integrator are responsible for Alexander's law. The integration of the ocular motor velocity command into a position command is necessary to counter centripetal elastic forces of the eye plant [4,5]. If neural integration is diminished, the fixation command is insufficient to keep a normal eye from drifting towards a central position, producing gaze-evoked nystagmus whose velocity increases with eccentricity. If gaze-evoked nystagmus is combined with the vestibular nystagmus, drift velocity in one gaze direction is reduced, but is increased in the opposite direction.

Robinson et al. (1984) investigated the time course of the development of the eye position dependency in three subjects during caloric induced nystagmus and found that it first occurred 20–46 s after the onset of nystagmus [2]. With natural vestibular stimulation (real movements of the head in space on a turntable), the eye position dependency was small, and did not evolve over time, which led to the proposition that Alexander's law is an adaptive response to un-natural vestibular stimulation. By 'un-natural', Robinson et al meant that a change in vestibular input from one side is not accompanied by the opposite change from the other side for 25 seconds. We will use the term non-physiologic to describe such stimulation patterns. If Alexander's law is produced by changes in the neural integrator, it could be considered an adaptive response, since eye velocity will be reduced for some eye positions, thus aiding vision.

During normal yaw head turns, one horizontal semicircular canal is stimulated while the other is inhibited. During non-physiologic unilateral caloric stimulation, on the other hand, only one canal changes its tonic activity depending on the stimulus (increase with warm and decrease with cold stimulation). This unusual pattern of stimulation might be detected and lead to Alexander's law.

In contrast, Doslak et al [6,7] proposed that the rotational vestibular ocular reflex (rVOR) command has a gaze position component which leads to Alexander's law. While this model can

provide an account for Alexander's law, it also predicts such effects for the normal VOR, which are not seen for head impulses [8], or 0.5 hz frequency head rotations [2].

We tested Robinson's hypothesis that only non-physiologic velocity commands evoke Alexander's law. We assumed that simultaneous irrigation at 44°C on one side (warm, excitatory) and 30°C (cold, inhibitory) on the contralateral side would produce a stimulation pattern similar to that produced by head rotations. If the intervestibular mismatch of non-physiologic stimulation would cause Alexander's law, then we would expect that it does not develop during simultaneous bilateral bithermal stimulation or would at least be weaker compared to unilateral caloric stimulation. Contrary to this expectation, we found that Alexander's law developed similarly in all conditions.

Materials and Methods

Subjects and equipment

Eleven subjects (8 male, 3 female) with no reported history of vestibular or oculomotor disorders participated, and each gave prior written consent after the experimental procedure was explained. The study was approved by the Ethics Committee of the Canton of Zurich, Switzerland, and was in accordance with the principles of the 1964 Declaration of Helsinki.

Subjects lay supine with the torso and head tilted up 30° to position the horizontal canals approximately vertical, which produces the strongest nystagmus. A neck cushion was used to reduce head motion. A 1.6 m×0.9 m screen was suspended from the ceiling, 1 meter from the subject and oriented perpendicular to the gaze line when subjects looked straight ahead. A mirror-galvanometer and laser under computer control projected a red target spot (~0.25° diameter) onto the screen to control gaze direction.

Horizontal and vertical positions of the right eye were recorded at 220 Hz with head mounted video cameras (EyeSeeCam, Munich). The center of the pupil was determined by ellipse fits to thresholded images of each eye. A custom-made calibration of eye position was made by having subjects fixate targets at ±40°, ±30°, ±20°, ±10°, and 0° horizontally, and ±10° vertically. In practice, eye positions beyond ±30° could not be reliably measured and were excluded.

Warm (44°C), cold (30°C), and simultaneous bilateral bithermal caloric irrigation was performed at ~230 ml/minute with ATMOS Variotherm plus systems. Caloric stimulation creates a temperature gradient along the lateral canals, introducing convection currents in the endolymph and movement of the cupula [9]. Cold stimulation produces utriculofugal flow of the endolymph, simulating a head rotation away from the irrigated ear and depressing activity in the vestibular nerve; warm stimulation has the opposite effect. Simultaneous bilateral bithermal stimulation (one side cold, the other warm; hereafter just called 'bithermal') thus approximates a normal horizontal head rotation. The altered temperature of caloric stimulation may also directly stimulate the vestibular nerve [10,11].

Procedure

Warm, cold, and bithermal stimulations were usually conducted on the same day in each subject. Each trial had 4 parts, with caloric stimulation in parts 3 and 4:

1. eye tracker calibration (35 sec)
2. baseline gaze holding (30 seconds)
3. Caloric stimulation (3 minutes):
4. Decline of nystagmus.

During baseline (part 2) and the first 2 minutes of stimulation, subjects were instructed to look in darkness at a pulsed target that moved every 4 seconds from 20° right to 20° left. The laser was pulsed (20 msec on, 2 sec off) so that we could direct the patient's gaze direction without suppressing nystagmus. Two minutes after stimulation began, the targets ±20°, ±10°, and 0°, were presented in a pseudorandom order, in order to collect data at more fixation positions to allow for higher order fits through the velocity versus position curve. Prior to the first caloric stimulation trial, a 1 minute control trial with 5 target positions and no caloric stimulation was completed.

Caloric stimulation lasted 3 minutes, but we continued measurements as eye velocity declined until no nystagmus was noticeable or the subject became uncomfortable. Short breaks, of around 5 minute's duration, were taken between recordings.

The stimulation order was constrained so that the direction of nystagmus changed for each trial. This required that the bithermal stimulation be either the first or last trial, and the unilateral stimulations be in the same ear. The first trial was warm for 3 subjects, cold for 4 subjects, and bithermal for 4 subjects. The unilateral stimulation was in the left ear for 5 subjects, and in the right ear for 6.

Analysis

All analyses were performed with MATLAB© (MathWorks Inc, Natick, MA, USA). Only horizontal eye movements were analyzed. We use the right-hand rule sign convention: looking left is positive and looking right is negative. To compare the data from different stimulation conditions, we converted the data to appear as if the subjects had right-sided excitation (warm right side, or cold left side), so slow phase eye movements were to the left.

Saccades were identified and removed with an interactive computer program that automatically detected saccades when velocity exceeded a threshold above the median eye velocity calculated over a 1 second window. With a window size this large there are more data points associated with slow phase movements than saccades, so the median is an estimate of the current slow-phase velocity, The threshold was typically set 20–30°/s from the median, depending upon the noise level. To ensure that saccadic components were not included, the initial 2 (~10 msec) and final 5 samples (~23 msec) were removed from each slow phase. The automatically-marked saccades could be manually adjusted and blink artifacts removed.

Nystagmus slow phases shorter than 50 msec were discarded, and slow phases longer than 100 msec were split into 2 or more parts of at least 50 msec. (This was done to ensure, for unbiased statistical analysis, that roughly the same number of data points occurred in each gaze direction.) For each of these slow phases we calculated the median position and velocity.

General estimates of the change of nystagmus velocity with eye position were made by linear regression of velocity versus position,

$$Velocity = \beta_0 + \beta_1 H.$$

β_0 is the intercept, or velocity at gaze straight ahead, and β_1 is the slope parameter that describes how velocity changes which horizontal position, H.

We created 'sliding' fits, by fitting lines to 30 seconds of data, and then advancing the time period every 5 seconds. These fits gave us the most accurate estimates of the time of peak nystagmus velocity and slope. To investigate the correlation of the nystagmus velocity and slope, we made fits to blocks of data 16 seconds in duration (4 changes of flashing target position). We then cross-

correlated the slopes and intercepts for each subject for the period when the nystagmus velocity was above 10% of the maximum velocity.

In patients suffering from spontaneous nystagmus due to an acute vestibular tone asymmetry, velocity varies with position in a non-linear fashion [12,13], so we also wished to test if this was the case with nystagmus induced by calorics. After the first 2 minutes of stimulation, the flashing laser target alternated between 5 positions: $\pm 20^\circ$, $\pm 10^\circ$, and straight ahead, which allowed us to describe the change in velocity with horizontal eye position in more detail. We did this by fitting second order equations via linear regression to the horizontal velocity versus position data to the data collected 2–3 minutes after the start of stimulation,

$$Velocity = \beta_0 + \beta_1 H + \beta_2 H^2.$$

We occasionally recorded data long enough to observe a reversal of nystagmus, presumably an adaptation to the persistent caloric stimulation. We analyzed the 30 seconds of data around the peak reversal nystagmus for changes in velocity with eye position with linear fits.

To test for differences between warm, cold, and bithermal stimulations, we performed one-way repeated-measures analysis of variance (ANOVA) with SPSS (version 19), and if a significant effect was found, we then performed multiple comparison tests with Sidak's correction. Correlations were performed with Spearmann's rank correlation.

Results

We first measured gaze holding prior to caloric stimulation by having subjects look to a flashing target that moved between positions of $\pm 20^\circ$, $\pm 10^\circ$, and straight ahead for 1 minute, and we fit second order equations to characterize the nystagmus velocity at straight ahead gaze (intercept), the first order change of the velocity with position (slope) and the 2nd order change of velocity with position. The average best fit parameters were -0.18°/s (standard deviation = 0.43), -0.005 1/s (0.019), and -0.00004 1/$^\circ$s (0.0003), none of which were significantly different from zero (p-values for difference from zero t-tests for the intercept, slope, and 2nd order term were 0.18, 0.34, and 0.64, respectively). However, individual subjects could exhibit significant drift: 8/11 showed significant drift at gaze straight ahead (with a maximum of 0.8°/s), 6/11 had significant slope parameters, and 3/11 had significant quadratic components. The small amount of gaze evoked nystagmus is typical for healthy people [2,14].

Development of Alexander's Law

Eye velocity typically increased rapidly with caloric stimulation, and would then plateau or decline modestly, until the irrigation stopped, and then velocity would drop rapidly (see bithermal example in Figure 1). For each data set, we fit straight lines to 30 seconds of data, and then shifted the time period every 5 seconds. The intercepts (Figure 2, top row) thus show how velocity at straight ahead evolves over time, and the slopes (Figure 2, middle row) show how the dependence of velocity on position changes with time. Nystagmus increased after stimulation began, peaking on average after 107 seconds (cold = 117 s, warm = 110 s, bithermal = 97 s). The change in velocity with eye position followed a similar time course, reaching minimums at 118, 119 s, and 113 s for cold, warm, and bithermal stimulation, respectively.

While nystagmus generally followed a smooth time course (Figure 2, top row), the fitted slopes were variable within and between subjects (Figure 2, middle row). Some of this variability was probably due to the difficulty subjects had in directing their gaze to the flashing target; in some trials subjects' eye position did not change over as large a range (40°) as desired, so the fitted slopes show more variability as a result. In addition, some subjects seemed surprised and distracted when the sensation of motion first appeared, and they did not track the flashing target. If eye position remained in one direction as the nystagmus increased, the resulting slope estimate was biased. This led to increased variability in the slope estimates shortly after the onset of stimulation.

At the time of maximum velocity (the peaks in Figure 2, top row), the average difference in intercepts from control across subjects were 23°/s, 40°/s, and 55°/s for cold, warm, and bithermal stimulation, respectively (Figure 3A; see Figure 4 for example fits). The one way ANOVA was significant ($F(2,20) = 24.3$; $p<0.001$), and multiple comparisons found that cold stimulation produced significantly less intense nystagmus than both warm ($p<0.001$) and bithermal ($p<0.001$) stimulation, and bithermal stimulation produced marginally greater nystagmus than warm ($p = 0.065$).

At the time of maximum nystagmus, the average difference in slopes across subjects, from control, were -0.085, -0.152, $-0.109^\circ/s/^\circ$ for cold, warm, and bithermal stimulation, respectively (Figure 3B). ANOVA did not find significant differences between the slopes ($F(2,20) = 0.83$, $p = 0.45$). With cold stimulation, 6 of 11 subjects had slopes that became more negative with stimulation, and 5 had no significant change. With warm stimulation, the slopes of 9 of 11 subjects became more negative, and 2 became significantly positive (a reversal of Alexander's law). For bithermal stimulation 8/11 had slopes that became more negative, 1 became significantly positive, and 2 had no significant change. In each condition, the average difference of slope was significantly different from zero (all $ps<0.02$) An integrator time constant can be inferred from the fitted equations by -1/slope; average time constants were thus about 12, 5, and 8 seconds for cold, warm, and bithermal stimulation, respectively. By way of comparison, an average time constant of 52 seconds was found for control data analyzed with simple linear fits.

The average slopes and intercepts followed similar time courses (Figure 2, bottom row). The time courses were compared by fitting lines to adjacent 16 second blocks of data, and cross correlating the fitted slopes and intercepts when the velocity was more than 10% of the maximum velocity. In 16 of 33 experiments the correlations were significant (5 cold, 7 warm, 4 bithermal) with average correlations of -0.43. On average, the intercept lagged the slope by 17 seconds, which was not significantly different from zero ($t = 1.0$, $p<0.3$). ANOVA did not find significant differences for the lag times for the different conditions ($F(2,20) = 2.3$, $p>0.1$). The lag of the intercept is most obvious in the cold condition when the nystagmus was declining, showing that the eye position effect tended to recover to normal slightly faster than the nystagmus decayed. Repeating the cross correlation for the data after the peak nystagmus velocity found an average correlation of -0.44, which was significant in 16 of 33 experiments (4 cold, 7 warm, 5 bithermal), and the average lag of the intercept was 48 seconds ($t = 2.9$, $p = 0.006$). In the cold condition, the intercept lagged by 84 seconds ($t = 2.5$, $p = 0.03$), in the bithermal condition the mean lag of the intercepted was 48 seconds ($t = 2.1$, $p = 0.059$), and in the warm condition the mean lag was 11 seconds ($t = 0.4$, $p = 0.6$). Correlations for the data when

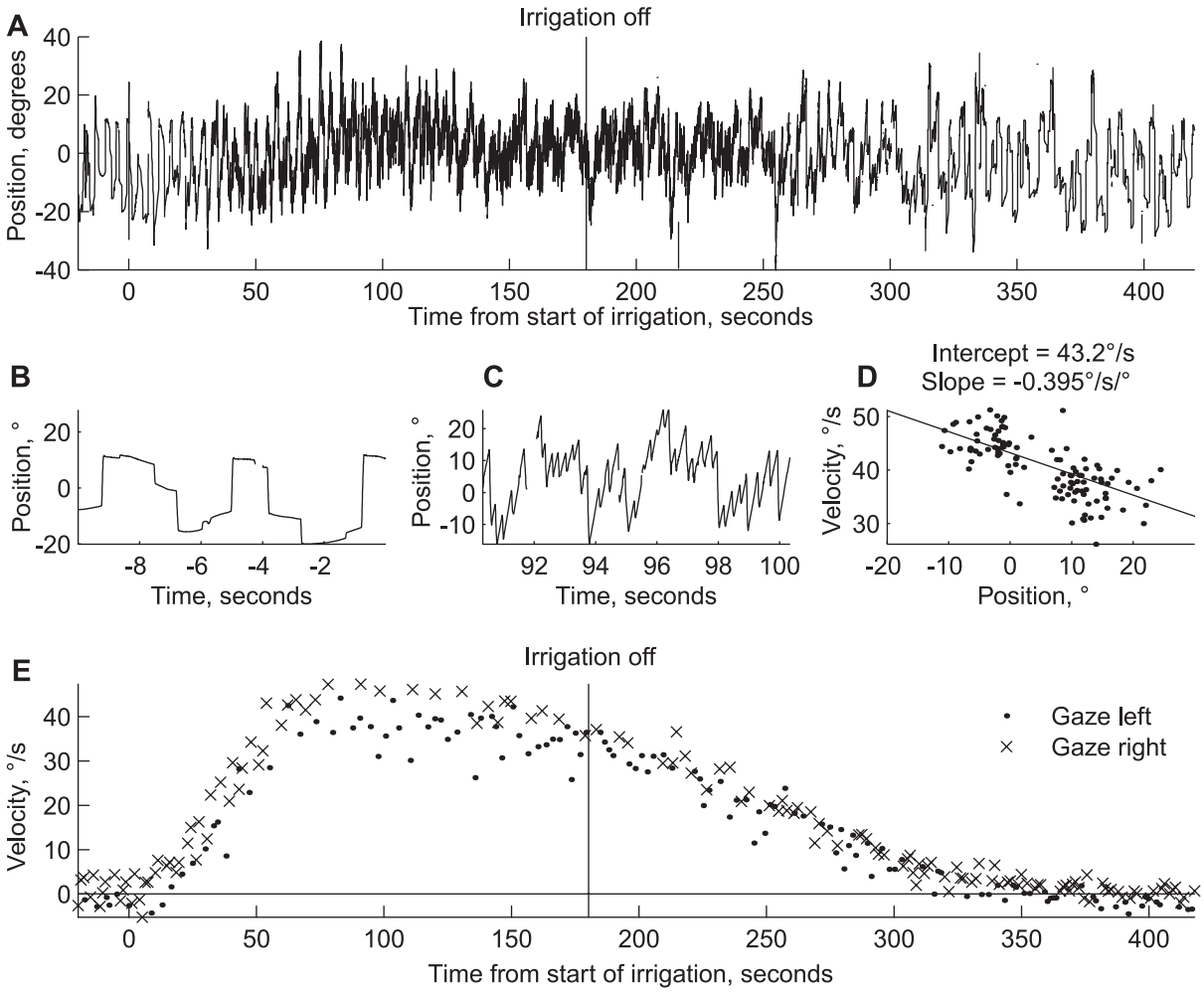

Figure 1. Example data. A. Horizontal eye position is shown for an experiment with bilateral, bithermal caloric stimulation. The subject looked into the direction of a flashing laser spot that first shifted between 20° left and right positions (time <120 s), and then the target shifted to targets at ±20°, ±10°, and 0° for the remainder of the experiment. B. Position traces before stimulation began, so little nystagmus is observed. C. Position traces from near the time of maximum velocity. D. Velocity is plotted versus position for 30 seconds of data selected at the time of maximum nystagmus. Each point is an individual slow phase. The best fit line and fitted parameters are also shown. E. The velocity of individual slow phases is shown, with different symbols used when subjects were looking left and right of straight ahead. For clarity, only 1 in 10 slow phases are shown.
doi:10.1371/journal.pone.0051409.g001

nystagmus was rising were less strong overall (significant in only 7 of 33 experiments, with a mean of −0.45), and the mean lag was 3 seconds, which was not different from zero ($t = 0.3$, $p = 0.7$). (Note that because nystagmus rose faster than it decayed, there was less data entering into these correlations.).

Focusing on the time of maximum nystagmus, there was a modest correlation between the nystagmus velocity and the slope (Figure 3C). Overall, the correlation was not quite significant (Spearmann's rho = −0.33, $p = 0.06$), though the correlation for warm stimulation was significant (rho = −0.655, $p = 0.034$).

Second Order Fits

We fit parabolas to the data from 2–3 minutes after the start of stimulation (when the target position shifted between 5 positions, instead of 2). While the quadratic component was often significant (5/10 cold, 4/10 warm, 4/10 bithermal), the sign of the components were not consistent, so the average quadratic components were not different from zero.

Eye Position Dependent Changes in Velocity Decline with the Decay of Vestibular Nystagmus

The fitted slopes returned towards control values as the nystagmus decayed (see Figure 2). When nystagmus velocity was higher, particularly with warm and bithermal stimulation, the direction of nystagmus could reverse a few minutes after stimulation stopped (after 2.8 minutes, on average). We did not always observe a reversal, though this could be because we stopped the experiment early. In 16 cases (3 cold, 6 warm, 7 bithermal) we could further analyze the data and so to characterize the reversal we fit straight lines to 30 seconds of data, centered on the peak reversal velocity. The average intercepts were 2.1°/s, 3.3°/s, and 3.7°/s for cold, warm, and bithermal stimulation, respectively. In 11/16 cases the fitted slopes were not significantly different from control. The slopes were more negative than control values in 4 cases (1 cold, 1 warm, 2 bithermal), that is, Alexander's law was followed in the reversal period. In 1 bithermal case the slope was more positive, or a reversal of Alexander's law.

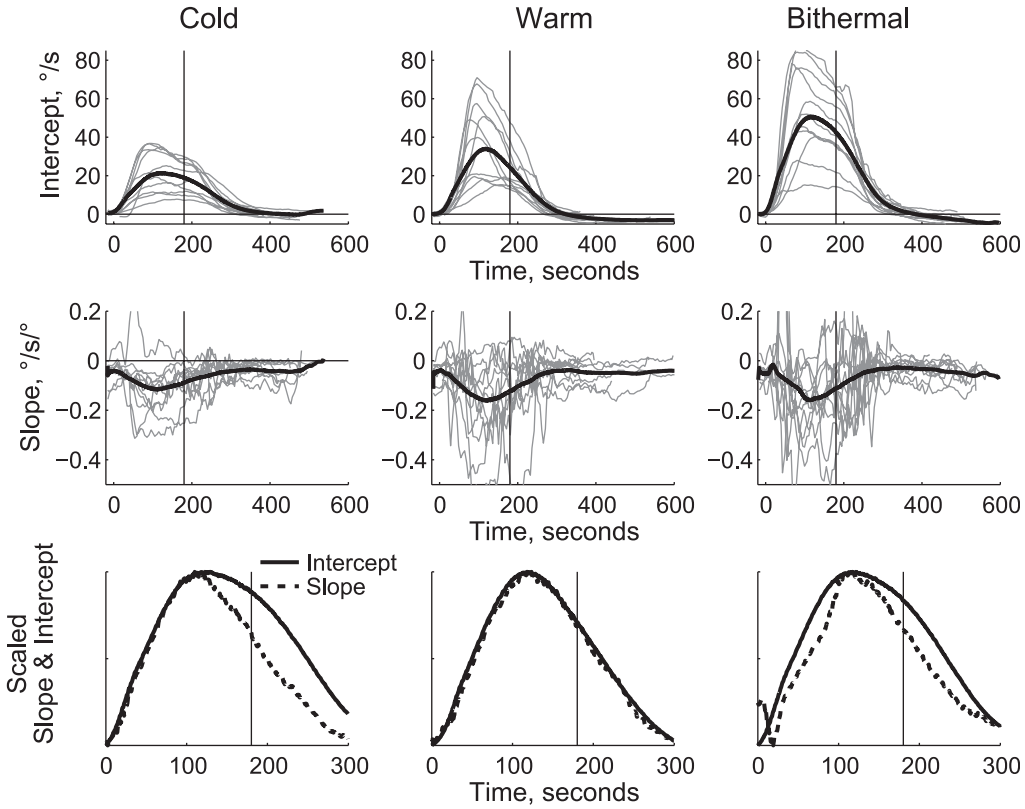

Figure 2. 'Sliding' fits to all data. We made linear fits to the velocity versus position data, using 30 seconds of data, and shifting the center time every 5 seconds. The fitted intercepts (top row) and slopes (middle row) for velocity versus position are shown for each stimulation condition. The thin grey lines are individual subject data, and the thick black line is the mean. Vertical lines mark the time when caloric irrigation was stopped. In the bottom row we scaled the mean intercept and slope curves to facilitate comparison of the curves.
doi:10.1371/journal.pone.0051409.g002

Discussion

We found that eye velocity depended upon position in accordance with Alexander's law when it was induced by warm, cold, and simultaneous bilateral bithermal caloric stimulation. The average velocity to position slope (-0.11) is very similar to the slopes we found in patients (-0.088 and -0.1) [12,13]. Our results provide little support for Robinson's et al [2] hypothesis that Alexander's law arises due to an adaptive response to unphysiologic stimulation. Bithermal stimulation mimics the 'push-pull' of normal vestibular stimulation, yet we usually observed Alexander's law in this condition.

The time course of the change in velocity with position, on average, closely followed that of the speed of nystagmus. There was, however, considerable variability in the velocity-position slopes, which made it difficult to determine the onset of Alexander's law, or any temporal delay of the rise of Alexander's law with the nystagmus velocity. Robinson's et al [2], in three subjects, reported that the time of peak Alexander's law lagged the time of peak nystagmus by 25 seconds, on average. Given the variability we observed in the slopes, however, such a measurement does not seem informative here. We correlated the slopes and intercepts over several minutes, and found the optimal temporal lag from the cross-correlation was not significantly different from zero. Since we binned the data in 16 second blocks, this would suggest that any lag is less than half the bin width, or 8 seconds, which is less than the 25 seconds suggested by Robinson et al [2]. This leads us to question whether it is really an adaptive phenomenon, since oculomotor adaptive effects typically need many minutes to develop, though rapid adaptation is not unprecedented (eg., [15,16]). Caloric stimulation, like peripheral vestibular disorders, has a frequency content that is much lower than that produced by natural head movements, and could explain why Alexander's law has not been observed during higher frequency head rotations. [2,8]. Perhaps very low frequency signals are not well integrated.

Our results seem to contradict those of Jeffcoat et al [17], who reported a 'reversed' Alexander's law with warm calorics. They interpret this result as supportive of Doslak's model of Alexander's law [6,7], which includes an eye-position dependency in the VOR pathway. However, in Supporting Information S1 we explain that this is a mis-interpretation of Doslak's model. Nonetheless, the results of Jeffcoat et al [17] with warm calorics are different than ours. However, they used a protocol that likely produced very low levels of nystagmus (the head was upright, whereas the optimal position for caloric stimulation is 60° pitched backwards; their example figures show velocity around 10°/s, whereas our average peak velocity was 40°/s). In the two cases where we observed a reversal of Alexander's law, the nystagmus velocity was quite low (see Figure 3C).

Our results also do not conclusively support the Doslak model. This model predicts that the eye-position dependent effect should be independent of the nystagmus speed (above a threshold), yet on average we find that the effect rises and falls with the nystagmus (see Figure 2 and Figure 3C). In addition, Doslak's model predicts that Alexander's law should be observed during normal head movements, yet this does not

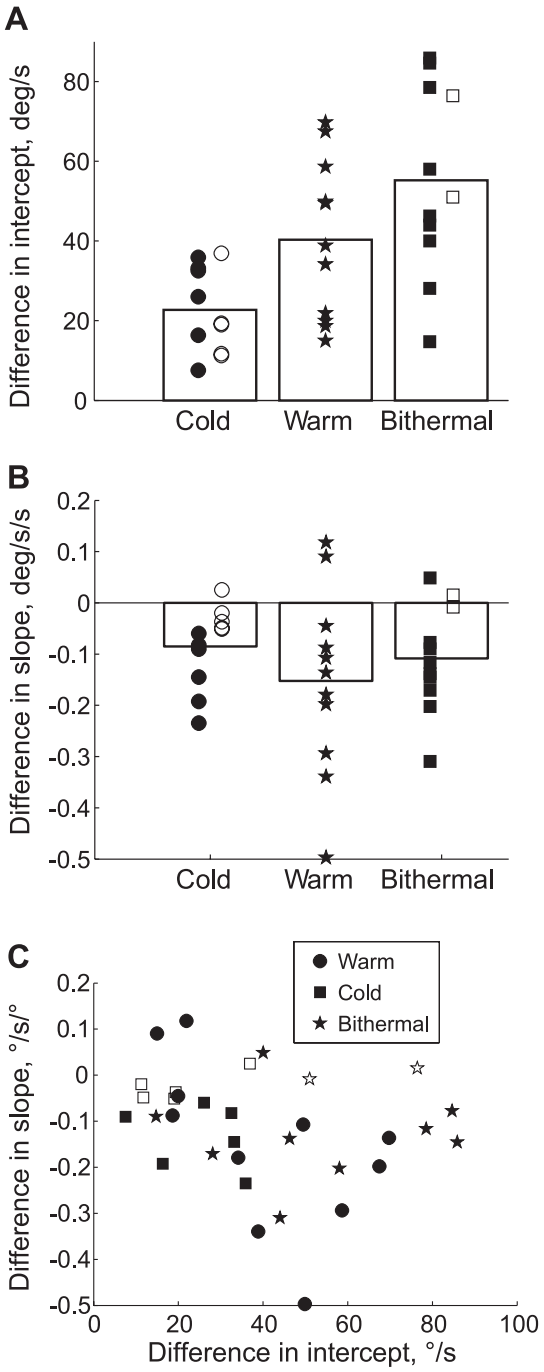

Figure 3. Linear regression of velocity on position at the time of peak nystagmus. A. Each point shows the difference in intercept from the control trial for an individual subject and the bars are means. Open symbols indicate the fitted *slopes* were not significantly different from control values. B. Each point shows the change in slope from the control trial for each subject and the bars are means. Open symbols indicate the difference in slopes from control values were not significantly different zero. C. The slopes (from panel B) are plotted against the intercepts (from panel A). Open symbols indicate the difference in *slopes* from control values were not significantly different from zero.
doi:10.1371/journal.pone.0051409.g003

seem to be the case for head impulses [8] or 0.5 Hz frequency head rotations [2].

What other mechanisms might account for Alexander's law? The translational VOR is highly dependent upon gaze direction, and backward head movements produce centripetal eye movements, which, if added to a rotational VOR signal would produce Alexander's law. The sensitivity of extraocular motor neurons varies with gaze position when stimulated with high intensity auditory stimuli (clicks) [18], which stimulate the otoliths organs [19,20], and Jeffcoat et al [17] proposed this as the basis of an explanation of Alexander's law. However, Alexander's law has not been found during high frequency head rotations [2,8]. There is evidence that caloric stimulation evokes horizontal linear VOR responses due to central processing to resolve the conflict between the dynamic canal stimulus and the static otolith signal [21]. To produce Alexander's law would require the target distance to vary (being nearer when in the fast phase direction since the gain of the linear VOR is higher for near targets). Similarly, the rotational VOR has been found to be modestly sensitive to vergence angle [22,23]. In our setup subjects viewed (flashing) targets on a flat screen and so the eccentric targets were more distant than central targets, but there was no left/right asymmetry which would provoke different vergence responses, so a contribution of vergence to Alexander's law seems unlikely. Thus, at this point the mechanism responsible for Alexander's law remains unclear. Our data do not fully support either the neural integrator hypothesis of Robinson et al [2], or the VOR modification model of Doslak [6,7], and a vergence mediated effect seems unlikely.

To explain our recent findings in patients with acute unilateral vestibular deficit, where slow-phase eye velocity varied nonlinearly with eye position [12,13], we developed a new model for Alexander's Law [24]. The simultaneous disfacilitation of the ipsilesional and hyperactivity of the contralesional vestibular nuclei following a peripheral vestibular lesion introduces an asymmetry in the responses of bilateral vestibular nuclei [25]. We hypothesize that this central asymmetry limits the linear operating range of the central responses. We showed that this results in eye position dependent gains in the central positive feedback loops that perform integration of velocity commands. Therefore, the time constant of the neural integrator becomes dependent on eye position, and nonlinear velocity-versus-position plots result. We further speculate that a similar mechanism could be responsible for Alexander's Law during calorics; a continuous low-frequency stimulation like calorics could in the same manner saturate or inhibit the central responses and influence the integrator in a matter of seconds.

We did not find consistent non-linear velocity-versus-position effects with caloric stimulation, leaving open the possibility that the effects found in patients might be the result of adaptive mechanisms to suppress nystagmus, since these patients typically had nystagmus for several days before they were measured. Thus, the patterns of eye position dependencies seen in patients could be the combination of two different mechanisms, an immediate linear effect as seen with caloric stimulation, and slower adaptive changes which produce the non-linear patterns. If changes in the neural integrator are responsible for these effects, it suggests the integrator time constant depends on gaze direction. Adaptation of the neural integrator time constant depending upon gaze direction has been suggest previously [26,27,28], and has also been proposed based on pharmacological inactivation studies in monkeys [29] and more recently in goldfish [30].

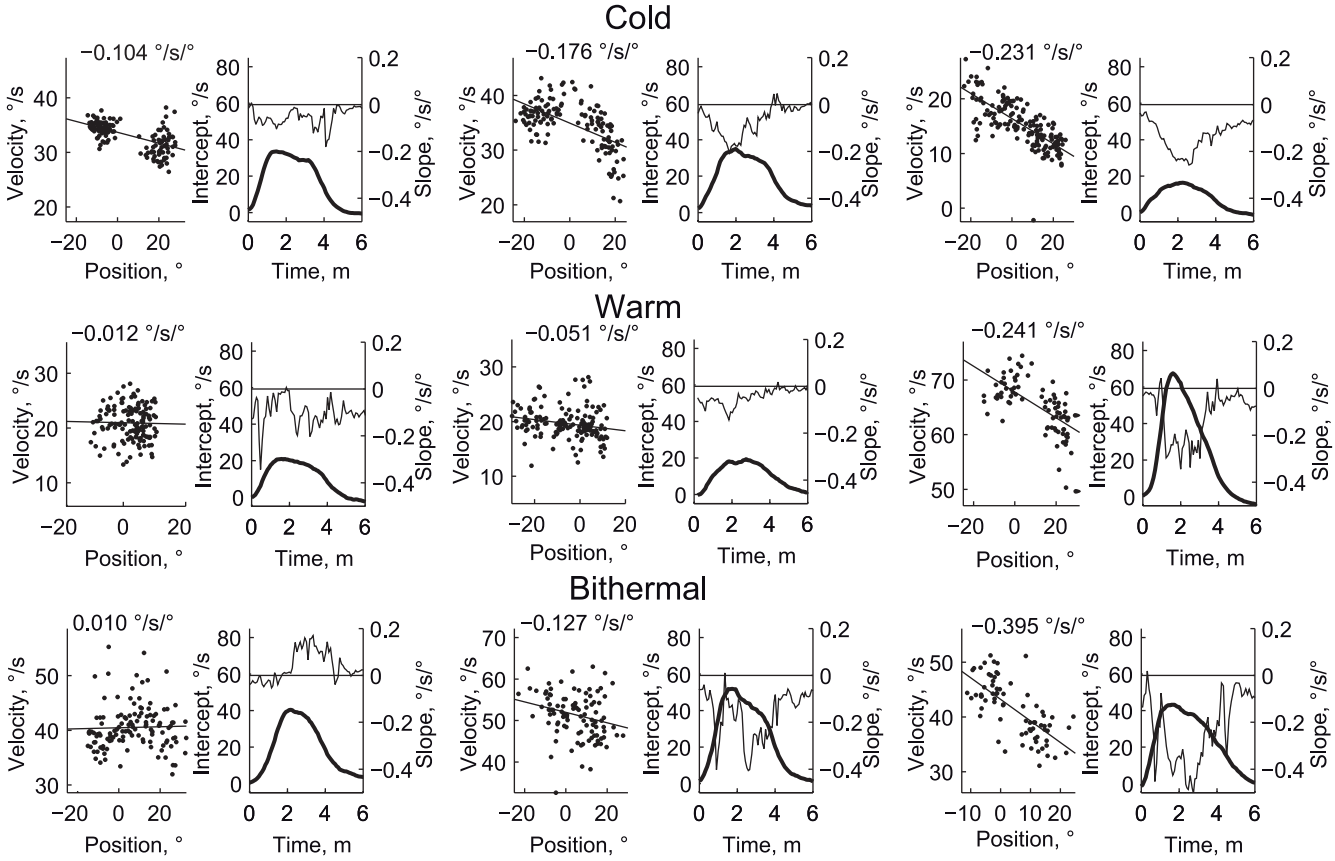

Figure 4. Example velocity versus position plots. Each row contains 2 pairs of plots, each pair showing the data from a different subject. The first plot in each pair is a scatter plot where each point shows the slow phase position and velocity from the 30 seconds centered on the time of maximum nystagmus velocity. The second plot in each pair shows the fitted intercepts (thick line, left-side axis) and slopes (thin line, right-side axis) for the first 6 minutes after the start of caloric stimulation. Each row shows a different stimulation condition (top = cold, middle = warm, bottom = simultaneous bilateral bithermal).
doi:10.1371/journal.pone.0051409.g004

Supporting Information

Figure S1 Predictions of Doslak's (1979) model for unilateral warm and cold calorics. Top, for a unilateral right side excitation, Doslak's model results in a vestibular induced velocity that is independent of eye position (the dashed line) plus an eye position dependent term (the dotted line). The sum is such that the absolute velocity is larger in the fast-phase direction (right) and smaller in the slow phase direction (left), as expected from Alexander's law. Bottom, in the same manner, a unilateral right side inhibition produces eye position dependent velocity in accordance with Alexander's law.
(EPS)

Supporting Information S1
(DOCX)

Acknowledgments

We would like to thank Marco Penner for technical support, and Martina Susac and Kathrin Schmidig for assistance in collecting preliminary data.

Author Contributions

Conceived and designed the experiments: SH CB DS. Performed the experiments: SH CB EK. Analyzed the data: CB. Wrote the paper: CB SH EK DS.

References

1. Alexander G (1912) Die Ohrenkrankheiten im Kindesalter. In: Schlossmann A, editor. Handbuch der Kinderheilkunde. Leipzig: Vogel. 84–96.
2. Robinson DA, Zee DS, Hain TC, Holmes A, Rosenberg LF (1984) Alexander's law: its behavior and origin in the human vestibulo-ocular reflex. Annals of Neurology 16: 714–722.
3. Hess K (1982) Do peripheral-vestibular lesions in man affect the position integrator of the eyes? Neuroscience Letters Suppl. 10: 242–243.
4. Robinson DA (1968) Eye movement control in primates. The oculomotor system contains specialized subsystems for acquiring and tracking visual targets. Science 161: 1219–1224.
5. Robinson DA (1975) Oculomotor control signals. In: Lennerstrand G, Rita P, editors. Basic mechanisms of ocular motility and their clinical implications. Oxford - New York - Toronto - Sydney - Braunschweig: Pergamon Press. 337–378.
6. Doslak MJ, Dell' Osso LF, Daroff RB (1979) A model of Alexander's law of vestibular nystagmus. Biological Cybernetics 34: 181–186.
7. Doslak MJ, Dell'Osso LF, Daroff RB (1982) Alexander's law: a model and resulting study. Ann Otol Rhinol Laryngol 91: 316–322.
8. Anagnostou E, Heimberger J, Sklavos S, Anastasopoulos D (2011) Alexander's law during high-acceleration head rotations in humans. Neuroreport 22: 239–243.
9. Oosterveld WJ, de Jong HA (1987) The caloric vestibular test in weightlessness. Arch Otorhinolaryngol 244: 155–158.
10. Paige GD (1985) Caloric responses after horizontal canal inactivation. Acta Otolaryngol 100: 321–327.
11. Scherer H, Brandt U, Clarke AH, Merbold U, Parker R (1986) European vestibular experiments on the Spacelab-1 mission: 3. Caloric nystagmus in microgravity. Exp Brain Res 64: 255–263.

12. Bockisch CJ, Hegemann S (2008) Alexander's law and the oculomotor neural integrator: three-dimensional eye velocity in patients with an acute vestibular asymmetry. Journal of Neurophysiolgy 100: 3105–3116.
13. Hegemann S, Straumann D, Bockisch C (2007) Alexander's law in patients with acute vestibular tone asymmetry–evidence for multiple horizontal neural integrators. J Assoc Res Otolaryngol 8: 551–561.
14. Becker W, Klein HM (1973) Accuracy of saccadic eye movements and maintenance of eccentric eye position in the dark. Vision Research 13: 1021–1034.
15. Melvill Jones G, Guitton D, Berthoz A (1988) Changing patterns of eye-head coordination during 6 h of optically reversed vision. Exp Brain Res 69: 531–544.
16. Miller JM, Anstis T, Templeton WB (1981) Saccadic plasticity: parametric adaptive control by retinal feedback. J Exp Psychol Hum Percept Perform 7: 356–366.
17. Jeffcoat B, Shelukhin A, Fong A, Mustain W, Zhou W (2008) Alexander's Law Revisited. Journal of Neurophysiolgy 100: 154–159.
18. Zhou W, Xu Y, Simpson I, Cai Y (2007) Multiplicative computation in the vestibulo-ocular reflex (VOR). 2007/01/26: 2780–2789.
19. Murofushi T, Curthoys IS (1997) Physiological and anatomical study of click-sensitive primary vestibular afferents in the guinea pig. Acta Otolaryngol 117: 66–72.
20. Murofushi T, Curthoys IS, Topple AN, Colebatch JG, Halmagyi GM (1995) Responses of guinea pig primary vestibular neurons to clicks. Exp Brain Res 103: 174–178.
21. Peterka RJ, Gianna-Poulin CC, Zupan LH, Merfeld DM (2004) Origin of orientation-dependent asymmetries in vestibulo-ocular reflexes evoked by caloric stimulation. J Neurophysiol 92: 2333–2345.
22. Paige GD, Telford L, Seidman SH, Barnes GR (1998) Human vestibuloocular reflex and its interactions with vision and fixation distance during linear and angular head movement. J Neurophysiol 80: 2391–2404.
23. Crane BT, Demer JL (1998) Human horizontal vestibulo-ocular reflex initiation: effects of acceleration, target distance, and unilateral deafferentation. J Neurophysiol 80: 1151–1166.
24. Khojasteh E, Bockisch CJ, Straumann D, Hegemann SCA (2012) A dynamic model for eye-position-dependence of spontaneous nystagmus in acute unilateral vestibular deficit. European Journal of Neuroscience:.
25. Smith PF, Curthoys IS (1989) Mechanisms of recovery following unilateral labyrinthectomy: a review. 14: 155–180.
26. Chan WW, Galiana HL (2005) Integrator function in the oculomotor system is dependent on sensory context. Journal of Neurophysiolgy 93: 3709–3717.
27. Chan WW, Galiana HL (2007) A non-linear model of the neural integrator in oculomotor control. Conf Proc IEEE Eng Med Biol Soc 1: 1156–1159.
28. Mensh BD, Aksay E, Lee DD, Seung HS, Tank DW (2004) Spontaneous eye movements in goldfish: oculomotor integrator performance, plasticity, and dependence on visual feedback. Vision Res 44: 711–726.
29. Crawford JD, Vilis T (1993) Modularity and parallel processing in the oculomotor integrator. Exp Brain Res 96: 443–456.
30. Aksay E, Olasagasti I, Mensh BD, Baker R, Goldman MS, et al. (2007) Functional dissection of circuitry in a neural integrator. Nature Neuroscience 10: 494–504.

Exp Brain Res
DOI 10.1007/s00221-013-3423-6

RESEARCH ARTICLE

Eye position dependency of nystagmus during constant vestibular stimulation

Christopher J. Bockisch · Elham Khojasteh · Dominik Straumann · Stefan C. A. Hegemann

Received: 8 November 2012 / Accepted: 15 January 2013

Abstract Alexander's law, the eye position dependency of nystagmus due to peripheral vestibular lesions, has been hypothesized to occur due to adaptive changes in the brainstem velocity-to-position neural integrator in response to non-reciprocal vestibular stimulation. We investigated whether it develops during passive head rotations that produce constant nystagmus for >35 s. The yaw rotation stimulus consisted of a 1-s acceleration (100°/s^2), followed by a lower acceleration ramp (starting at 7.3°/s^2 and increasing at 0.04°/s^2/s) until 400°/s was reached after 38 s. This stimulus was designed to offset the ~15 s vestibular ocular reflex time constant (and the 150 s adaptation time constant) and produce constant velocity slow phases. In contrast to peripheral lesions, this vestibular stimulation is the result of real head turns and has the push–pull characteristics of natural movements. The procedure was successful, as the average velocity of 31°/s was unchanged over the final 35 s of the acceleration period. In all 10 healthy human subjects, we found a large and stable Alexander's law, with an average velocity-versus-position slope of −0.366 in the first half that was not significantly different in the second half, −0.347. These slopes correspond to integrator time constants of <3 s, are much less than normal time constants (~25 s), and are similar to those observed in patients with peripheral vestibular lesions. Alexander's law also developed, on average, in 10 s. We conclude that Alexander's law is not simply a consequence of non-reciprocal vestibular stimulation.

Keywords VOR · Nystagmus · Vestibular · Adaptation · Alexander's law

Introduction

Spontaneous nystagmus in patients with vestibular lesions often has a dependency on eye position, first described in 1912 (Alexander 1912) and called Alexander's law, where the slow-phase velocity is highest with gaze in the fast-phase direction. Modern measurements have further quantified Alexander's law in patients (Hegemann et al. 2007; Bockisch and Hegemann 2008), and caloric stimulation has been used to simulate peripheral vestibular disorders in healthy subjects and evoke similar patterns of eye position dependency as have been described in patients (Doslak et al. 1982; Robinson et al. 1984; Jeffcoat et al. 2008; Bockisch et al. 2012).

Hess (1982), and shortly thereafter Robinson et al. (1984), proposed that Alexander's law arose from changes in the brainstem/cerebellar velocity-to-position neural integrator, such that the integrator produces a smaller-than-normal command to compensate for elastic forces produced by

Electronic supplementary material The online version of this article (doi:10.1007/s00221-013-3423-6) contains supplementary material, which is available to authorized users.

C. J. Bockisch (✉) · D. Straumann
Department of Neurology, University Hospital Zürich, Frauenklinikstrasse 26, 8091 Zurich, Switzerland
e-mail: chris.bockisch@usz.ch

C. J. Bockisch
Department of Ophthalmology, University Hospital Zürich, Zurich, Switzerland

C. J. Bockisch · E. Khojasteh · S. C. A. Hegemann
Department of Otorhinolaryngology, Head and Neck Surgery, University Hospital Zürich, Zurich, Switzerland

C. J. Bockisch · D. Straumann · S. C. A. Hegemann
Zürich Centre for Integrative Human Physiology (ZIHP), University Hospital Zürich, University of Zürich, Zurich, Switzerland

Published online: 06 February 2013

the extraocular tissues that pull the eye back to a central position. This would then result in centripetal drift of the eyes, which when added to the constant velocity signal from the vestibular system produces the eye position dependency of velocity.

The oculomotor velocity-to-position neural integrator has been localized to the brainstem [nucleus prepositus hypoglossi (Cannon and Robinson 1987; Cheron and Godaux 1987) and medial vestibular nucleus (McFarland and Fuchs 1992; McConville et al. 1994) for horizontal eye position, and the interstitial nucleus of Cajal for vertical and torsional position (King et al. 1981; Crawford et al. 1991; Crawford and Vilis 1993; Crawford 1994; Helmchen et al. 1998; Farshadmanesh et al. 2007)] and cerebellum (Takemori and Cohen 1974; Zee et al. 1981; Waespe et al. 1983). Typically, the brainstem is modeled as a positive position feedback system that increases the neural integrator time constant to around 12 s, and the cerebellum is modeled as a negative velocity feedback system that further increases the time constant to ~25 s (Optican and Zee 1984; Glasauer 2006).

Robinson et al. (1984) suggested that the process producing Alexander's law is an adaptive response to the vestibular lesion. Centripetal drift caused by a leaky integrator, when added to the constant velocity drift produced by the vestibular lesion, will reduce eye velocity in the direction of the slow phase, thus aiding vision for some gaze directions. Robinson et al. (1984) also performed several experiments to support the adaptation hypothesis. First, they reported that Alexander's law is not seen during 0.5-Hz sinusoidal head oscillations in normal humans, concluding it is not due to the normal vestibular ocular reflex (VOR). Second, they reported during caloric stimulation the emergence of Alexander's law is delayed by about 25 s relative to the onset of nystagmus, thus giving it the appearance of an adaptive response to non-reciprocal (unilateral) vestibular stimulation (which Robinson et al. called 'unnatural'). Unilateral caloric stimulation, as well as peripheral vestibular lesions, produces non-reciprocal stimulation in the sense that vestibular input from one side is not accompanied by the opposite change from the other side. Finally, during low constant head acceleration on a turntable ($2.1°/s^2$ after a velocity step of 30°/s), Alexander's law was found but was reported to be weak and constant during the 60 s of stimulation. They interpreted this as meaning that a natural head rotation signal does not evoke Alexander's law; rather, a non-reciprocal pattern of stimulation (unilateral caloric or peripheral lesions) is necessary to provoke the adaptive mechanism.

We recently observed Alexander's law with bilateral bithermal stimulation (cold on one side, warm on the other) (Bockisch et al. 2012), which preserves the normal push–pull pattern of stimulation from real head movements, which suggests Robinson et al.'s (1984) hypothesis should be re-evaluated. Peripheral vestibular disorders and caloric stimulation contain frequencies that are much lower than those produced by natural head movements and could help explain why Alexander's law has not been observed with higher-frequency head rotations (Robinson et al. 1984; Anagnostou et al. 2011). We therefore sought a stronger test of Robinson et al.'s (1984) hypothesis that only non-reciprocal patterns of stimulation produce Alexander's law. We chose a variant of their constant stimulation experiment, but did so with a paradigm that produces higher levels of nystagmus (simply by using higher velocities and accelerations), because our work in patients found that the strength of Alexander's law increased with higher levels of slow-phase velocity (Hegemann et al. 2007; Bockisch and Hegemann 2008), thus opening the possibility that Alexander's law was low in Robinson et al.'s (1984) constant stimulation experiments because the stimulus was too weak.

Methods

Subjects and equipment

Ten subjects with no reported visual or vestibular problems were studied. The experiments conformed to the principles of the Declaration of Helsinki and were approved by the local ethics committee. Subjects gave informed, written consent after the experimental procedure had been explained.

Subjects sat on a rotatable chair controlled with three motor-driven axes (Acutronic, Jona, Switzerland). Only the earth-vertical axis was used in these experiments. Subjects were secured in the chair with safety belts, and the head was fixed to the chair with individually adjusted masks (Sinmed BV, Reeuwijk, the Netherlands). The mask, made of a thermoplastic material (Posicast), was molded to the contour of the head. The center of the head was positioned in or near the chair rotation axis.

Search coils, produced by Skalar (Delft, the Netherlands) or Universal Trading Ventures, Inc (Cleveland, USA), were used to record the three-dimensional movements of both eyes. Orthogonal magnetic fields with frequencies of 80, 96, and 120 Hz were produced by a head-fixed coil frame ($0.5\ m^3$). A fast Fourier transform was computed in real time by a digital signal processor to determine the voltage induced by each magnetic field (Primelec, Regensdorf, Switzerland). Eye position signals were digitized with 12-bit accuracy and sampled at 1,000 Hz using National Instruments (Austin, Texas) hardware and Labview software. Data were analyzed off-line with MatLab software (The MathWorks, Boston, MA). Coils were calibrated in vivo by having subjects fixate

targets from 0° to ±25°, horizontally and vertically, in 5° increments.

A laser spot (~0.25° diameter) controlled by two mirror galvanometers was projected onto a chair-fixed screen positioned 80 cm in front of the subject for visual targets.

We first collected data for control trials to measure horizontal gaze evoked nystagmus. In darkness, subjects looked at a pulsed target that moved every 2 s from 20° right to straight ahead, and 20° left, for 1 min. We will refer to each consecutive period of right, center, and left fixations as a fixation sequence. The laser was pulsed (20 ms every second) so that we could direct the subject's gaze direction without visually suppressing nystagmus. Subjects were instructed to look in the direction where they last saw the flashed target and to attempt to keep looking in that direction until they saw a flashed target in a different position.

The goal of the acceleration trials was to produce a vestibular stimulus that would create a constant rotational velocity signal for a long period. The stimulus consisted of an initial velocity step, followed by a period of acceleration that increased slowly with time. We used estimated properties of the vestibular system (yaw time constant of 15 s and adaptation time constant of 150 s) to determine the required rotation profile to produce a constant velocity signal of 100°/s. (The existence of the adaptation time constant has been determined from studies of long-lasting vestibular stimulation (Leigh et al. 1981; Boumans et al. 1983; Furman et al. 1989). A plausible explanation of such a mechanism is to null small tonic imbalances between the left- and right-side canals.) The stimulus consisted of a 1-s acceleration ramp from 100°/s^2 to 107°/s^2, followed by a lower acceleration ramp starting at 7.3°/s^2 and increasing at 0.04°/s^2/s (Fig. 1). We approximated the initial acceleration period by a 1-s period of constant acceleration of 100°/s^2, and thereafter, the acceleration stepped to 7.3°/s^2 and increased once a second by 0.04°/s^2 (in other words, we approximated the continuous function by changing the acceleration once per second). The acceleration continued until the velocity reached 400°/s. After a delay to allow nystagmus to decline, we used the same acceleration sequence, but in the opposite direction to change the rotation speed from 400°/s to −400°/s. Figure 1a, b shows the acceleration and velocity profiles. Figure 1c shows the expected response from a system consisting of dominant time constants of 10, 15, or 20 s, an adaptation time constant of 150 s, and a gain of 0.5. The initial period of a nearly constant response lasts approximately 38 s. When the acceleration stops, the vestibular response decays and reverses direction due to the adaptation component. During the experiment we monitored eye velocity and did not start the second acceleration period until nystagmus appeared to stop (typically about 4 min). The second acceleration period, during the change from 400°/s to −400°/s, lasted about 78 s. Finally, the chair decelerated to zero using the same profile as the initial acceleration.

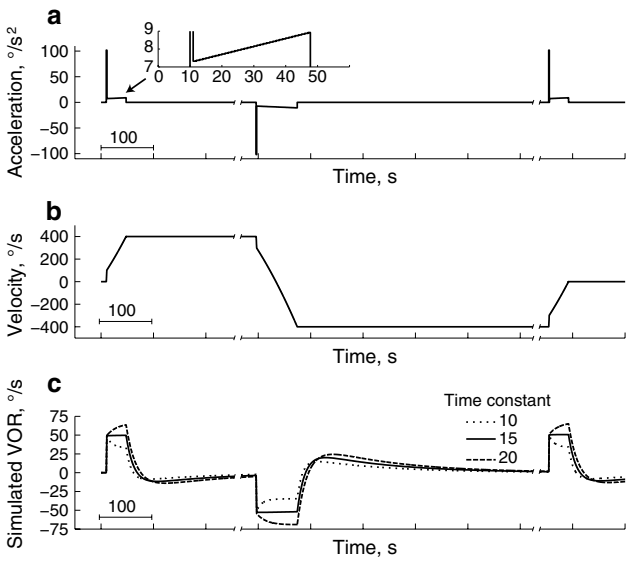

Fig. 1 The *top* and *middle panels* show the stimulus used in the experiments, with head acceleration in **a** and velocity in **b**. The stimulus was an initial step of velocity to about 100°/s, followed by a slowly increasing acceleration (see inset of **a** that shows an expanded view of the initial 50 s, and "Methods" for details). After the rotation reached 400°/s, the acceleration stopped, and the velocity remained constant until the subject's nystagmus stopped. The acceleration profile was then inverted, so that there was an initial velocity step from 400°/s to 300°/s, followed by a slow change in acceleration until the chair reached −400°/s. In **c**, the simulated responses to the stimulus from a system consisting of dominant time constants of 10, 15, or 20 s, and an adaptation time constant of 150 s, and a gain of 0.5 are shown. The velocity response is nearly constant during the acceleration phase, and then during the constant velocity phase, the response declines and reverses direction, before returning toward zero before the next acceleration phase

The initial rotation direction was to the right in half the subjects and to the left in the other half.

Analysis

Data were first filtered with a zero-phase distortion 200-Hz butterworth lowpass filter (butter.m and filtfilt.m, Mathworks). Only horizontal position and velocity were analyzed, and positive rotations are to the left. Since the results for the left and right eyes were similar, we only report the results of the movements of the right eye. Saccades were identified and removed with an interactive computer program that automatically detected saccades when velocity exceeded a threshold (typically 20–30°/s, depending upon the noise level) above the median eye velocity calculated over a 1-s window. The automatically marked saccades could be manually adjusted and blink artifacts removed. To ensure that saccadic components were not included in the slow phases, in particular the initial portion which can be

influenced by the more gradual end of saccades, the first 10 and final five samples of each slow phase were discarded.

Nystagmus slow phases shorter than 50 ms were discarded, and slow phases longer than 100 ms were split into two or more parts of at least 50 ms, to ensure, for unbiased statistical analysis, that roughly the same number of data points occurred in each gaze direction. For each of these slow phases (or parts thereof), we calculated the median position and velocity.

Estimates of the change of nystagmus velocity with eye position were made by fitting second-order equations with linear regression to the velocity-versus-position data:

$$\text{Velocity} = \beta_0 + \beta_1 H + \beta_2 H^2,$$

where β_0 is the intercept (with units of °/s), or velocity at gaze straight ahead, β_1 (s^{-1}) is the slope parameter that describes how velocity changes with horizontal position, H, and β_2 (1/°s) is the second-order component. Inspection of the data showed that velocity generally built up for 3 s following the onset of the change in acceleration and then was fairly constant. So, we discarded the first 3 s of data before further analysis. We did fits to the entire acceleration period (excluding the first 3 s), as well as doing fits to the first and second half of the period, and tested whether the fitted parameters changed using a dummy variable to code for the two time periods (Kleinbaum et al. 1988). Finally, we did linear fits to each fixation sequence, so we could analyze the change in nystagmus in more temporal detail. In order to determine when the slope during the acceleration period first became significantly different from control values, we used Bonferroni-corrected p values.

When combining data across different rotation directions, we first took the absolute value of the fitted intercepts.

Results

We first measured gaze holding prior to stimulation. The average best-fit, second-order parameters were −0.2°/s, −0.031 1 s^{-1}, and 3.7×10^{-6} 1/°s. The average intercepts and second-order terms were not significantly different from zero (t test, ps > 0.3), but the average slope term was less than 0 ($t = 2.9$, $p < 0.05$). A leaky velocity-to-position neural integrator with time constant τ will produce velocity that varies with horizontal position H according to the following equation:

$$\text{Velocity} = -\frac{H}{\tau} + \text{bias}$$

where bias is the velocity produced by the vestibular stimulation. So, an integrator time constant can be inferred from the fitted equations by −1/slope. The average time constant was 32 s.

Development of Alexander's law

Eye velocity increased rapidly in the first several seconds after the onset of acceleration. Figure 2 shows examples from three subjects (see also Online resource 1). For the subject in the top row, after the initial increase in eye velocity at the start, the velocity was fairly constant for the remainder of the acceleration period. The fitted second-order equations for the first and second halves are shown in Fig. 2b and are nearly identical, indicating that the eye velocity was very stable. For the subject shown in panels C and D, eye velocity increased from the first to the second halves, whereas

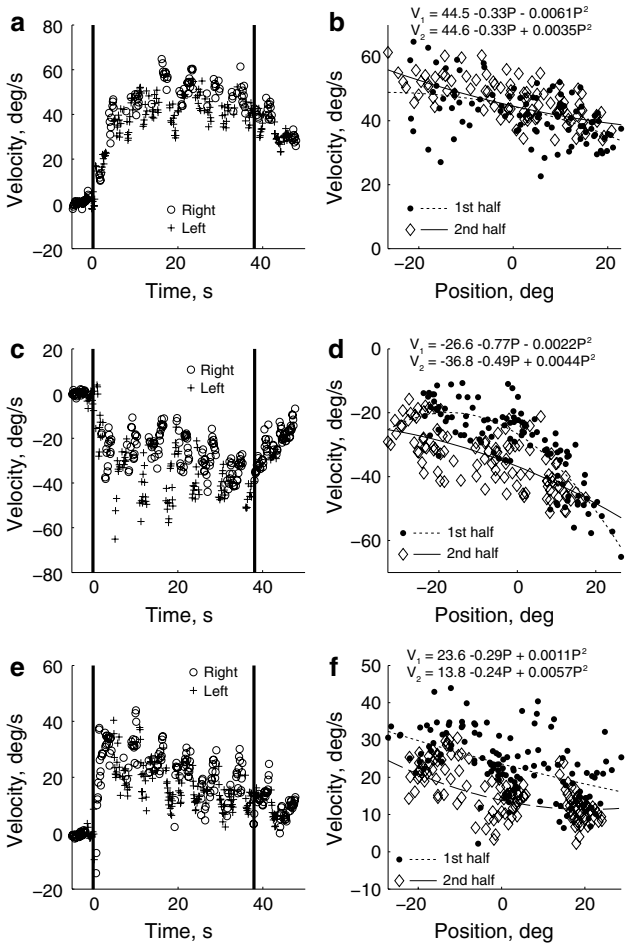

Fig. 2 Example data, with different subjects shown in each row. The *left column* shows the eye velocity of individual slow phases plotted as a function of time, with different symbols to indicate whether the subject was looking left or right of straight ahead. *Vertical lines* mark the start and end of the acceleration period. The *right column* shows eye velocity of individual slow phases plotted against horizontal position for the acceleration period, excluding the first 3 s. *Different symbols* indicate when the data point was from the first or second half of the experiment. The best-fit, second-order equations for the first and second half of the data are shown at the *top* (V velocity, with the subscript indicating the first or second half, P is position)

Table 1 The average parameters from the best-fit, second-order equations for the control and each acceleration period

Acceleration period	Intercept (°/s)		Slope (s^{-1})		Quadratic (1/°s)	
	Mean	Δ	Mean	Δ	Mean	Δ
Control	−0.245		−0.031*		3.7×10^{-6}	
1st	30.39***	−0.41	−0.380***	−0.074	−0.0007	−0.0030
2nd	31.09***	−1.17	−0.331*	−0.058	−0.0049	−0.0037
3rd	33.90***	−2.28	−0.483**	0.095**	−0.0068	−0.0049

The column marked "Δ" provides the difference between the first and the second halves (2nd − 1st) of each acceleration period

t test results: *** $p < 0.001$, ** $p < 0.01$, * $p < 0.05$

eye velocity decreased over time for the subject in panels E and F.

The second-order fits to the entire acceleration period found that while the average slope term was significantly different from zero (−0.38, $t = 9.6$, $p < 0.001$), the average quadratic term was not (−0.001, $t = 0.3$, $p = 0.76$) (Table 1). In addition, the slope term was significant in all 10 subjects, whereas the quadratic term was significant in only three.

Overall, there was little change in the best-fit, second-order equations between the first and second periods (Fig. 3). The average magnitudes of the intercepts were 30.8°/s and 30.4°/s for the first and second halves, respectively, and were not significantly different ($t = 0.2$, $p = 0.84$). Likewise, the best-fit slopes (−0.366 and −0.347) were not significantly different ($t = 0.4$, $p = 0.68$), nor were the second-order terms different (0.0013 and −0.0017; $t = 0.92$, $p = 0.38$).

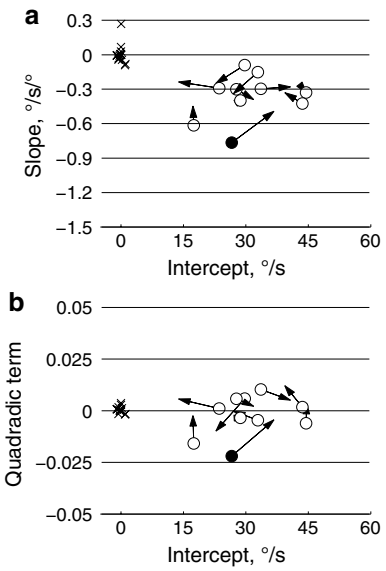

Fig. 3 The parameters of the best-fit, second-order equations to velocity-versus-position data are shown for the first acceleration period. Panel **a** plots the slope versus the intercept, and **b** plots the quadratic term versus the intercept. *Circles* show the fits to the first half of the acceleration period, and the arrows end at the values for the second half of the acceleration period. *Filled circles* indicate the change in slope (**a**) or quadratic (**b**) terms were significant. The *X*'s show control data

To analyze how nystagmus evolved over time in more detail, we did linear fits (since the second-order terms in the previous analysis were not significantly different from zero overall) to each fixation sequence (Fig. 4), including the 3 min after the acceleration in order to analyze the decay of nystagmus. For the first fixation sequence, six of the ten subjects showed slopes that were significantly different from control trials during the first fixation sequence (mean intercept = 30°/s, mean slope = −0.3). The first significant slope occurred, on average, 10 s after the start of the acceleration. Eye velocity declined rapidly after the acceleration ended and then reversed direction (Fig. 4a). The average maximum reversal velocity (intercept) was −9°/s and occurred 59 s after the end of the acceleration. The slopes declined rapidly, but did not reverse (Fig. 4b); rather, they declined to a value of about −0.1 and then decayed with a time course similar to that of the intercept. Figure 4c shows an apparent relationship between the slope and the intercept, as higher intercepts tend to be associated with steeper slopes.

The results for the second and third acceleration periods were similar (see Table 1). The mean slopes were significantly different from control in all periods, whereas the average quadratic term was not. Recall that the second acceleration period was 78 s long, compared to 38 s for the first and third periods, which could have increased the ability to detect changes in the parameters over time. Nonetheless, the fitted parameters were very stable, with only a small reduction in the slope in the third acceleration period.

Discussion

We found an eye position dependency of the slow phase of nystagmus during constant vestibular stimulation similar to Alexander's law. Like Robinson et al. (1984), we found it was mostly stable during the entire period of stimulation, as

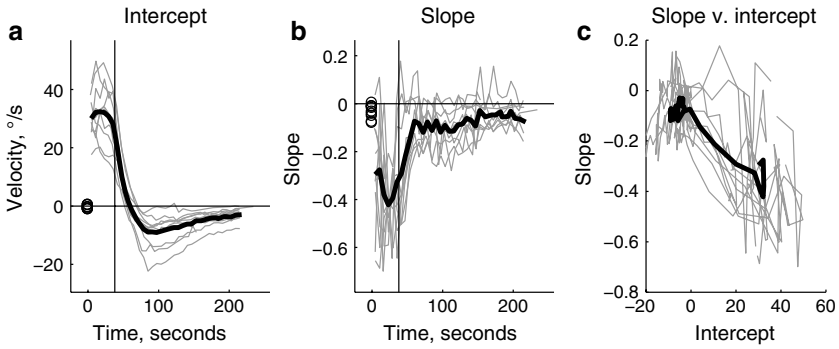

Fig. 4 The time course of linear fits to each fixation sequence. *Thin lines* are individual subjects, and the *thick black line* is the mean. *Circles* at time = 0 are control data. **a** Intercepts. **b** Slopes. **c** The slopes are plotted relative to the intercepts

the magnitude was similar in the first and second halves of the acceleration period. Alexander's law was also apparent in 6/10 subjects in the first fixation sequence and occurred on average 10 s after the onset of acceleration. Unlike the results of Robinson et al. (1984), however, the size of the effect was large and similar to what occurs in patients. Here, we found slopes of about −0.4 for nystagmus velocities of 30°/s, which are comparable to our patient studies where we found slopes of about −0.3 to −0.4 for velocities around 25°/s (Hegemann et al. 2007; Bockisch and Hegemann 2008).

Robinson et al. (1984) concluded that the eye position dependency found during constant acceleration (natural stimulation, in the sense that normal push–pull stimulation pattern is maintained, albeit for an unusual duration) was different from that observed in patients and with caloric stimulation (non-reciprocal and therefore unnatural stimulation, because a change in vestibular input from one side is not accompanied by the opposite change from the other side), because (1) the magnitude was small and (2) it did not evolve over time. This led Robinson et al. to conclude that Alexander's law was an adaptive response, as it reduced eye velocity in some gaze directions, to non-reciprocal stimulation. We suggest this is incorrect for three reasons. First, the small magnitude was likely because the velocity and acceleration were lower than what we used (a 30°/s velocity step followed by 2.1°/s^2, compared to a 107°/s step followed by an acceleration ramp that began at 7.1°/s^2), since the magnitude of Alexander's law increases with increasing nystagmus. Second, in their caloric stimulation study of three subjects, they report that the peak of Alexander's law was delayed, on average, 25 s from the peak of nystagmus velocity, and from this they concluded that Alexander's law needs 25 s of non-reciprocal stimulation to develop. However, in their data a clear eye position dependency is apparent before the peak nystagmus; the fact that the peak position dependency was delayed cannot be used to conclude that Alexander's law was not developing earlier. In our experiment, Alexander's law was found on average 10 s after the onset of stimulation. Third, in our recent study with caloric stimulation, we observed Alexander's law with bilateral bithermal stimulation (cold on one side, warm on the other) (Bockisch et al. 2012). This stimulus preserves the push–pull pattern of natural stimulation and is further evidence against the Robinson et al.'s (1984) hypothesis.

Doslak (Doslak et al. 1979, 1982) proposed that Alexander's law occurs because of an eye position dependency within the VOR pathway. According to the model, whenever the difference between the right and left canal signals exceeds a threshold, an eye velocity signal is added that depends upon eye position. Our finding that Alexander's law occurs with constant vestibular stimulation, with very little change over time, supports the Doslak model. However, the Doslak model also predicts that the velocity-versus-position slope should be independent of nystagmus speed (above a threshold), but that is not the case in our study (Fig. 4c), nor with caloric stimulation (Bockisch et al. 2012). The model of Doslak et al. also predicts Alexander's law should occur with the normal VOR, yet it is not found with 0.5-Hz sinusoidal head rotations on a turntable (Robinson et al. 1984) or head impulses (Anagnostou et al. 2011; Anastasopoulos and Anagnostou 2012).

Jeffcoat et al. (2008) proposed a different account of Alexander's law, where the gain of extraocular motor neurons varies with position and whether the velocity inputs come from increased or decreased canal activity. This hypothesis was based on the findings that eye movements and abducens neuron responses to short duration auditory stimuli depend upon eye position (Zhou et al. 2004, 2007). Jeffcoat et al. (Jeffcoat et al. 2008) proposed that with decreased canal activity, the abducens neuron gain *decreases* with adducting eye position, thus producing Alexander's law in patients with vestibular lesions and unilateral cold caloric stimulation. With increased canal activity, abducens neuron gain *increases* with adducting eye position. This model thus predicts a reversed Alexander's law with unilateral warm caloric stimulation, which they reported (Jeffcoat et al. 2008). With normal, reciprocal stimulation of the canals, the gain changes with eye position cancel, producing a VOR that does not depend on eye position. Thus, this model does

not predict Alexander's law during constant acceleration protocols, as we observed here, nor with bilateral bithermal caloric stimulation (Bockisch et al. 2012).

Constant acceleration and caloric stimulation protocols that show Alexander's law produce very low-frequency stimulation, whereas the VOR studies that do not show Alexander's law use higher-frequency stimuli. Alexander's law then may be a consequence of the velocity-to-position neural integrator being insensitive to very low-frequency signals. One reason for this could be that natural head movements contain mainly high-frequency components. Another reason could be to make the integrator insensitive to small imbalances in the tonic stimulation from the left and right vestibular canals. While another mechanism to compensate for such imbalances exists [up-regulation of tonic inputs following peripheral lesion (Smith and Curthoys 1989)], this mechanism operates on a timescale of hours or days (Ris and Godaux 1998).

If Alexander's law is a consequence of low-frequency stimulation, then it is tempting to speculate on the role of the velocity-storage mechanism, which enhances the low-frequency canal response in order to correctly interpret linear acceleration signals from the otoliths (Laurens and Angelaki 2011). While the linear VOR is highly eye position dependent, to produce Alexander's law would require target distance to change with eye position, being nearer when in the fast-phase direction. The flashed targets in our setup were presented on a flat screen, with no distance difference for left and right targets. Thus, there is not an obvious functional connection between the velocity-storage mechanism and Alexander's law.

A different explanation of Alexander's Law in acute unilateral vestibular deficit has recently been proposed by Khojasteh et al. (2012). Due to the vestibular lesion and insufficient tonic activity on the ipsilesional primary afferents, the ipsilesional vestibular nucleus is silenced, while the contralesional vestibular nucleus becomes hyperactive (Smith and Curthoys 1989). Khojasteh et al. (2012) suggested that this asymmetry in the response of the bilateral vestibular nuclei reduces the linear operating range of the central VOR circuits, which perform the integration of velocity signals. The gain of the brainstem positive feedback loop thus becomes dependent on the merging neural activity, making the integration process dependent on eye movement signals. They hence propose that in the slow-phase direction (side of the lesion) integration of eye signals is insufficient (leaky), while in the fast-phase direction the integrator could become unstable. Khojasteh et al. (2012) further speculated that the persistent stimulation of the primary vestibular afferents by very low-frequency stimuli could in the same manner saturate the vestibular nucleus on one side, while pushing the other vestibular nucleus into inhibitory cutoff, thus producing eye position–dependent integration similar to unilateral vestibular lesions.

Patients suffering from spontaneous nystagmus due to an acute vestibular tone asymmetry show velocity that varies with position in a nonlinear fashion (Hegemann et al. 2007; Bockisch and Hegemann 2008). We did not find similar effects here, or in our experiments with caloric stimulation (Bockisch et al. 2012). Perhaps, in patients there are adaptive mechanisms to suppress nystagmus which cause the nonlinear behavior, since these patients typically had nystagmus for several days before being measured. In their model of the velocity-to-position neural integrator, which was developed to describe congenital nystagmus, Optican and Zee (1984) proposed that eye position–dependent nonlinearities were necessary to account for changes in nystagmus waveforms with eye position that occur in these patients. Perhaps, modifications to such mechanisms require either more time than was available in the protocol used here (patients were typically measured hours or days after the onset of symptoms) or the presence of retinal slip information that was excluded in our experiments by performing them in the dark.

Clinicians often treat the presence of Alexander's law in spontaneous nystagmus as a sign of a peripheral vestibular lesion, though we suggest it is not conclusive. If Alexander's law is in fact a consequence of low-frequency velocity inputs to the velocity-to-position neural integrator, from any source, then Alexander's law ought to occur. One example of this is pursuit after-nystagmus (Marti et al. 2005). However, with other forms of nystagmus, such as infantile nystagmus syndrome, the Alexander's law mechanism might be invoked, but the variation in eye velocity with position would be difficult to detect due to the complex (and temporally unstable) velocity inputs.

Acknowledgments We would like to thank Beckey Trihn for collecting data on preliminary experiments and Marco Penner for technical support. This study was financially supported by the Swiss National Science Foundation, the Betty and David Koetser Foundation for Brain Research, Zurich, Switzerland, and the Center of Integrative Human Physiology, University of Zurich, Switzerland. E. Khojasteh receives the FQRNT postdoctoral scholarship from Quebec, Canada.

References

Alexander G (1912) Die Ohrenkrankheiten im Kindesalter. In: Schlossmann A (ed) Handbuch der Kinderheilkunde. Vogel, Leipzig, pp 84–96

Anagnostou E, Heimberger J, Sklavos S, Anastasopoulos D (2011) Alexander's law during high-acceleration head rotations in humans. NeuroReport 22:239–243. doi:10.1097/WNR.0b013e3283451769

Anastasopoulos D, Anagnostou E (2012) Invariance of vestibulo-ocular reflex gain to head impulses in pitch at different initial eye-in-orbit elevations: implications for Alexander's law. Acta Otolaryngol 132:1066–1072. doi:10.3109/00016489.2012.682120

Bockisch CJ, Hegemann S (2008) Alexander's law and the oculomotor neural integrator: three-dimensional eye velocity in patients with an acute vestibular asymmetry. J Neurophysiol 100:3105–3116

Bockisch CJ, Khojasteh E, Straumann D, Hegemann S (2012) Development of eye position dependency of slow phase velocity during caloric stimulation. PLoS ONE 7:e51409. doi:10.1371/journal.pone.0051409

Boumans LJ, Rodenburg M, Maas AJ (1983) Response of the human vestibulo-ocular reflex system to constant angular acceleration. II. Experimental investigation. ORL J Otorhinolaryngol Relat Spec 45:130–142

Cannon SC, Robinson DA (1987) Loss of the neural integrator of the oculomotor system from brain stem lesions in monkey. J Neurophysiol 57:1383–1409

Cheron G, Godaux E (1987) Disabling of the oculomotor neural integrator by kainic acid injections in the prepositus-vestibular complex of the cat. J Physiol 394:267–290

Crawford JD (1994) The oculomotor neural integrator uses a behavior-related coordinate system. J Neurosci 14:6911–6923

Crawford JD, Vilis T (1993) Modularity and parallel processing in the oculomotor integrator. Exp Brain Res 96:443–456

Crawford JD, Cadera W, Vilis T (1991) Generation of torsional and vertical eye position signals by the interstitial nucleus of Cajal. Science 252:1551–1553

Doslak MJ, Dell' Osso LF, Daroff RB (1979) A model of Alexander's law of vestibular nystagmus. Biol Cybern 34:181–186

Doslak MJ, Dell'Osso LF, Daroff RB (1982) Alexander's law: a model and resulting study. Ann Otol Rhinol Laryngol 91:316–322

Farshadmanesh F, Klier EM, Chang P, Wang H, Crawford JD (2007) Three-dimensional eye-head coordination after injection of muscimol into the interstitial nucleus of Cajal (INC). J Neurophysiol 97:2322–2338

Furman JM, Hain TC, Paige GD (1989) Central adaptation models of the vestibulo-ocular and optokinetic systems. Biol Cybern 61:255–264

Glasauer S (2006) Cerebellar contribution to saccades and gaze holding: a modeling approach. Ann N Y Acad Sci 1004:206–219

Hegemann S, Straumann D, Bockisch C (2007) Alexander's law in patients with acute vestibular tone asymmetry—evidence for multiple horizontal neural integrators. J Assoc Res Otolaryngol 8:551–561. doi:10.1007/s10162-007-0095-6

Helmchen C, Rambold H, Fuhry L, Buttner U (1998) Deficits in vertical and torsional eye movements after uni- and bilateral muscimol inactivation of the interstitial nucleus of Cajal of the alert monkey. Exp Brain Res 119:436–452

Hess K (1982) Do peripheral-vestibular lesions in man affect the position integrator of the eyes? Neurosci Lett Suppl 10:242–243

Jeffcoat B, Shelukhin A, Fong A, Mustain W, Zhou W (2008) Alexander's law revisited. J Neurophysiol 100:154–159

Khojasteh E, Bockisch CJ, Straumann D, Hegemann SCA (2012) A dynamic model for eye-position-dependence of spontaneous nystagmus in acute unilateral vestibular deficit. Eur J Neurosci. doi:10.1111/ejn.12030

King WM, Fuchs AF, Magnin M (1981) Vertical eye movement-related responses of neurons in midbrain near intestinal nucleus of Cajal. J Neurophysiol 46:549–562

Kleinbaum DG, Kupper LL, Muller KE (1988) Applied regression analysis and other multivariable methods. PWS-Kent Publishing Company, Boston

Laurens J, Angelaki DE (2011) The functional significance of velocity storage and its dependence on gravity. Exp Brain Res 210:407–422. doi:10.1007/s00221-011-2568-4

Leigh RJ, Robinson DA, Zee DS (1981) A hypothetical explanation for periodic alternating nystagmus: instability in the optokinetic-vestibular system. Ann N Y Acad Sci 374:619–635

Marti S, Bockisch CJ, Straumann D (2005) Prolonged asymmetric smooth-pursuit stimulation leads to downbeat nystagmus in healthy human subjects. Invest Opththalmol Vis Sci 46:143–149

McConville K, Tomlinson RD, King WM, Paige G, Na EQ (1994) Eye position signals in the vestibular nuclei: consequences for models of integrator function. J Vestib Res 4:391–400

McFarland JL, Fuchs AF (1992) Discharge patterns in nucleus prepositus hypoglossi and adjacent medial vestibular nucleus during horizontal eye movement in behaving macaques. J Neurophysiol 68:319–332

Optican LM, Zee DS (1984) A hypothetical explanation of congenital nystagmus. Biol Cybern 50:119–134

Ris L, Godaux E (1998) Spike discharge regularity of vestibular neurons in labyrinthectomized guinea pigs. Neurosci Lett 253:131–134

Robinson DA, Zee DS, Hain TC, Holmes A, Rosenberg LF (1984) Alexander's law: its behavior and origin in the human vestibulo-ocular reflex. Ann Neurol 16:714–722

Smith PF, Curthoys IS (1989) Mechanisms of recovery following unilateral labyrinthectomy: a review. Brain Res Brain Res Rev 14:155–180

Takemori S, Cohen B (1974) Loss of visual suppression of vestibular nystagmus after flocculus lesions. Brain Res 72:213–224. doi:10.1016/0006-8993(74)90860-9

Waespe W, Cohen B, Raphan T (1983) Role of the flocculus and paraflocculus in optokinetic nystagmus and visual-vestibular interactions: effects of lesions. Exp Brain Res 50:9–33

Zee DS, Yamazaki A, Butler PH, Gucer G (1981) Effects of ablation of flocculus and paraflocculus of eye movements in primate. J Neurophysiol 46:878–899

Zhou W, Mustain W, Simpson I (2004) Sound-evoked vestibulo-ocular reflexes (VOR) in trained monkeys. Exp Brain Res 156:129–134. doi:10.1007/s00221-003-1778-9

Zhou W, Xu Y, Simpson I, Cai Y (2007) Multiplicative computation in the vestibulo-ocular reflex (VOR). J Neurophysiol 2780–2789

OPEN ACCESS Freely available online

PLOS ONE

Gaze Holding in Healthy Subjects

Giovanni Bertolini[1]*, Alexander A. Tarnutzer[1], Itsaso Olasagasti[1], Elham Khojasteh[2], Konrad P. Weber[1,3], Christopher J. Bockisch[1,2,3], Dominik Straumann[1], Sarah Marti[1]

1 Department of Neurology, University Hospital Zurich, Zurich, Switzerland, **2** Departments of Otorhinolaryngology, Head and Neck Surgery, University Hospital Zurich, Zurich, Switzerland, **3** Department of Ophthalmology, University Hospital Zurich, Zurich, Switzerland

Abstract

Eccentric gaze in darkness evokes minor centripetal eye drifts in healthy subjects, as cerebellar control sufficiently compensates for the inherent deficiencies of the brainstem gaze-holding network. This behavior is commonly described using a leaky integrator model, which assumes that eye velocity grows linearly with gaze eccentricity. Results from previous studies in patients and healthy subjects suggest caution when this assumption is applied to eye eccentricities larger than 20 degrees. To obtain a detailed characterization of the centripetal gaze-evoked drift, we recorded horizontal eye position in 20 healthy subjects. With their head fixed, they were asked to fixate a flashing dot (50 ms every 2 s)that was quasi-stationary displacing(0.5 deg/s) between $\pm$40 deg horizontally in otherwise complete darkness. Drift velocity was weak at all angles tested. Linearity was assessed by dividing the range of gaze eccentricity in four bins of 20 deg each, and comparing the slopes of a linear function fitted to the horizontal velocity in each bin. The slopes of single subjects for gaze eccentricities of $\pm$0$-$20 deg were, in median,0.41 times the slopes obtained for gaze eccentricities of $\pm$20$-$40 deg. By smoothing the individual subjects' eye velocity as a function of gaze eccentricity, we derived a population of position-velocity curves. We show that a tangent function provides a better fit to the mean of these curves when large eccentricities are considered. This implies that the quasi-linear behavior within the typical ocular motor range is the result of a tuning procedure, which is optimized in the most commonly used range of gaze. We hypothesize that the observed non-linearity at eccentric gaze results from a saturation of the input that each neuron in the integrating network receives from the others. As a consequence, gaze-holding performance declines more rapidly at large eccentricities.

Citation: Bertolini G, Tarnutzer AA, Olasagasti I, Khojasteh E, Weber KP, et al. (2013) Gaze Holding in Healthy Subjects. PLoS ONE 8(4): e61389. doi:10.1371/journal.pone.0061389

Editor: Susana Martinez-Conde, Barrow Neurological Institute, United States of America

Received September 19, 2012; **Accepted** March 8, 2013; **Published** April 26, 2013

Funding: This study was supported by Swiss National Science Foundation (32003B_130163/1), Koetser Foundation for Brain Research, Zurich; Bonizzi Theler Foundation, Zurich; and Center for Integrative Human Physiology, University of Zurich. The funders had no role in study design, data collection and analysis, decision to publish, or preparation of the manuscript.

Competing Interests: The authors have declared that no competing interests exist.

* E-mail: bertoweb@gmail.com

Introduction

Most healthy human subjects display a physiological centrifugal horizontal nystagmus at extreme lateral gaze in darkness ([1]). This 'end-point nystagmus' suggests that the gaze-holding system's performance noticeably degrades at larger eccentricities. The occurrence of end-point nystagmus is, however, quite variable and subjects showing no end-point nystagmus at all, regardless of eccentricity, have been reported ([2], [3], [4], [5]) while others show such nystagmus already at small gaze eccentricities ([2], [5]). These contrasting findings have been explained by the strong influence of the physical status of the subjects ([6] for review). For example alcohol consumption ([7], [8], [9]) as well as sleep deprivation ([5]) decrease the minimal horizontal gaze eccentricity at which end-point nystagmus appears.

In general, however, gaze shifts to moderate horizontal eccentricities evoke, even in darkness, only very weak centripetal eye drift in healthy subjects, as cerebellar control sufficiently compensates for the inherent leakiness of the brainstem gaze-holding network ([10], [11], [12], [13], [14]). Cerebellar disease unmasks the deficient behavior of the brainstem gaze holding system and leads to prominent gaze-dependent centripetal drift at small horizontal gaze-eccentricities, i.e. gaze-evoked nystagmus ([1], [15]). Patients affected by cerebellar disease often also show a transient nystagmus in the direction of the previous gaze eccentricity upon returning to primary gaze position after sustained eccentric fixation. This nystagmus, usually called rebound nystagmus ([16], [17]), is a consequence of a mechanism that reduces excessive drift velocity during a sustained eccentric fixation. Minimal rebound nystagmus has also been observed in some healthy subjects ([4], [18], [19]). Its presence in healthy subjects - although infrequent - suggests that physiological drift velocities may be sufficient to activate the adaptive mechanisms generating it.

To better understand the physiological and pathological manifestations of the inherent deficiencies of the gaze holding system, it is crucial to clarify how the centripetal horizontal eye drift grows in relation to eccentric gaze position. Several studies reported drift velocity for only one or very few specific horizontal gaze eccentricities (typically 30, 40 or 50 deg) ([3], [4], [18], [20]). This approach does not allow a detailed investigation of the relationship between the ability to hold gaze stable and concurrent eye eccentricity, but it is sufficient to characterize it under a simple modeling hypothesis: in order to obtain the eye position command for the ocular motor neurons, the velocity command needs to be integrated by a network of neurons, which is modeled as a leaky integrator ([11], [21]) with a time constant usually estimated between 10 s and 70 s ([1], [22]). Such a model results in an eye

drift velocity that grows linearly with eye eccentricity with a slope equal to the reciprocal of the leaky integrator time constant ([11], [12], [21]).The cerebellum is hypothesized to provide a feedback loop in the model, which prolongs the time constant of the integrator, scaling down the slope of the eye drift with eye eccentricity ([23]). Early studies in patients ([24], [25]) observed nonlinear behavior in pathological nystagmus and therefore proposed modifications to the leaky integrator model, introducing an eye eccentricity dependent nonlinearity in the gain of the cerebellar feedback loop to account for nonlinear behavior. These nonlinearities were mainly considered to describe specific pathological conditions, although nonlinear growth of centripetal eye drift velocity with gaze eccentricity has also been observed in healthy human subjects ([3]). Nonlinear behavior at large eccentricities is not surprising since integration, the ability to maintain and update multiple levels of persistent activity, requires neuronal and network processes, that include nonlinearities such as the inhibitory cutoff in neuronal firing and possibly nonlinear synaptic transmission ([26], [27]). This supports a modeling hypothesis alternative to the leaky integrator, based on a network of neurons, whose properties mimic those observed from the neurons believed to be part of the gaze holding network. Such a model could explain both the leakiness and the nonlinearity, as they arise naturally from neuronal behavior. Additionally it could simulate the dependence of behavior on the tuning, which can be hypothesized to be under cerebellar control.

The purpose for the present study is, therefore, to characterize the relation between centripetal eye drift velocity and gaze eccentricity in healthy human subjects and clarify the limit of applicability of the single time constant leaky integrator model.

Methods

Subjects

Twenty healthy human subjects (8 females; mean age ± 1 SD: 41 ± 11 years; range 24–67 years) participated in the study. Informed consent of all participants was obtained in written form after full explanation of the experimental procedures. The protocol was approved by the Ethics Committee of the Canton of Zurich, Switzerland (Protocol N° E-33/2007), and was in accordance with the ethical standards laid down in the 1964 Declaration of Helsinki for research involving human subjects.

Experimental setup

Participants were comfortably seated upright on a chair mounted on a two servo-controlled motor-driven axes turntable system (Tönnies D561, Freiburg i.Br., Germany; control system: Acutrol® ACT2000, Acutronic, Switzerland Ltd.). The two independent motor-driven axes are coincident and earth vertical. One rotates the chair and the other a cylinder (Optokinetik Drum, radius: 74 cm) mounted concentrically to the chair. Remotely controlled LEDs are attached to the cylinder at the level of subject's eyes. Safety belts around the feet and the shoulders restrained the subject. An adjustable chin rest and a forehead strap were used to stabilize the subject's head.

Recording of eye movements. Horizontal eye movements were recorded at 220 Hz with a head-mounted video-oculography (VOG) device ("EyeSeeCam") ([28], [29]) consisting of swimming goggles with two mounted infrared cameras. A model of the eye rotation is used by the VOG system to derive the horizontal eye position from the pupil position recorded in the coordinate system of the cameras. An additional offline calibration was performed to improve the accuracy. Using the LED attached to the motorized cylinder, before the beginning of the experiment, we asked the subjects to look at a sequence of fixation points. We then fitted a second order polynomial function to the corresponding eye angles provided by the VOG system.

Experimental procedure

Participants were asked to fixate a briefly flashing (50 ms every 2 s) red LED without moving the head. The LED was positioned at the level of the eyes in the range of horizontal gaze eccentricity from 40 deg left to 40 deg right. Each subject was tested in two subsequent runs, changing the order of presentation of the requested gaze eccentricities. Specifically the LED always started straight-ahead and slowly displaced (0.5 deg/s) up to 40 deg of eccentricity in one of the two possible directions (the initial direction was in one run leftward and in the other rightward, randomly selecting the first one), then the direction was reversed, continuing the displacement until the 40 deg of eccentricity of the opposite side was reached, when it was reversed again to return to straight ahead position, where it stopped. Both eyes were recorded simultaneously.

Data analysis

Data analysis was done offline on a PC using interactive programs written in MATLAB (The Mathworks, Natick, MA), version 7.5. Velocity traces were obtained as the derivative of horizontal eye position traces. Saccades and blinks were interactively removed using a custom program that identifies all the data points exceeding by a given threshold the median velocity calculated over a time window moving in steps of one third of its width. The data points that exceeded the threshold at least two times were considered part of a saccade. The beginning and the end of each saccade were identified by searching for the closer reversals of the velocity. All data points belonging to saccades were removed. The threshold was set to 3 deg/s and the width of the window was 0.5 sec. Missing data or unreliable data (due to blinks, or if the pupil could not be reliably found at eccentric positions due to coverage by the eye lids) were not interpolated. We calculated median eye velocities recorded from every single subject within 4 non-overlapping, 20 deg wide bins of eye eccentricity (i.e. 0–20 deg and 20–40 deg for both sides), keeping the two runs (which differ by the starting direction), the two directions of target displacement and the two eyes, separated. Individual median eye velocities from all subjects were compared within each bin using a repeated measures three-way analysis of variance (Matlab function RMAOV33.m) ([30]) with the direction of target displacement, the run and the eye as factors, using post hoc Bonferroni correction to compensate for multiple comparisons.

The behavior of eye drift as a function of gaze eccentricity was analyzed using two separate procedures, one focused on single subject data and the other on pooled whole population data. The first provided a test of the reliability of the linear modeling, by testing the consistency of the parameters estimated by linear fit of different ranges of gaze eccentricity. The second allowed defining the general behavior of gaze holding, evaluating which function can best represent the growth of the drift velocity with gaze eccentricity.

Subject-based data analysis

Instantaneous eye velocity values from both eyes, directions of target displacement and runs were pooled for each subject. The resulting data were sorted according to their eye eccentricity and then split in four 20 deg wide bins from 40 left to 40 right (i.e. 0–20 and20–40 for both sides). Under the assumption of linear behavior, the slopes obtained fitting the data from different bins should be the same within each subject. Calling V the instanta-

neous eye drift velocity and E the horizontal eye eccentricity the following function was fitted to each bin:

$$V = m * E + c_1 \quad (1)$$

The linear slope m and the offset c_1 were optimized with an algorithm (Matlab function quantreg.m) ([31]) for quantiles regression minimizing a sum of squared residuals with respect to the median ([32]), as the assumption of normality of the data required for the ordinary least squares regression was not confirmed. Lilliefors test ([33]) indicated that the slopes in each bin across subjects were not normally distributed. To investigate the linearity of the behavior we performed a paired Wilcoxon signed rank test, between the coefficients estimated from the 0–20 deg bin and those obtained in the 20–40 deg bin, pairing those from each side. Additionally we calculated the ratio of the paired coefficients. A Wilcoxon signed rank test was used to test whether the ratios came from a population with a median different from 1. A median significantly smaller than 1indicates that the rate of growth of the drift velocity increased with gaze eccentricity, demonstrating that a linear fit does not capture the real behavior.

Analysis of the pooled population

Each subject's instantaneous velocity was smoothed as a function of eye eccentricity using a weighted linear least-squares robust regression method (Matlab function smooth.m with "rloess" algorithm) based on a second order polynomial model ([34]) applied on a moving window equal to 20% of the whole range of gaze angles tested (16 deg). The results were interpolated every 0.1 deg from 40 deg left to 40 deg right. Lilliefors test ([33]) was consistent with the normality of the distribution of resulting velocities across subjects at each eccentricity. The mean velocity of all subjects was calculated at each interpolated eye position and fitted with Eq.1 and with the following equations:

$$V = \tan(k * E) + c_2 \quad (2)$$

$$V = \sinh(h * E) + c_3 \quad (3)$$

where *tan* and *sinh* are the tangent and the hyperbolic sine functions, k and h are scaling coefficient and c_2 and c_3 are offsets. Variance accounted for ([35])was used to compare the quality of fit of the three functions. To check for possible distortions of the shape of the curve due to boundary effects of the smoothing process, we repeated the procedure decreasing the size of the moving window to 5% of the whole range of gaze angles tested (4 deg) and compared the obtained parameters.

Mathematical model of a network simulating the gaze holding behavior

To illustrate how the underlying nonlinearities in the brainstem gaze holding networks could surface at extreme eye positions, we used a mathematical model of a network of neurons. The network simulates eye drift velocity by mimicking the physiological behavior of the neurons. The equations of the model were derived as follows.

Electrophysiological data have shown that, during eye fixations, neurons thought to be part of the neural integrator network in the brainstem ([36], [37], [38]) fire approximately linearly with eye position. Mathematically:

$$r_i = [k_i(E - U_i)]_+ \quad (4)$$

The subscript indexes the neurons; r is the firing rate and E the eye position. The two parameters in this expression are the slope, k_i, and the eye position threshold, U_i, which can be measured experimentally. The inhibitory cutoff (there are no negative firing rates) is the only nonlinearity considered in equation 4. We simulated a bilateral network of rate neurons based on published work ([26], [39]) composed of 40 neurons (20 per side). In order to simplify, we consider that the same neurons can lead to both excitatory and inhibitory postsynaptic currents. The firing rate of the neurons in the network is determined by the total amount of input current: excitatory contributions from ipsilateral neurons, inhibitory contributions from contralateral neurons, a tonic input T and a command input B. The postsynaptic current is characterized by a synaptic activation variable s, which determines the active proportion of the maximum synaptic current. We write the weight of the connection from neuron 'j' to neuron 'i' as a product of two factors: the postsynaptic factor ξ_i and the presynaptic factor η_j. NMDA synaptic transmission, with decay time constant on the order of 100 ms, is hypothesized to play an important role in network based persistent activity ([40]). Therefore we will be working in a regime in which synaptic dynamics is slower than firing rate dynamics and we can consider that the firing rate adapts instantaneously to the synaptic input dynamics. In such cases, for a right side neuron i, we can write ([41]):

$$r_{R,i} = \left[\xi_{R,i}\left(\sum_j \eta_{R,j} s_{R,j} - \sum_j \eta_{L,j} s_{L,j}\right) + B_{R,i} + T_{R,i}\right]_+ \quad (5)$$

A similar relation can be written for neurons in the left side population. To model the synaptic current that each neuron creates in the postsynaptic neuron, we use a synaptic activation function $s_\infty()$ with first order dynamics ([26]):

$$\tau_s \frac{ds_i}{dt} = -s_i + s_\infty(r_i) \quad (6)$$

with $\tau_s = 100\ ms$, as suggested by Seung and colleagues ([26]). As mentioned above, this is the order of magnitude of the decay time constant of postsynaptic currents through NMDA receptors. It follows from the above equation that all firing rates depend on the combination:

$$\Delta \equiv \sum_j \eta_{R,j} s_{R,j} - \sum_j \eta_{L,j} s_{L,j} \quad (7)$$

whose dynamic equation can be obtained by differentiating equation 5 and using equations 5 and 6.

$$\tau_S \frac{d\Delta}{dt} = -\Delta + \sum_i \eta_{R,i} s_\infty \left(\left[\xi_{R,i}(\Delta + B_R) + T_{R,i} \right]_+ \right) - \sum_i \eta_{L,i} s_\infty \left(\left[\xi_{L,i}(-\Delta + B_L) + T_{L,i} \right]_+ \right) \quad (8)$$

That is, the dynamics of the network can be reduced to a single equation. This network will maintain stable fixations for any values of Δ for which the right hand side of equation 5, itself a function of Δ, is zero in the absence of driving inputs (when B_R and B_L are zero). For such stable values, equation 5 gives:

$$r_{R,i} = \left[\xi_{R,i}\Delta + T_{R,i} \right]_+ \quad (9)$$

Comparing with equation 4, it is possible to assign Δ to the internal representation of eye position, ξ to the slope of the tuning function and T to the combination $-kU$. The values for ξ and T can be obtained from neurons' tuning curves, which are experimentally accessible ([39]). We generated these values by choosing equally spaced eye position thresholds within right and left populations of the network and by assigning slopes that are slightly increasing as eye thresholds become more ipsilateral to anatomic location of the neurons. The presynaptic factors η are undetermined and can be used to minimize the right hand side of equation 8 in the absence of eye movement commands. We considered both linear and saturating forms of the activation functions s_∞ and used equation 8 to find the values of η that minimize the drift in Δ, which is expressed by the cost function in Eq.10.

$$V = \sum_\Delta \left[-\Delta + \sum_i \eta_{R,i} s_\infty \left(\left[\xi_{R,i}(\Delta + B_R) + T_{R,i} \right]_+ \right) - \sum_i \eta_{L,i} s_\infty \left(\left[\xi_{L,i}(-\Delta + B_L) + T_{L,i} \right]_+ \right) \right]^2 \quad (10)$$

In the dark, the ability to maintain fixations depends on the behavior of equation 8, which gives the drift as a function of Δ. In our simulations, we will consider Δ as a proxy for eye position and derive position velocity plots (PV plots) directly from equation 8.

Results

Figure 1 shows left eye position recorded in one typical subject as a function of time. The presence of a centripetal drift is evident at extreme gaze eccentricities, where a clear end-point nystagmus appears (inset 1 in figure 1-panel A). It is, however, noticeable (inset 2 and 3 in figure 1-panel A) that for lower eye eccentricity the eye position trace did not show centripetal drift. On the contrary, the eyes position displays a rather constant slope, which appears to be related to the direction of target displacement. This is confirmed when looking at the velocity trace in panel C of figure 1, representing the velocity corresponding to eye eccentricities larger than 10 deg (figure 1 - panel B). The eye velocities recorded at 10 degree of eccentricity with the target moving in opposite directions (the two ends of the plot in panel C) have two different values, one for each direction of target displacement, which nearly match the rate of the target displacement (±0.5 deg/s). Panel C in figure 1 also shows that the effect of the deficiency of the gaze holding system is already visible at 25 deg (around 60 s, according to figure 1- panel B), where the end-point nystagmus is absent, but the positive velocity value observed at 10 deg of eccentricity began to decrease.

The constant value of the velocity signal observed in figure 1 (panel C – left end) between 10 deg and 25 deg of eccentricity suggests the presence of a velocity signal, that, at higher eccentricity, is summed to the position dependent centripetal drift that represents the object of our study. To understand how to best account for such a signal when estimating the eye centripetal drift, we plot the medians of the eye velocity recorded within single bins (width = 1 deg) centered at every degree of eye eccentricity in the range tested as a function of gaze, keeping data obtained with the target moving in opposite directions separated (figure 2). As already observable in panel C of figure 1, an eye velocity matching the one of the target displacement is clearly visible at low eccentricity. This is also confirmed by the right panel of figure 2, where the difference between the eye velocities recorded with target moving in opposite directions is reduced after subtraction of the target velocity.

To find out whether the direction of target displacements or other factors affect the recorded instantaneous eye velocity, we calculated for each subject the medians of the velocity within four non-overlapping 20 deg wide bins in the range tested, keeping the different runs (which differ by the starting direction), the different directions of the target displacement and the two eyes separated. Pooling the data of all our subjects, we used a repeated measure three-way ANOVA within each bin separately. After applying Bonferroni correction for multiple comparisons, we found that the run (i.e. initial displacement toward right vs. initial displacement toward left) and the eye (i.e. left vs. right eye) were not associated with a significant difference in any bin. The direction of target displacement was instead a significant factor ($p<0.001$; $F(1,38) = 32.5$ and $F(1,38) = 39.8$ for left and right eccentricities, respectively) in the two central bins (between 0 and 20 deg on both sides), with higher horizontal eye velocities when the target was moving toward the subjects' straight-ahead position, but not in the two outer bins (between 20 and 40 deg on both sides). The median difference between eye velocities recorded at the same eccentricity with the target moving in opposite directions was 0.45 deg/s; approximately half of the value expected considering the two opposite velocity offsets needed to match the target displacement in both directions. This finding, together with the statistical analysis, suggests that the velocity signal observed in figure 1 varied mainly with eye eccentricity and cannot be subtracted as a direction dependent offset. Therefore we pooled the data from both directions at a given gaze angle to cancel the velocity signal, which causes the difference between the two directions of target displacement (figure 2). The resulting median velocity represents the eye centripetal drift velocity due to the gaze holding deficiency.

To investigate the behavior of eye drift as a function of gaze eccentricity we applied two separate analyses to our data: one fitting single subject data and the other evaluating the average of the whole population.

In the first of these analyses, instantaneous velocity recorded from each single subject was sorted as a function of gaze eccentricity, pooling data from the two eyes, the two runs and the directions of target displacement. Data of each subject were separated in four bins defined as for the statistical analysis above. We fitted a linear function of the eye eccentricity (Eq.1) to the values in each bin separately. Figure 3 shows an example of this fitting procedure in a typical subject. The goal of this analysis was to quantify the reliability of the parameters estimated by a linear fit for different ranges of gaze eccentricity.

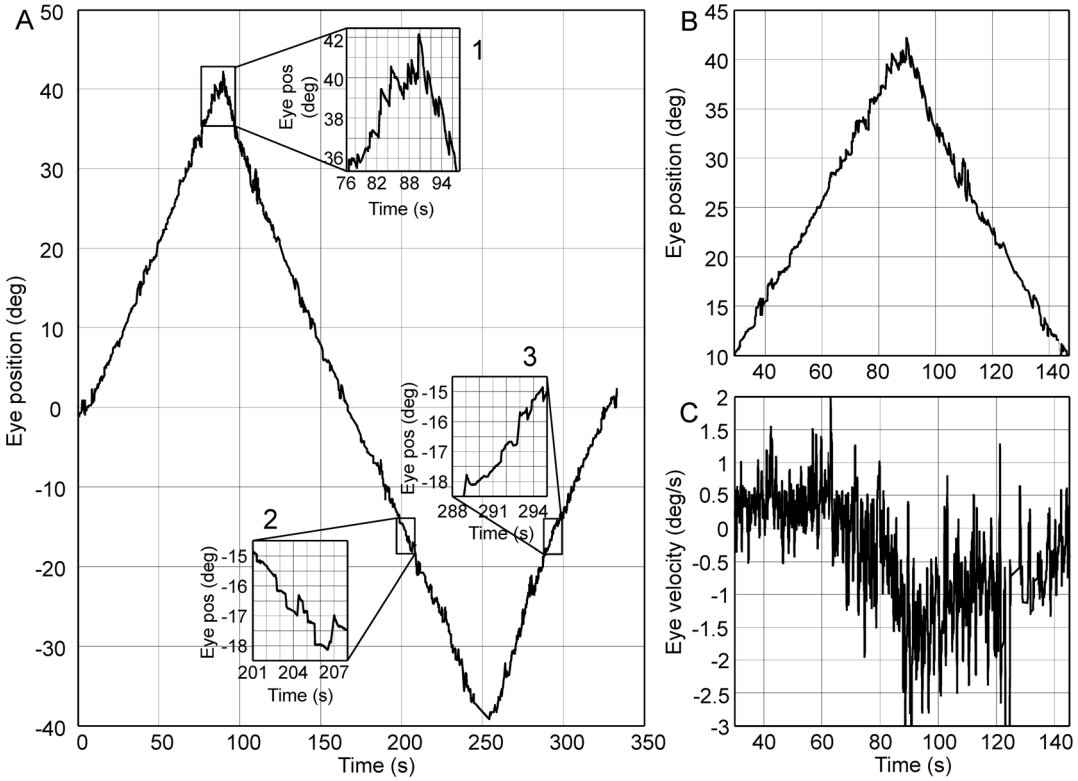

Figure 1. Raw data recorded in a single trial from a typical subject. Panel A - Left eye position plotted as function of time. Positive angles correspond to right eccentricities as seen by the subject. In this trial the dot was moving (0.5 deg/s) rightward at first. Inset 1: At extreme eccentricities the centrifugal beating nystagmus is clearly visible and the slow phase shows the tendency of the eye to return toward the primary position. Inset 2 and 3: Difference in the slope of the position trace at the same eccentricities when the dot is moving outward or inward. Panel B and C - Position (panel B) and velocity (panel C) of the eye at eccentricities larger than 10 deg right. The eye velocity begins to decrease from its baseline before the onset of the nystagmus, showing the growing centrifugal drift. Note that the baseline velocity is not zero but is positive between 10 and 25 deg of gaze eccentricity. When returning to 10 deg, however, the velocity is negative, showing the asymmetry in the baseline velocity showing the subject's attempt to match the target displacement velocity.
doi:10.1371/journal.pone.0061389.g001

Using a paired Wilcoxon signed rank test we found that the slopes fitted from each subject for gaze eccentricities between 0 and 20 on one side were significantly ($p<0.05$) smaller than those obtained in the same subject for gaze eccentricities between 20 and 40 deg on the same side. The median ratios (median absolute deviation in square brackets) of the paired slopes were 0.44 [0.29] on the left side and 0.32 [0.25] on the right side, respectively. Ratios of the slopes were significantly lower than 1 ($p<0.01$), confirming the significant increase of the rate of growing of the eye drift velocity with gaze eccentricity and therefore indicating a non-linear behavior. Pooling both sides the median ratio was 0.41 [0.29]. The mean slopes of the fitted subjects are reported in table 1.

The second analysis aimed at identifying a function that better represents the drift behavior, showing an improvement over the linear one. We characterized the behavior of the whole population by smoothing the individual instantaneous eye velocity traces of all subjects as a function of gaze eccentricity and interpolating them for all angles between 40 deg left to 40deg right in steps of 0.1 deg. Lilliefors test ([33]) confirmed that the obtained eye velocities at every step of interpolated eccentricity can be assumed to be normally distributed across subjects. We therefore calculated the mean eye velocity at each interpolated gaze eccentricity (figure 4) and fit each side with a linear, a tangent and a hyperbolic sine function (Eq. 1, Eq.2 and Eq.3, respectively). The variance-accounted-for evaluated in the range 0–20 deg scores were 0.90 and 0.97 for the linear fit on the right and left side, 0.98 and 0.95 for the tangent fit and 0.95 and 0.96 for the hyperbolic sine fit on the right and left side, respectively. When evaluating the fit in the range 20–40 deg these values however dropped considerably for the linear fit (0.84 and 0.81 for the right and the left side respectively) and moderately for the hyperbolic sine fit (0.92 and 0.87) but were almost unaffected for the tangent fit (0.98 and 0.92). The slopes of the linear fit were $-0.036\ s^{-1}$ on the right and $-0.029\ s^{-1}$ on the left side, corresponding to a time constant of 28 and 34 s, respectively. The values of k, the scaling factor of the tangent function, that provide the best fit of the data were 1.53 and 1.28 for right and left side, respectively. The values of h, the scaling factor of the hyperbolic sine function, that provide the best fit of the data were 0.031 and 0.025 for right and left side, respectively. To check for possible distortions due to boundary effects of the smoothing procedure, we repeated the analysis reducing the width of the moving windows used to smooth from 16 deg to 4 deg. The estimated parameters changed by less than 2% of their previous values, proving the robustness of our estimate to boundary effects.

Results of the simulations of a network of neurons

To show how the observed behavior can stem from the nonlinearities that affect the integrator network at the neuronal level, we simulated a mathematical model of a network incorporating some of the known characteristics of those involved in the velocity signal integration in the goldfish and showing the

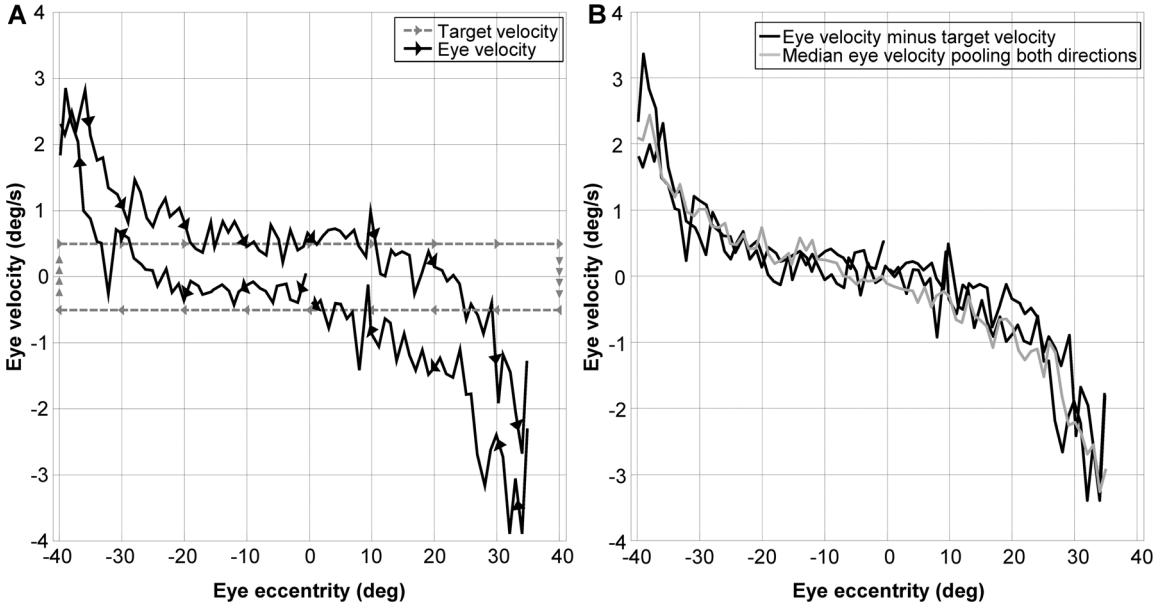

Figure 2. Position-Velocity plot considering target direction. Panel A - Black lines: Medians of the eye velocity within a 1 deg-wide bin plotted as a function of gaze eccentricity keeping the direction of target displacement separated. Gray lines: velocity of the target as a function of its position during the whole recording period. Note that the eye velocity matches the target velocity from the beginning suggesting that the offset observed around the straight ahead gaze is not due to a memory effect. The arrows show the directions of target and eye displacement. Panel B - Black lines: Velocity traces from the left panel after subtracting the correspondent target velocity. Gray line: Medians of the eye velocity within a 1 deg-wide bin plotted as a function of gaze eccentricity after pooling data from different directions of target displacement.
doi:10.1371/journal.pone.0061389.g002

effect of different tuning of the free parameters (see Methods). Without tuning (using the same value for every η), the drift grows rapidly with eye eccentricity (figure 5). Interestingly, however, the overall shape shows a clear nonlinear behavior evidencing the intrinsic nonlinearity of the drift pattern due to the influence of the neurons' natural nonlinearities (the only nonlinearity considered in

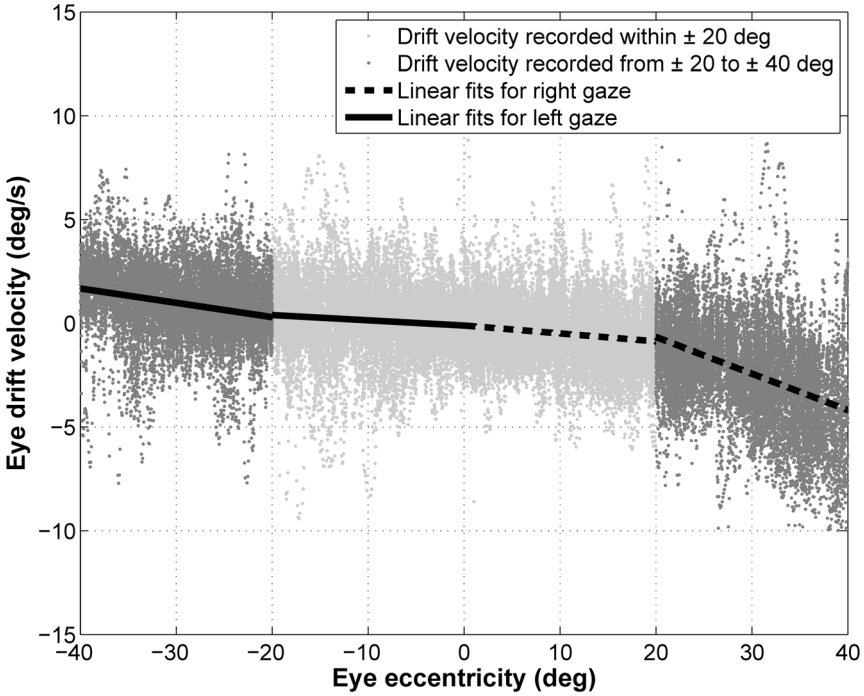

Figure 3. Position-Velocity plot and linear fit. Gray dots: Instantaneous velocity plotted as a function of the eye eccentricity. Light gray dots: Velocity in the 0–20 deg bins; dark gray dots: Velocity in the 20–40 deg bins; black line: linear fit of the velocity in the 0–20 deg bins and in the 20–40 deg bins.
doi:10.1371/journal.pone.0061389.g003

Table 1. Summary of the drift velocity and the slopes estimated from single subjects.

	0 deg to 20 deg	20 deg to 40 deg
Left gaze		
Median	0.33 ± 0.17	1.21 ± 0.56
Slope	−0.021±0.014	−0.045±0.022
Ratio to 20–40 deg	0.44 [0.29]	1
Right gaze		
Median	−0.36 [0.30]	−1.31 [0.54]
Slope	−0.020[0.010]	−0.047[0.045]
Ratio to 20–40 deg	0.32 [0.25]	1

doi:10.1371/journal.pone.0061389.t001

this simulation is the inhibitory cutoff since we assumed a linear synaptic activation function).

As the eye spends less time in the most eccentric positions than in the center, we considered a reasonable assumption to use a non-uniform tuning procedure, which will weigh more the drifts occurring in more central eye positions. This can be simulated by weighting Eq.10, which represents the error to minimize, with a Gaussian function of the eye eccentricity Δ (figure 6). We obtained almost perfect integration in the central eye range, corresponding to the almost flat region in figure 6 (bottom panel). Outside this range the performance of the network decreases dramatically and the drift explodes.

If we set a gaze-dependent tolerance for allowed drift in the minimization procedure, simulating a mechanism favoring leakiness over instability, it is possible to obtain a plot (figure 7) qualitatively resembling the mean trace depicted in figure 4. This was obtained by zeroing all the values of Eq.10 below the inverse of a Gaussian function of the eye eccentricity Δ and which will cause a centripetal drift.

To illustrate that different hypotheses in the network design can also generate simulations that mimic the experimental data, we include a simulation with saturating synaptic activation functions and a partial overlap of the activation thresholds in the center of the eye position range (Figure 8, constant weights).

Random perturbations around the weights used in Figure 7, generated patterns similar to Figure 4 in the main text (figure 9).

Discussion

Centripetal drift of the eye in eccentric positions is a known phenomenon possibly caused by non-ideal integration of the eye velocity command when generating the position command for the motoneurons driving the eyes ([1] for references). This process is usually approximated by a leaky integrator ([11], [21]) with a time constant that ranges between 10 s and 70 s ([22]). Such approximation implies that the drift velocity grows linearly with gaze eccentricity, with a slope equal to the inverse of the time constant. Although it has been shown in a few studies that this approximation may not hold for all eccentricities ([2], [3]), a detailed characterization of the gaze dependent centripetal drift was missing.

In this study we investigated gaze-holding performance in healthy human subjects by measuring eye drift velocity as a function of gaze eccentricity over a ±40 deg range. Pooling all subjects, we found a clear drift pattern with approximately linear behavior only within the central 20 deg of gaze eccentricity. For

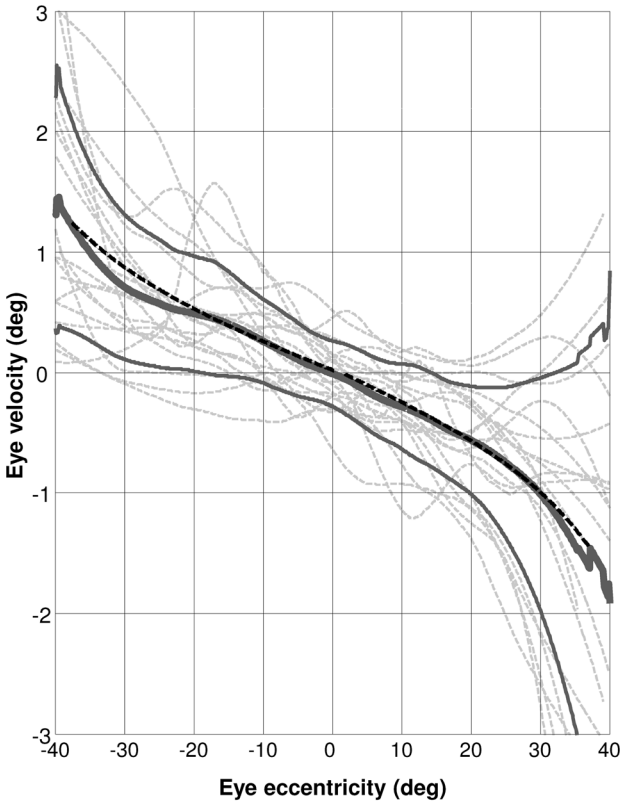

Figure 4. Smoothed Position -Velocity plot of the whole population. Dashed gray lines: Individual position-velocity curves obtained after smoothing and interpolating instantaneous velocity as a function of eye eccentricity; solid thick gray line: mean of the smoothed individual position-velocity curves; solid medium gray line: mean ±1 standard deviation of the smoothed individual position-velocity curves; dashed black line: tangent fit of the mean of the smoothed individual position-velocity curves.
doi:10.1371/journal.pone.0061389.g004

larger eccentricities the slope increased gradually, resulting in a curve that was better fit by a tangent function (figure 4). Our results therefore contradict the assumption of linearity of horizontal drift velocity with respect to eye eccentricity, showing that modeling the gaze holding network as a leaky integrator with a single time constant ([11], [21]) might be misleading if used on eye eccentricities larger than 20 deg. According to our data, this assumption is indeed consistent with the observed behavior only in a limited range around the primary position, where the linear fit scored the same variance-accounted-for value as the tangent one. Such a range is likely to coincide with the most commonly used eye position, since sustained horizontal gaze exciding 30 degrees is quite rare under normal conditions as head rotations integrate gaze shifts when exploring visual scene. This may suggest that the gaze holding system is optimized to behave linearly within a given range, while at larger eccentricities it gets nonlinear, an observation potentially relevant when investigating pathological forms of nystagmus, like gaze-evoked nystagmus and rebound nystagmus.

It may be argued that the specific characteristics of our paradigm affected the recorded drift velocity. In contrast to the reported earlier studies that used large gaze shifts between different recorded positions, we slowly displaced the target to obtain a sequence of quasi-continuous position steps. This allowed us to minimize the distance between the evaluated gaze eccentricities, keeping the recording time short, and not sacrificing

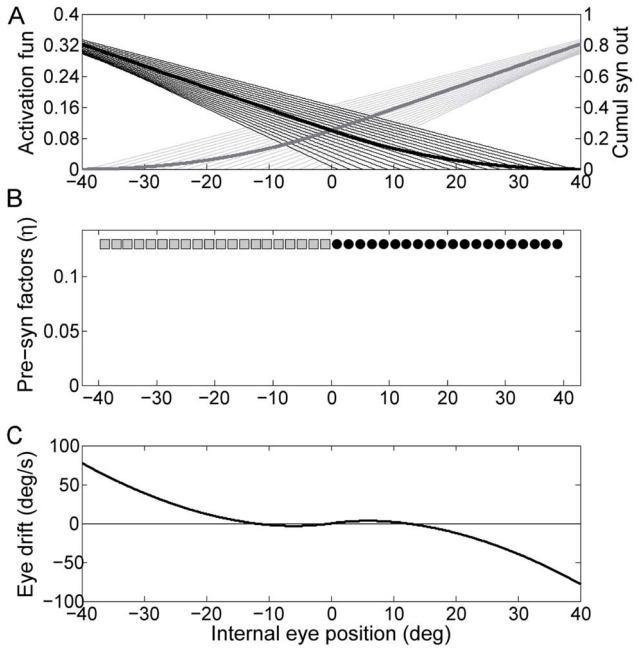

Figure 5. Simulation of the network without tuning. Panel A shows the output of the synaptic activation function of each neuron (thin lines) as a function of the internal representation of eye eccentricity (Δ), the zero of each line indicates the neuron threshold, i.e. the eccentricity at which the inhibitory cutoff takes place. The thick lines are the cumulative output of both sides of the network, obtained by combining all the synaptic activation functions with their factor η. Panel B shows the presynaptic factor η of each neuron, indexed according to the threshold shown in the upper panel, here set to the same value for all neurons to illustrate the general features of a non-tuned network. Panel C shows the PV plot for the internal representation of eye position.
doi:10.1371/journal.pone.0061389.g005

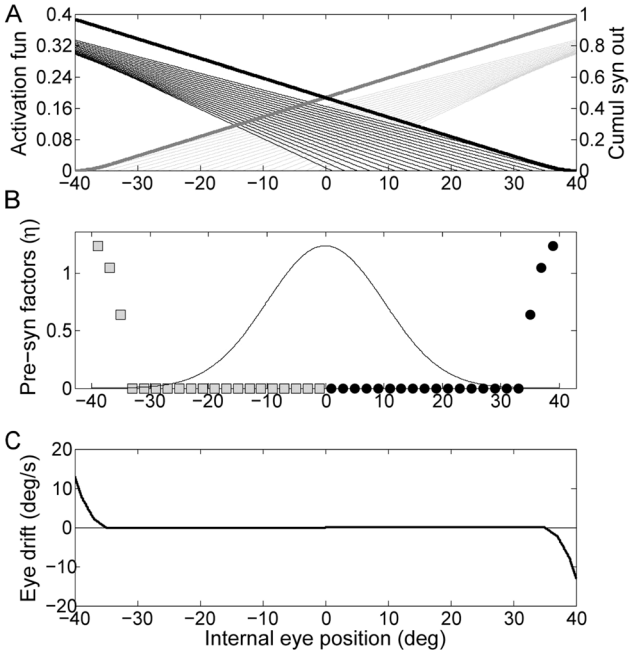

Figure 6. Simulation of the network tuned with non-uniform error function. The Gaussian function of the eye eccentricity represented by the solid line in the central panel has been multiplied to the resulting drift, i.e. the error to minimize, during the optimization procedure. The contents of the panels are as in figure 1A.
doi:10.1371/journal.pone.0061389.g006

the range tested. A saccade-based paradigm usually requires the subject to rapidly look eccentrically to elicit centripetal drift, and to look back to straight head after each trial to guarantee the same starting condition in each trial. This approach is inefficient if one aims at acquiring the same number of eccentric gaze positions as we recorded, as it would require two gaze shifts for every gaze eccentricity and only the very first second of every eccentric fixation could be used. For our experimental setup, which uses LEDs embedded in a motorized drum surrounding the subject, a quasi-static displacing target was a good compromise between the efficient data acquisition and recording time. We reasoned that, considering the characteristics of the system, there is, in principle, no reason to prefer one method over the other, as both require the integration of a velocity command to reach the desired eccentricity and none of the two guarantees that the possible nonlinearity of the integration network will not affect the estimation of the centripetal drift. For small gaze angles we found an evident velocity offset of a magnitude similar to the velocity of target displacement. This offset caused a significant difference between the instantaneous velocities recorded when the eye moved rightward or leftward (figure 2). The strong similarity of the left panel of figure 2 with a hysteresis trace may suggest the hypothesis that a memory-like effect, developed when reaching large gaze eccentricities, is responsible for the offset. However, since the offset is immediately present during the first outward directed movement (see figure 1 and 2), it cannot be caused by a hysteresis phenomenon. We hypothesized that such an offset results from

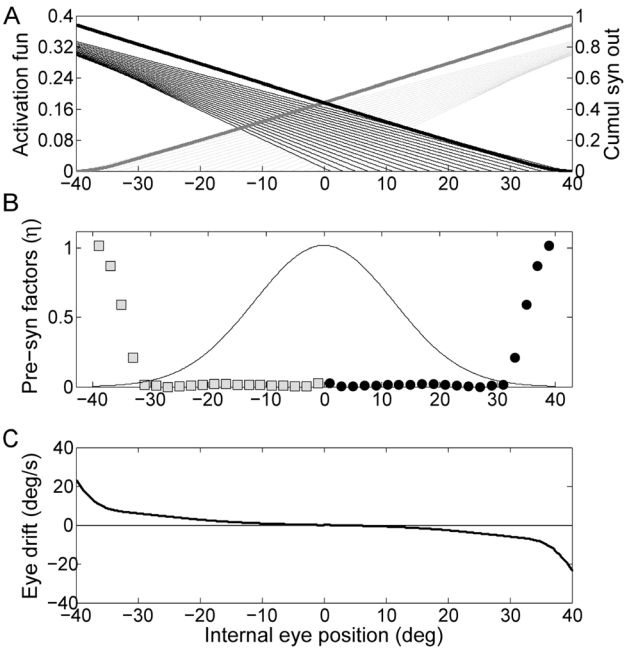

Figure 7. Simulation of the network tuned favoring leakiness against instability. The inverse of the Gaussian function of the eye eccentricity shown by the solid line in the central panel has been used as a gaze-dependent threshold for the non-penalized drift during the optimization procedure. The contents of the panels are as in figure 1A.
doi:10.1371/journal.pone.0061389.g007

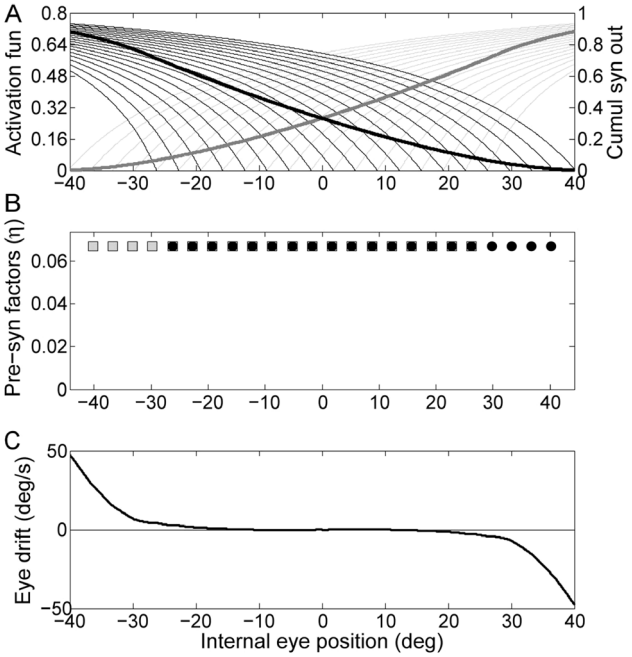

Figure 8. Simulation of the network using nonlinear synaptic activation functions. The contents of the panels are as in figure 5.
doi:10.1371/journal.pone.0061389.g008

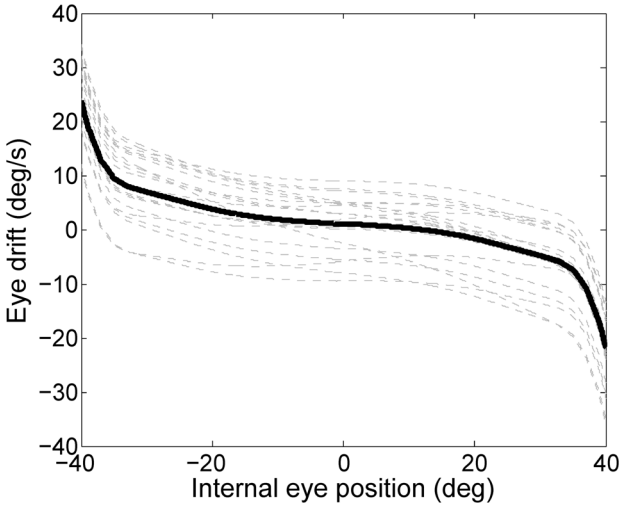

Figure 9. PV plots of random perturbations of tuned network. Effect of modifying the tuned values of η by a random fraction of 5% of the value used in figure 7. Dashed gray lines shows 20 different perturbations. The black solid line represents their mean.
doi:10.1371/journal.pone.0061389.g009

the velocity command needed to keep the eye on the flashing target, estimated by the brain by extrapolation from the displacement of the flashing target observed over time, possibly through the smooth pursuit system. Since the difference between rightward and leftward directed movements disappeared with larger eccentricities, subtraction of target velocity was not justified. A possible explanation is that the smooth pursuit gain decreased with eccentricity or that the integration of the velocity command becomes less efficient the more the eyes moved away from the center, causing a decrease of the observed velocity offset. Although theoretically it can be argued that the offset can bias the analysis of the centripetal drift velocity, we assumed that, by pooling the velocities recorded with the target moving in both directions, the effect of the two offsets into opposite directions would cancel out. A perfect cancellation would be obtained, if the smooth pursuit gain was symmetric in the two directions, as the offset would have the same magnitude at each given eccentricity but opposite signs when the target moved in opposite directions. In the case of an asymmetry between leftward and rightward smooth pursuit gain, the effect on our data would be that of adding a vertical bias to the whole velocity curve, causing a non-zero velocity when the subject is looking straight ahead, which is not present in our data and that would not affect the nonlinearity of the behavior in any case.

Although the nonlinear behavior emerges clearly when considering the population mean curve, the high variability across subjects, shown by the light gray dashed lines in figure 4, representing smoothed position-velocity curves of single subjects, make more difficult to observe a clear behavior when considering single subject data. Nonetheless, we found that, within subjects, the slopes of a linear function changed significantly ($p<0.05$) when fitting different portions of the range of recorded gaze positions. Specifically, between 0 deg and 20 deg of eye eccentricity the slope of the drift velocity was, in median, 0.41 times the one obtained between 20 and 40 deg. Such a ratio, which was significantly ($p<0.01$) lower than 1, confirms the nonlinear behavior evidenced by the population approach discussed above.

Considerable variability between subjects is a common observation in both the papers on end-point nystagmus reporting eye drift velocities ([3], [18]) and in those discussing the angle of nystagmus onset ([2], [4], [5], [42]). This is usually explained by the strong influence of the physical status of the subjects ([6] for review). A direct comparison with results from previous studies ([3], [18]) must be made with caution because of differences in the range of gaze eccentricities tested. Gordon and colleagues ([18]) reported an eye drift velocity of 0.3 deg/s at 30 deg of gaze eccentricity, which is lower than what we found in most of our subjects. On the other hand they also reported that the eye drift velocity was 6.8 deg/s at 55 deg. Since the maximal gaze angle reached by all of our subjects was 40 deg, a direct comparison is not possible. Although different from those found in our study, the velocities observed by Gordon and colleagues confirm by themselves a nonlinear growth, which was not further evaluated in their study. Eizenman ([3]) categorized subjects according to whether they developed nystagmus due to fatigue or whether they were showing a sustained nystagmus from the beginning of eccentric fixation. Our results are in line with the values reported by Eizenman at 40 deg for the subjects showing sustained nystagmus.

Although previous studies did not measure eye drift velocities in a continuous range of gaze eccentricities, a decrease of the integrator time constants at large angles of gaze was already reported ([3]). This suggests that the integration process might work differently at different angles. Some models already proposed a nonlinearity in the integration process ([24], [25], [43]). These models, however, dealt with pathological nystagmus (congenital nystagmus, gaze evoked nystagmus and spontaneous nystagmus, respectively)and used eye position nonlinear positive feedback loops to obtain the desired behavior. In a similar way, more recent models proposed the use of dynamic non-linear gains, which depend on eye eccentricities to explain the eye position dependence of rotational vestibulo-ocular reflex behavior ([44], [45], [46], [47]). By appropriately adjusting the eye-eccentricity dependence, all these model structures ([25], [24], [45]) could possibly describe the gaze holding behavior observed in our data.

However, our aim was to find a simple function able to encapsulate the main features of the observed dependence of eye drift velocity on eye position, i.e. of the measurable manifestation of the leakiness of the integration process. We showed that for eccentricities between 20 and 40 deg, the linear approximation of the position-velocity curves worsened, while a tangent function can better capture both the weak linear growth of eye drift around primary position and the rapid nonlinear increase observed at larger eccentricities, without the need for two different strategies as suggested before ([25]).

Although the tangent function is not derived from a specific model, the described behavior is consistent with the biological constraints that the brain has to overcome to hold gaze steady ([26], [27]). To illustrate this point we considered neural networks similar to those introduced by Aksay and colleagues ([39]). These authors showed that a network of neurons incorporating some of the known characteristics of those involved in the velocity signal integration in the goldfish can be trained to approximate a perfect integrator within a certain range of eye eccentricities. We simulated a similar network, showing that it is able to mimic the nonlinear behavior that we found experimentally. However, we stress that it is in principle possible to obtain any arbitrary drift pattern by choosing the right parameters and that we are not implying that the tuning strategies we used are actually implemented by the brain. As the goal and the mechanisms used by the brain to tune the network are not known, we did not use our network to fit our data. Instead, our aim was to show that leakiness and non-linearity arise naturally as the behavior of the integrator network in the brain is affected by a number of nonlinearities at neuronal level. Our simulations indeed show that simply considering the inhibitory cutoff, the most known nonlinearity affecting neurons, the network needs to be finely tuned to obtain a linear behavior in the most frequently used eye positions. Inhibitory cutoff is only one of the problems the brain has to overcome to provide integration of an input velocity signal given a limited number of nonlinear neurons. Nonetheless we showed that it may already lead to an outcome which is qualitatively similar to the experimental data. Implementation in the network of nonlinear synaptic activation functions led to simulations that resembled the experimental data more closely, although still quantitatively different, as more complex interactions should be considered to model the actual integration network in the brainstem. In general, whatever the characteristics of the actual integrator network in the brain are, the activity of each neuron should be sustained by the inputs it receives from the others in the network. Moreover such inputs should increase anytime the network needs to reach a new persistent state, required to keep the eye in an increasingly eccentric position. We hypothesize that the nonlinearity we observed occurs due to a progressive saturation of the input that each neuron in the integrating network receives from the others when the eyes approach maximum eccentricity. Given a limited pool of neurons, the brain might optimize the recruitment strategy to obtain the best performance in the range of gaze eccentricity most commonly used. This comes at the cost of saturation of the network output, as well as that of the input to each neuron in the network, beyond a certain angle of gaze eccentricity. This saturation would imply a progressive decline of integration performance, as the needed firing rate cannot be maintained.

Conclusion

We conclude that gaze holding in healthy humans does not follow a linear function, but is much better characterized by a tangent. The nonlinearity of the gaze holding behavior in healthy subjects is well grounded on neuronal physiology and the use of a tangent function provides a compact and simple characterization of healthy behavior to be used as a reference when investigating pathological conditions of gaze holding, e.g. in patients with progressive degenerative vestibulo-cerebellar disease.

Acknowledgments

The authors thank M. Penner for technical assistance.

Author Contributions

Model development: IO. Revised the manuscript: GB AAT SM CJB EK KPW DS. Conceived and designed the experiments: GB SM KPW AAT DS. Performed the experiments: GB AAT. Analyzed the data: GB. Contributed reagents/materials/analysis tools: GB CJB EK. Wrote the paper: GB.

References

1. Leigh RJ, Zee DS (2006) The neurology of eye movements. Oxford Press.
2. Abel LA, Parker L, Daroff RB, Dell'Osso LF (1978a) End-point nystagmus, Invest. Ophthalmol Vis Sci17: 539–544.
3. Eizenman M, Cheng P, Sharpe JA, Frecker RC (1990) End-point nystagmus and ocular drift: an experimental and theoretical study. Vision Res 30(6): 863–877.
4. Shallo-Hoffmann J, Schwarze H, Simonsz HJ, Mühlendych H (1990) A reexamination of end-point and rebound nystagmus in normal. Invest Ophthalmol Vis Sci31(2): 388–392.
5. Whyte CA, Petrock AM, Rosenberg M (2010) Occurrence of physiologic gaze-evoked nystagmus at small angles of gaze. Invest Ophthalmol Vis Sci 51:2476–2478.
6. Rubenzer SJ, Stevenson S (2010) Horizontal Gaze Nystagmus: A review of vision science and application issues. J of Forensic Sci 55(2): 394–409.
7. Aschan G, Bergstedt M (1975) Positional alcoholic nystagmus in man following repeated alcohol doses, Acta Otolaryngol. Suppl 330:15–29.
8. Citek K, Ball B, Rutledge DA (2003) Nystagmus testing in intoxicated individuals, Optometry 74: 695–710.
9. Citek K, Elmont AD, Jons CL, Krezelok CJ, Neron JD, et al. (2011) Sleep Deprivation Does Not Mimic Alcohol Intoxication on Field Sobriety Testing. Journal of Forensic Sciences 56: 1170–1179.
10. Westheimer G, Blair SM (1973) Oculomotor defect in cerebelloctomized monkeys, Invest. Ophthalmol 12: 618–621.
11. Robinson DA (1974) The effect of cerebellectomy on the cat's vestibulo-ocular integrator. Brain Res 71: 195–207.
12. Zee DS, Leigh RJ, Mathieu-Millaire F (1980) Cerebellar control of ocular gaze stability. Ann Neurol 7: 37–40.
13. Zee DS, Yamazaki A, Butler PH, Gücer G (1981) Effects of ablation of flocculus and parafloccculus on eye movements in primate. J Neurophysiol 46: 878–899.
14. Nakamagoe K, Iwamoto Y, Yoshida K (2000) Evidence for brainstem structures participating in oculomotor integration. Science 288: 857–859.
15. Leech J, Gresty M, Hess K, Rudge P (1977) Gaze failure, drifting eye movements, and centripetal nystagmus in cerebellar disease. Br J Ophtalmol 61: 774–781.
16. Hood JD, Kayan A, Leech J (1973) Rebound nystagmus. Brain 96:507.
17. Bondar RL, Sharpe JA, Lewis AJ (1984) Rebound nystagmus in olivocerebellar atrophy: A clinicopathological correlation. Ann Neurol 15:474.
18. Gordon SE, Hain TC, Zee DS, Fetter M (1986) Rebound nystagmus in normals subjects. ARVO Abstracts. Invest Ophthalmol Visual Sci 27:158.
19. Wild F, Shallo-Hoffmann J, Mühlendych H (1991) Physiologischer und pathologischer Rebound-Nystagmus, Fortschr. Ophthalmol 88: 73–77.
20. Wilson E, Sng K, Somers JT, Reschke MF, Leigh RJ (2005) Studies of eccentric gaze stability: effects of pitch head position on horizontal gaze-holding in patients with cerebellar disease. Ann N Y AcadSci 1039:593–596.
21. Robinson DA (1973) Models of the saccadic eye movement control system. Kybernetik 14: 71–83.
22. Becker W, Klein HM (1973) Accuracy of saccadic eye movements and maintenance of eccentric eye positions in the dark. Vision Res. 13: 1021–1034.
23. Glasauer S (2003) Cerebellar contribution to saccades and gaze holding. A modeling approach, Ann NY AcadSci 1004: 206–219.
24. Optican LM, Zee DS (1984) A hypothetical explanation of congenital nystagmus. Biological Cybernetics 50: 119–134.
25. Abel LA, Dell'Osso LF, Daroff RB (1978b) Analog Model for Gaze-Evoked Nystagmus, IEEE transaction on biomedical engeneering 25, 1: 71–75.

26. Seung HS, Lee DD, Reis BY, Tank DW (2000) Stability of the memory of eye position in a recurrent network of conductance-based model neurons. Neuron 26: 259–271.
27. Goldman MS, Compte A, Wang XJ (2009) Neural Integrator Models, In Encyclopedia of Neuroscience, L. R. Squire, Ed. Oxford Academic Press 6: 165–178.
28. Schneider E, Dera T, Bard K, Bardins S, Boening G, et al. (2005) Eye movement driven head-mounted camera: it looks where the eyes look. IEEE IntConfSyst Man Cybern 3:2437–2442.
29. Dera T, Boening G, Bardins S, Schneider E (2006) Low-latency video tracking of horizontal, vertical, and torsional eye movements as a basis for 3-DOF realtime motion control of a head-mounted camera. In Proceedings of the IEEE conference on systems, man and cybernetics 5191–5196.
30. Trujillo-Ortiz AR, Hernandez-Walls, Trujillo-Perez FA (2006) RMAOV33: Three-way Analysis of Variance With Repeated Measures on Three Factors Test. A MATLAB file. Available: http://www.mathworks.com/matlabcentral/fileexchange/loadFile.do?objectId = 9638.
31. Grinsted A (2008) quantreg.m: Quantile regression. Available: http://www.mathworks.com/matlabcentral/fileexchange/32115-quantreg-m-quantile-regression.
32. Koenker R, Hallock K (2001) Quantile Regression,Journal of Economic Perspectives 15: 143–156.
33. Lilliefors H (1967) On the Kolmogorov–Smirnov test for normality with mean and variance unknown. Journal of the American Statistical Association 62: 399–402.
34. Cleveland WS (1979) Robust locally weighted regression and smoothing scatterplots. J Am Stat Assoc 74: 829–836.
35. Galiana HL, Smith HL, Katsarkas A (1995) Comparison of linear vs. non-linear methods for analysing the vestibulo-ocular reflex (VOR). ActaOtolaryngol 115: 585–596.
36. Lopez-Barneo J, Darlot C, Berthoz A, Baker R (1982) Neuronal activity in prepositus nucleus correlated with eye movement in the alert cat. J Neurophysiol 47: 329–352.
37. McFarland JL, Fuchs AF (1992) Discharge patterns in nucleus prepositus hypoglossi and adjacent medial vestibular nucleus during horizontal eye movement in behaving macaques. J Neurophysiol 68: 319–332.
38. Aksay E, Baker R, Seung HS, Tank DW (2000) Anatomy and discharge properties of pre-motor neurons in the goldfish medulla that have eye-position signals during fixations. J Neurophysiol 84: 1035–1049.
39. Aksay E, Olasagasti I, Mensh BD, Baker R, Goldman MS, et al. (2007) Functional dissection of circuitry in a neural integrator. Nat Neurosci 10: 494–504.
40. Wang X-J (1999) Synaptic basis of cortical persistent activity: the importance of NMDA receptors to working memory. J Neurosci 19: 9587–9603.
41. Ermentrout B (1994) Reduction of Conductance-Based Models with Slow Synapses to Neural Nets. Neural Computation 6:679–695.
42. Booker JL (2001) End-position nystagmus as an indicator of ethanol intoxication. Sci Justice 41:113–116.
43. Khojasteh E, Bockisch C, Straumann D, Hegemann S (2013) A dynamic model for eye-position-dependence of spontaneous nystagmus in acute unilateral vestibular deficit (Alexander's Law). Eur J Neurosci 37: 141–149.
44. Khojasteh E, Galiana HL (2006) A nonlinear model for context-dependent modulation of the binocular VOR, IEEE Trans. Biomed. Eng 53:986–995.
45. Khojasteh E, Galiana HL (2009) Implications of gain modulation in brainstem circuits: VOR control system. J ComputNeurosci 198(1):1–18.
46. Chan WW, Galiana HL (2005) Integrator function in the oculomotor system is dependent on sensory context. J Neurophysiol 93: 3709–3717.
47. Chan WW, Galiana HL (2007) A non-linear model of the neural integrator in oculomotor control. Proc IEEE Eng Med BiolSoc 1: 1156–1159.

EJN fens EUROPEAN JOURNAL OF NEUROSCIENCE

European Journal of Neuroscience, pp. 1–9, 2012 doi:10.1111/ejn.12030

A dynamic model for eye-position-dependence of spontaneous nystagmus in acute unilateral vestibular deficit (Alexander's Law)

Elham Khojasteh,[1] Christopher J. Bockisch,[1,2,3] Dominik Straumann[2] and Stefan C. A. Hegemann[1]
[1]Department of Otorhinolaryngology, University Hospital Zurich, CH-8091, Zurich, Switzerland
[2]Department of Neurology, University Hospital Zurich, Zurich, Switzerland
[3]Department of Ophthalmology, University Hospital Zurich, Zurich, Switzerland

Keywords: neural disease modeling, neural integration, ocular-motor system, spontaneous nystagmus, vestibulo-ocular reflex

Abstract

Spontaneous nystagmus (SN) is a symptom of acute vestibular tone asymmetry. Alexander's Law (AL) states that slow-phase velocity of SN is higher when looking in the direction of fast-phases of nystagmus and lower in the slow-phase direction. Earlier explanations for AL predict that during SN, slow-phase eye velocity is a linear function of eye position, increasing linearly as eye deviates towards the fast-phase direction. Recent observations, however, show that this is often not the case; eye velocity does not vary linearly with eye position. Such new findings necessitate a re-evaluation of our understanding of AL. As AL may be an adaptive response of the vestibular system to peripheral lesions, understanding its mechanism could shed light on early adaptation strategies of the brain. Here, we propose a physiologically plausible mechanism for AL that explains recent experimental data. We use a dynamic control system model to simulate this mechanism and make testable predictions. This mechanism is based on the known effects of unilateral vestibular deficit on the response of the ipsi- and contralesional vestibular nuclei (VN) of the brainstem. This hypothesis is based on the silencing of the majority of ipsilesional VN units, which creates an asymmetry between the responses of the ipsi- and contralesional VN. Unlike former explanations, the new hypothesis does not rely on lesion detection strategies or signals originating in higher brain structures. The proposed model demonstrates possible consequences of acute peripheral deficits for the function of the velocity-to-position neural integrator of the ocular motor system and the vestibulo-ocular reflex.

Introduction

Unilateral vestibular deficit (UVD) results when the resting discharge rate of primary vestibular afferents on the right or left side of the head decreases or becomes absent and the firing rate no longer modulates with vestibular stimuli. This is a common observation in clinical practice and is the result of a number of pathologies, including lesions to the vestibular organs, labyrinthectomy, lesions to the vestibular nerve (e.g. vestibular neuritis) and neurectomy. In acute stages, this imbalance induces behavioral symptoms such as vertigo, postural instability and spontaneous nystagmus (SN). The SN consists of slow eye drift towards the lesioned side (slow-phases), interspersed with quick reorienting eye movements towards the healthy side (fast-phases). During SN, the slow-phase eye velocity is higher when the patient looks in the direction of fast-phases and decreases in the slow-phase direction. This property is known as Alexander's Law (AL) (Alexander, 1912). Figure 1A shows a typical nystagmus pattern observed in a patient with mild vestibular neuritis on the left side, measured several hours following the onset of symptoms. Figure 1B depicts slow-phase eye velocity versus eye position generated from the data in Fig. 1A, demonstrating AL.

The mechanism that causes AL remains unknown. Normal vestibulo-ocular reflex (VOR), evoked by sinusoidal en-block rotations at 0.5 Hz (Robinson *et al.*, 1984) or head impulse stimuli with high-frequency content (Anagnostou *et al.*, 2011), is shown to be independent of eye position. This suggests that the visco-elastic properties of the eye plant (i.e. the eye ball, the extra-ocular muscles and the orbital tissue, collectively) are not responsible for eye-position effects during SN. Doslak *et al.* (1979) proposed that if the vestibular tone asymmetry is large enough, then a gaze-dependent command is added to the total VOR drive at the level of vestibular nuclei (VN), which is otherwise gated by an inhibitory signal. The effect of this additional drive is to generate an eye position-dependent movement whose velocity is larger when looking in the direction of fast-phases and decreases linearly as the eye is directed towards the slow-phase direction. Alternatively, Hess (1982) and later Robinson *et al.* (1984) suggested that AL is an adaptive response triggered when prolonged imbalanced tonic activity is detected on the primary afferents. They hypothesized that when the brain decides it is receiving incorrect sensory signals, it deactivates its vestibular-perseverating mechanisms (i.e. the velocity storage

Correspondence: Dr E. Khojasteh, as above.
E-mail: elham.khojasteh@mail.mcgill.ca

Received 26 June 2012, revised 11 September 2012, accepted 19 September 2012

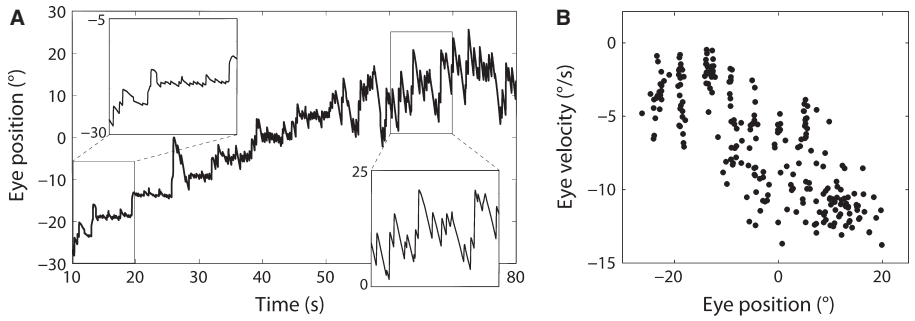

FIG. 1. (A) Typical nystagmus record from a 45-year-old patient with mild left-side vestibular neuritis, in the first several hours after the onset of symptoms (data from Hegemann *et al.*, 2007). The patient attempts fixation of a flashing target that moves in 5° steps from the left side to the right side. Data from 10–20 s (while looking to the left) and 60–70 s (looking to the right) are magnified for better visualization (same vertical scale). In accordance with Alexander's Law, slow-phase eye velocity is larger when looking in the contralesional direction compared with ipsilesional direction. (B) Slow-phase eye velocity is plotted versus median slow-phase eye position for the patient shown in A. Velocity of slow-phases increases as the patient looks more in the direction of the healthy side (right side).

mechanism and the velocity-to-position neural integrator). The time constant of the velocity-to-position neural integrator (NI) of the oculomotor system is consequently reduced. Therefore, the NI no longer provides sufficient command signals for motor neurons to maintain a desired eye position. This causes the eye position p to drift from a desired position p_0 towards the null position, following an exponential pattern with the time constant τ determined by the NI: $p = p_0 e^{(-t/\tau)}$. The velocity of this drift, $p' = \mathrm{d}p/\mathrm{d}t = -p/\tau$, is a linear function of eye position. This centripetal drift, when superimposed on the SN, counteracts SN when eye position is in the direction of slow-phases, creating a region in the visual field where nystagmus is less intense or absent.

While both theories discussed above account for AL, they propose rather different mechanisms through which AL is induced; the former suggests changes in the VOR gain but not its dynamics (i.e. time constants) and the latter suggests modifications in the NI. Both theories are nevertheless unclear about the underlying neural mechanism that triggers and guides these modifications. Furthermore, recently Hegemann *et al.* (2007) showed that in patients with acute UVD the slow-phase velocity of SN is not a linear function of eye position. In other words, they found that in these patients the rate of change of velocity with position is itself a function of eye position, suggesting an eye position-dependent integrator function. This finding led them to suggest multiple horizontal neural integrators each with a distinct integration direction.

Temporal integration of neural signals to create short-term memories is an important task of the neural networks in the brain (e.g. Goldman-Rakic, 1995; Taube & Bassett, 2003; Huk & Shadlen, 2005). Among those, the NI of the ocular motor system is one of the best studied. Understanding the underlying cause for AL could lead to deeper knowledge about neural integration in the ocular motor system, as well as early adaptation strategies employed by the central nervous system in response to peripheral lesions. To account for new experimental data, in this article we propose an alternative explanation for AL based on changes in the population responses of the bilateral VN after the onset of UVD. This hypothesis relies on the silencing of many ipsi-lesional VN units because of insufficient incoming baseline activity on the primary afferents (Smith & Curthoys, 1988a,b, 1989). Unlike former hypotheses, the proposed mechanism does not rely on any additional triggering/guiding signals, nor does it employ switches or other unknown gating signals. Here, a commonly accepted feedback control model for the VOR is used to demonstrate that this transformation in the central VOR circuits is enough to cause AL and also to simulate some recent findings.

Methods

In this section the physiological basis for the model is reviewed and expressions for the gain and time constant of the system are provided. Then the proposed mechanism through which AL is induced in acute UVD is presented.

Description of model structure (healthy system)

The model used here (Fig. 2) is a feedback structure for the canal-driven conjugate horizontal VOR during slow phases (Galiana & Outerbridge, 1984; Galiana *et al.*, 1984; Galiana, 1991). The lowercase letter 's' is the complex frequency and all notations are expressed in Laplace domain. The input to the model is the difference in discharge between the right and left vestibular primary afferents: $\Delta c(s) = c_R(s) - c_L(s)$. The output, $E(s)$, is conjugate eye position defined as the mean right and left eye positions. Solid arrows in the schematic present population projections (neural path-

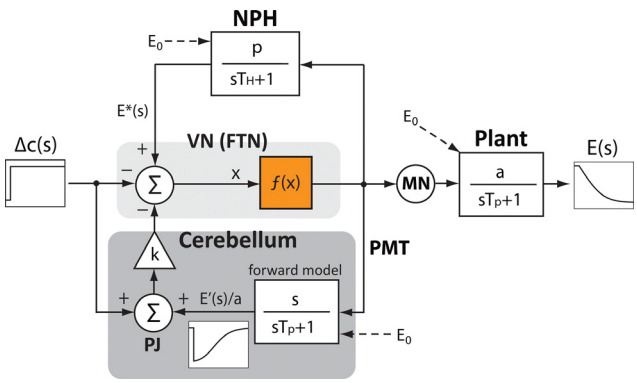

FIG. 2. Model structure for the horizontal canal-driven conjugate VOR during slow-phases. Solid arrows indicate neural projections. Dashed arrows show where initial eye position is preset for integrators. All notations are in Laplace domain and lower-case letter 's' is the complex frequency. Δc is the difference between the right and left primary vestibular afferents and E is the conjugate eye position. E^* is the efference copy of eye position. E' is eye velocity. $f(x)$ is the static population transfer function of the vestibular nuclei. Abbreviations: VN, vestibular nuclei; FTN, flocculus target neurons in the vestibular nuclei; PJ, Purkinje neurons; NPH, nucleus prepositus hypoglossi; PMT, paramedian tract neurons; MN, motor nuclei. T_p is the time constant of the plant; a is the plant gain; T_H is the time constant of the neural filter at the NPH; p is the gain of the neural filter at the NPH; and k is the projection weight of PJ neurons to the FTN. Numerical values are given in Table 1.

ways). Rightward movements and positions are considered positive. Subscripts R and L refer to the right and left side.

In the most direct VOR pathway (three-neuron-arc of the VOR), canal signals are carried directly to the VN via the primary vestibular afferents. The VN project to the motor nuclei (MN), which in turn drive the eye plant. Here, the eye plant is modeled as a first-order low-pass filter with time constant T_p and gain a. The mathematical integration of the VOR velocity commands is accomplished through a distributed network of neurons, mainly the VN, nucleus prepositus hypoglossi (NPH) and the vestibular cerebellum, i.e. flocculus/ventral paraflocculus (Fukushima & Kaneko, 1995; Kaneko, 1997). The effect of this network is to augment the time constant of the gaze holding response above the ~200 ms time constant of the eye plant, as originally proposed by Skavenski & Robinson (1973). In the model, this is achieved by two feedback loops around the VN: a positive position feedback through the NPH and a negative velocity feedback through the flocculus. The NPH performs the first integration in the brainstem, generating and distributing an internal estimate of eye position, $E^*(s)$. Here, the NPH is modeled as a first-order low-pass system with time constant T_H and gain p. The dynamics of this leaky integrator are set equal to those of the eye plant for simplicity of analyses (i.e. $T_H = T_p$). In a more general case, the dynamics of the NPH low-pass filter do not match those of the eye plant (i.e. $T_H > T_P$), and the positive feedback does not fully cancel the eye plant dynamics but will only lengthen the dominant time constant of the response. A second integration is done through the flocculus/ventral paraflocculus of the cerebellum (Zee *et al.*, 1981; Nakamagoe *et al.*, 2000). The flocculus receives a copy of the motor neuron drive from the paramedian tract (PMT) neurons in the brainstem via mossy fibers (Büttner-Ennever *et al.*, 1989). It is believed that the flocculus constructs an efference copy of eye velocity using a stored forward model of plant dynamics (for a review see Lisberger, 2009). The flocculus also receives vestibular signals, perhaps from floccular projecting neurons in the VN (Cheron *et al.*, 1996). As shown by Lisberger *et al.* (1994), floccular gaze-velocity Purkinje neurons (PJ) make inhibitory projections (with a weight of k in the model) to the flocculus target neurons (FTN) in the VN, closing the negative feedback loop around the VN. This negative velocity feedback was also proposed by Glasauer (2003) in a gaze holding model. In the model, the desired (or initial) eye position E_0 is preset for each leaky integrator, as indicated by the dashed arrows in Fig. 2.

Resting discharge rates for different neural populations are not included in the model. This means that in model simulations, all firing rates modulate around zero; a negative population discharge means a discharge rate that is below the resting firing rate of the population.

As the purpose of this study was to prove a concept using a simple model structure, a conjugate VOR model was used instead of a complete bilateral structure. Here, the VN represents the effective overall contribution of the right and left vestibular nuclei to conjugate VOR response, i.e. $VN = VN_R - VN_L$.

Choice of a sigmoidal transfer function for the VN

If each individual neuron in the VN acts as a piece-wise linear unit with individual cut-off and saturation thresholds, then the transfer function of a large population of such units with scattered thresholds can be approximated by a sigmoidal function (Fig. 3). A qualitative representation of these sigmoidal transfer functions for the right and left VN is shown in Fig. 4A. Hereafter, the 'operating region' of the transfer function refers to the region between cut-off and saturation,

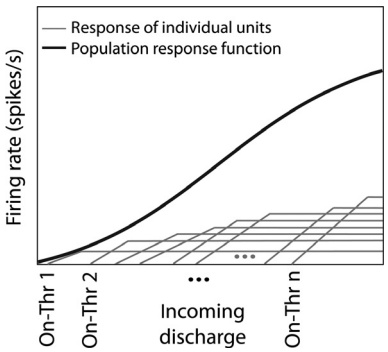

FIG. 3. A qualitative demonstration for constructing a sigmoidal transfer function from a population of saturating neurons. Single neurons are modeled as quasi-linear functions with distinct on-thresholds (On-Thr) and a discharge rate that saturates above some distinct input value. If the incoming discharge is in the off-direction of neurons, they remain in cut-off region. As the total incoming discharge activity increases above the on-threshold of neurons, gradually more neurons are recruited and finally when all neurons are recruited and saturated the total response saturates. This recruitment order produces an overall sigmoidal population response. If the operating region of the sigmoid is large enough, it can be approximated by a quasi-linear function.

where the transfer function has a non-zero gain re. input. In an intact system, where the responses of the right and left VN are balanced and symmetric, the *effective population response function of the bilateral* VN (i.e. $VN_R - VN_L$) is also a sigmoid with a much larger operating region, as shown in Fig. 4A. This overall static transfer function, called $f(x)$ hereafter, can be approximated by a quasi-linear function that saturates for large inputs and cuts-off for inputs in the off-direction. In other words, inside the operating region $f(x) \cong gx$, where the constant $g = f(x)/x$ defines the instantaneous gain (or sensitivity) of the response to the total incoming neural activity x.

Derivation of the input–output relationship for the model (healthy system)

If the system is linearized assuming $f(x) \cong gx$, where g is a constant that does not vary with the input x, eye velocity can be derived as:

$$E'(s) = G_{VOR} T_{VOR} \frac{s}{sT_{VOR} + 1} \Delta c(s) - \frac{1}{sT_{VOR} + 1} E_0 \qquad (1)$$

where T_{VOR} and G_{VOR} are the time constant and gain of the VOR system, respectively, given by:

$$T_{VOR} = \frac{T_P + gk}{1 - gp} \qquad (2)$$

$$G_{VOR} = -\frac{ag(1+k)}{T_P + gk}. \qquad (3)$$

The first component in Eqn (1) presents the forced system response to the vestibular stimulus Δc and the second component is the transient response to the initial eye position E_0. The effect of feedback loops on the time constant of the response can be seen from Eqn (2). To maintain system stability, the term $1 - gp$ should be positive. Model parameters (listed in Table 1) are chosen such that for a healthy system the response gain is almost unity and the time constant is about 30 s. For a vestibular tone asymmetry of the amplitude A: $\Delta c(s) = A/s$, the expression for eye velocity in the time domain is:

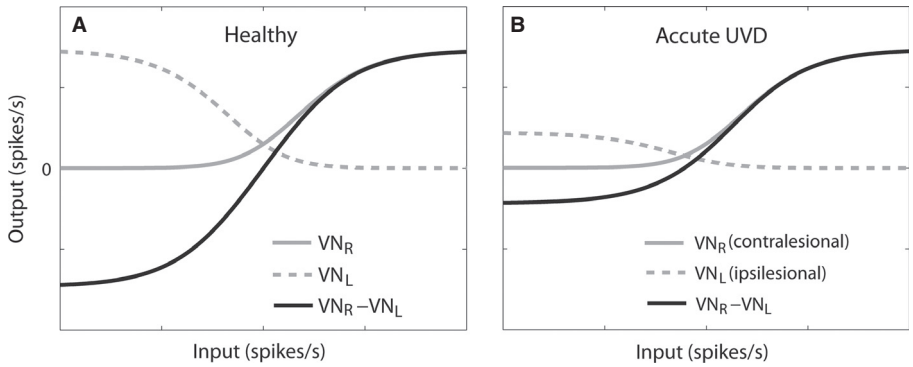

FIG. 4. A qualitative representation for the response function of the right and left VN, assuming that the right VN dominates integration of eye signals in the right half-plane and vice versa. Gray curves show the right (solid line) and left VN (dashed line) responses, and the black curve shows the effective overall contribution of both: $VN_R - VN_L$. (A) The case where the responses of both sides are balanced and symmetric and (B) the case for a left-side UVD. The effective overall response in A is symmetric with a large operating region between cut-off and saturation. In contrast, in B the overall response function becomes asymmetric, having larger gain for positive inputs. It also has a smaller operating range.

$$E'(t) = AG_{\mathrm{VOR}} e^{-\frac{t}{T_{VOR}}} - \frac{E_0}{T_{VOR}} e^{-\frac{t}{T_{VOR}}}. \quad (4)$$

It is important to note that according to Eqns (2) and (3), changes in VN sensitivity g affect both T_{VOR} and G_{VOR}; a larger g results in larger VOR gain and time constant. Also outside the operating region, where the VN response saturates or cuts-off, the gain g is zero and no further integration of eye signals is achieved.

Changes to the model caused by acute UVD

Immediately following UVD, many of the VN neurons ipsilateral to the lesion are silenced because of insufficient incoming tonic activity from primary vestibular afferents. Simultaneously, some of the contralesional secondary vestibular neurons increase their baseline activity because of the silencing of inhibitory commissural across midline projections (Smith & Curthoys, 1988a,b, 1989). This causes an asymmetry between the population responses of the bilateral VN, altering the effective overall neuronal responses in acute UVD, as shown in Fig. 4B. The assumption made here is that such a change in neural responses affects the overall VN response function $f(x)$ in at least two aspects: (i) the total sensitivity to the input, g, is reduced; and (ii) the transfer function becomes asymmetric and the operating range for which the linear approximation $f(x) \cong gx$ is valid becomes too small, such that the criteria under which the system may be approximated by a linear system are no longer satisfied (Fig. 4B).

Hence in the analyses of the model in acute UVD the sigmoidal transfer function is not linearized. This means that the sensitivity g of the VN is not a constant but will itself depend on the input: $g = g(x)$. In the model, the input to the VN consists of vestibular as well as eye-movement related signals:

$$x = -(1+k)\Delta c - (k/a)E' + E^*. \quad (5)$$

Therefore any of these quantities can change the input x and consequently the VN sensitivity, $g(x)$.

A desired eye position, E_0, as required by the fixation target, determines an operating point x_0 on the sigmoidal curve. SN then modulates the input x about this operating point. Consider a left-side UVD, which evokes a SN with left drifting slow-phases. Left-drifting slow-phases decrease the total input to the VN, x, as seen from Eqn (5). As shown in Fig. 5, when looking to the right (target T_R), a decrease in input x results in an increase in g. From Eqns. (2) and (3), an increase in g increases the VOR gain and time constant. Therefore, as leftward slow-phases decrease the total input x, they increase g along the way, increasing G_{VOR} and T_{VOR}. But for a fixation point on the left (target T_L in Fig. 5), the opposite of this scenario is true; leftward slow-phases decrease g, reducing G_{VOR} and T_{VOR}. Therefore, for a fixation point on the left side, the forced response in Eqn (1) will be smaller (i.e. a smaller G_{VOR}). Plus, for this fixation point, the time constant T_{VOR} is also smaller (as g is smaller), causing a larger drift velocity towards the null position. Hence for target T_L the small forced response will be counteracted by an even larger transient response in the opposite direction, resulting in an overall smaller eye velocity.

Choosing the parameters of the sigmoidal function

For simulations of the model, the following analytical formulation was used for the sigmoidal function:

$$f(x) = \alpha + \beta(1 + \tau \exp(-\gamma(x-\mu)))^{-\frac{1}{\tau}}. \quad (6)$$

Equation (6) represents a generalized logistic function. Numerical values for the parameters (α, β, γ, μ, τ) are provided in Table 1, and the function is displayed in Fig. 5A. Figure 5B shows the instantaneous gain of this function, $g(x)$.

It is important to note here that it is the inherent characteristics of a sigmoidal shape that produces AL in the model, not a specifically

TABLE 1. Numerical values for model parameters used in simulations; the subscript H refers to healthy case and D to acute UVD

					Sigmoid parameters (healthy)					Sigmoid parameters (UVD)				
Parameter	a	p	k	T_p (ms)	α_H	β_H	γ_H	μ_H	τ_H	α_D	β_D	γ_D	μ_D	τ_D
Value	0.7	2	1	200	–122.1	244.3	0.008	0	1	–81.4	172.7	0.011	22.1	1.3

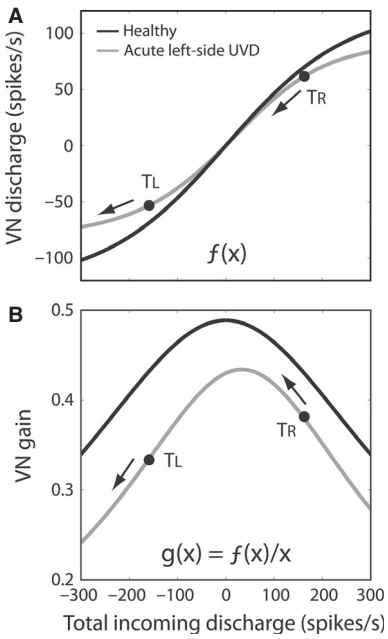

FIG. 5. For a healthy system, the overall population response of the bilateral VN can be approximated with a quasi-linear sigmoidal function *f(x)* as shown in A with the black curve. In case of UVD, this response function is better described by an asymmetric sigmoidal function, and not a linear approximation of it, as shown in A with the gray curve. The bell-shaped function in B is the instantaneous gain of the sigmoidal function *f(x)* in A and represents the sensitivity of the VN with respect to the input. For a left-side UVD, the arrows in A and B show the direction of slow-phase eye movement around an operating point defined by the fixation target ($T_{R,L}$). When the target position is on the right (T_R), i.e. in the fast-phase direction, slow-phases move the eye in a direction that increases the VN gain. While for a fixation point on the left (T_L), slow-phases move the eye such that the VN gain decreases. Parameters for sigmoidal function in both healthy and UVD are provided in Table 1.

optimized parameter set. In general, a sigmoidal function as expressed in Eqn (6) has high sensitivity around input level $x = \mu$ (like a 'tuning region') while this sensitivity decreases smoothly as the input level moves away from this tuned value. With reference to Fig. 5B, the section of the sigmoidal curve around which the input x modulates during SN is determined by target position. The average gain of this section is always larger when modulation occurs about an eye position in the fast-phase direction than for eye position in the slow-phase direction. This is because slow-phases are centripetal (i.e. towards higher g values) for an eye position in the fast-phase direction, but centrifugal for eye position in the slow-phase direction. In other words, the sigmoidal function is not strictly tuned to produce a specific result. In fact, the only restrictions applied when choosing the parameters of the sigmoidal function were: (i) to maintain system stability for all inputs; and (ii) to decrease the sensitivity, $g = f(x)/x$, smoothly from its maximum value at the null position to about one-half at the most eccentric eye positions at 60°. Therefore, as long as the system stability criteria are met, any sigmoidal shape with a reasonable gain drop at eccentric eye positions will produce AL.

Fast-phase strategy

Fast-phases of the SN are not explicitly modeled in this study. Nevertheless, a switching strategy is embedded in the model to be able to simulate the complete nystagmus pattern. In the nystagmus mode, the output of the model (eye position) is constantly compared with a desired value that represents target position. When the difference between the two is greater than 10°, a fast-phase is triggered, resetting eye position (i.e. the initial condition of the model integrators) to within ± 5° of the desired value.

Simulation results

Simulations were performed in MATLAB SIMULINK (The MathWorks Inc., Natick, MA, USA), with an integration step size of 1 ms. Unless otherwise stated, the model simulates a *left-side* UVD, which means the input to the model is a positive step function whose amplitude is indicator of the severity of the deficit. Therefore, slow-phases are to the left and the resulting eye velocity is negative.

Gaze holding in the dark

The gaze holding behavior of the model was first examined with no vestibular input to the model. The drift velocity versus eye position (i.e. the *P–V* curve) is plotted in Fig. 6. From the figure it can be seen that the centripetal drift velocity increases in acute UVD compared with a healthy case, meaning that integration deteriorates in acute UVD. This is because the effective overall sensitivity of the VN in the model, g, decreases as a result of the change in the population response. Furthermore, both in acute UVD and in the healthy system, integration becomes worse at more eccentric eye positions. This is because the right and left vestibular nuclei (that dominate integration of eye signals on the right and left side, respectively) gradually saturate at large eye positions (Fig. 4). Therefore their gain, g, decreases for large eccentric eye positions, adversely affecting integration. The model hence predicts that even in a healthy subject at more eccentric gaze angles the integrator does not function as effectively as for central gaze. For the healthy case, a linear fit to the data points estimates a time constant of 25 s for eye position within ± 10° from straight ahead, and a time constant of 8 s for more eccentric positions in the [10° 30°] range.

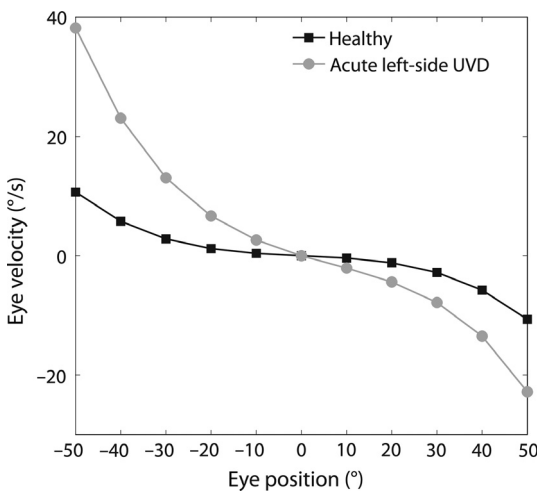

FIG. 6. Model behavior during simulated gaze holding in darkness. Each marker represents the drift velocity at the corresponding eye position. The black plot corresponds to a healthy system and the gray plot to left-side UVD. For both cases the slope increases at far eccentric eye positions, suggesting a deteriorated integration function.

Simulations in the slow-phase and nystagmus modes

In Fig. 7, the effect of eye position on eye velocity is demonstrated for a vestibular tone imbalance of +60 spikes/s (i.e. a left-side deficit). In other words, the input to the model was a step of size +60 at time 100 ms. The model was simulated with this input in both the slow-phase and the nystagmus mode, for three conditions: eye straight ahead (dark gray), and at 20° to the right (light gray) and to the left (black). The eye velocity is largest when the eye is deviated 20° to the right (i.e. the fast-phase direction). As explained in the Methods, this difference is a result of a smaller VOR gain at −20° as well as a larger counteracting centripetal drift at this position.

The effect of severity of the deficit

The input to the VN in the model includes both the efference copy of eye position and vestibular signals (see Eqn 5). Therefore, not only the eye position but also the amount of the vestibular imbalance in UVD modulates the VN sensitivity g to the incoming discharge. To examine how the severity of the imbalance affects model behavior, the model was stimulated with rightward steps of different magnitudes at multiple eye positions, again simulating a left-side UVD. Figure 8 shows the resulting eye velocity as a function of fixation position for each step amplitude. For smaller input amplitudes, the *P–V* plots are almost symmetric around the straight ahead position. But for larger input values, the plot saturates in the fast-phase direction (i.e. on the right side), demonstrating a reduced rate of change with eye position in the fast-phase direction.

Reversal of nystagmus direction

Figure 8 also shows that for smaller vestibular tone imbalance, if eye position is far enough into the slow-phase direction (here: left side) there could be a region where the direction of nystagmus reverses and slow-phases drift to the right instead of left (as indicated by positive eye velocity). For instance, if the tonic imbalance is 10 spikes/s, then for eye positions that are further than 30° to the left, the nystagmus changes direction. As shown, this threshold position beyond which nystagmus reverses depends on the severity of the deficit and is smaller for smaller tonic imbalance.

The effect of the sigmoidal function

The sigmoidal function that was used in model simulations so far was chosen based on the fact that following UVD many of the ipsilesional VN units are silenced, causing a reduction in the ipsilesional VN sensitivity (see Fig. 4B for a graphical explanation). This sigmoidal function is shown in Fig. 5A (gray curve) and again in Fig. 9A (black curve).

Furthermore, the contralesional VN also increases its baseline activity because inhibitory cross-midline projections from the ipsilesional VN are silenced. If this increase in baseline activity of the contralesional VN coincides with an increase in population sensitivity, an even greater asymmetry in the responses of the right and left VN would result. To reflect this further change in the contralesional VN, the sigmoidal function was modified as shown in Fig. 9A (gray curve, parameters: $\alpha = -76$, $\beta = 209$, $\gamma = 0.011$, $\tau = 0.5$, $\mu = 25$). The model was then stimulated with a rightward step of 60 spikes/s at various eye positions. The resulting *P–V* plot from this modified

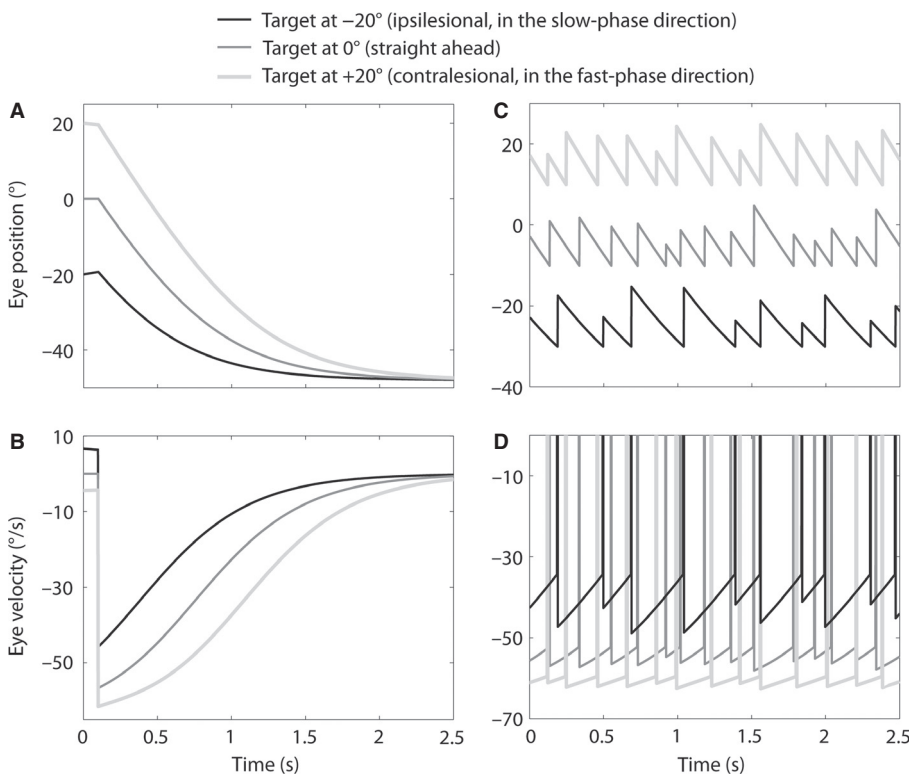

FIG. 7. Simulation results for a left-side UVD. The input to the model was a rightward pulse at time 100 ms with amplitude of +60 spikes/s. The eye position was set at three different values at the start of simulation. In A and B the model was simulated in slow-phase mode only; in C and D the nystagmus model was simulated. Eye velocity was greatest when the eye was initially at 20° to the right (i.e. in the fast-phase direction) and lowest for the eye position in the slow-phase direction. The difference in response amplitude is caused by a larger VOR gain at +20° as well as a smaller counteracting centripetal drift velocity.

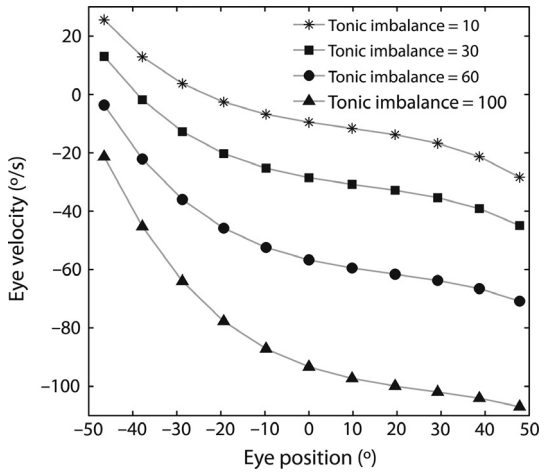

FIG. 8. The response of the model is compared for various simulated degrees of left-side unilateral deficit by changing the input amplitude. The model was stimulated with steps of different amplitudes (shown by distinct markers) and eye velocity at the time of the step is plotted as a function of fixation position. For smaller values of the input and eye positions near straight ahead, the *P–V* plot is relatively symmetric around the straight ahead position. For larger inputs the *P–V* plot saturates in the fast-phase direction. Also, if the eye is deviated far enough into the slow-phase direction (for example at −40° or −50°) the direction of nystagmus reverses.

sigmoidal function is shown in Fig. 9B (gray) where it can be compared with the original *P–V* plot (black) for the same input amplitude. The gray plot shows that if the sensitivity of the contralesional VN is simultaneously increased, the slope of the *P–V* plot could become positive in the fast-phase direction, suggesting that in the fast-phase direction the integrator has become unstable.

Discussion

A new physiologically plausible mechanism is proposed to explain the effects of eye position on SN and its performance is tested through model simulations. The new hypothesis is based on UVD-induced changes in the responses of ipsi- and contralesional VN, which have been shown in several experimental studies (reviewed by Smith & Curthoys, 1989). The assumption made here is that this change in the population response function and the resulting asymmetry between the bilateral VN responses reduce the effective linear operating range of the VN. Based on this assumption, it is proposed that in acute UVD, a sigmoid better describes the population response function of the bilateral VN, which in a healthy system could be approximated by a quasi-linear function. To simulate AL effects, the parameters of the sigmoidal function were neither specifically tuned nor optimized; the only criteria were to maintain system stability as well as a smooth drop in the sensitivity of the sigmoidal function at more eccentric eye positions. To investigate the performance of this hypothesis through model simulations, a simple feedback control system for the VOR was used. In addition to replicating and explaining the experimental data, model simulations make some novel testable predictions which are discussed below.

In a healthy system, the integration of eye velocity signals deteriorates at eccentric eye positions

We suggest that in a balanced and healthy system, the population response function of the bilateral VN is also sigmoidal (albeit one with a quasi-linear behavior inside a large operating region). Hence we propose that even in a healthy system, the integrator time constant decreases at eccentric eye angles because of the lower sensitivity of the sigmoidal function at eccentric positions (Fig. 6). This behavior has been documented by Eizenman *et al.* (1990), who reported a decrease in the time constant for eye positions beyond 20°. They proposed that an eye position-dependent gain in the cerebellar feedback loops causes smaller time constants at eccentric eye positions. This explanation is similar to the present hypothesis, except that here the eye position-dependent gain is assumed in the vestibular nuclei of the brainstem. Our hypothesis is also in agreement with the results of nonlinear identification of the VOR system by Chan & Galiana (2008). They found that in both healthy subjects and vestibular patients the integration of VOR commands could be dependent on eye position and suggested that perhaps integration is best close to the origin and deteriorates at lateral eye positions.

Nevertheless, this does not mean that in a healthy system vestibular nystagmus is dependent on eye position and head velocity. As proposed by Galiana (1991), during normal vestibular nystagmus, when vestibular or eye movement signals exceed the linear range of sensors or central processing stages, a quick-phase is triggered to reorient the eye and bring the activity back inside the linear range. Therefore, fast-phases could extend the linear range of the response beyond the linear range of individual elements in the system.

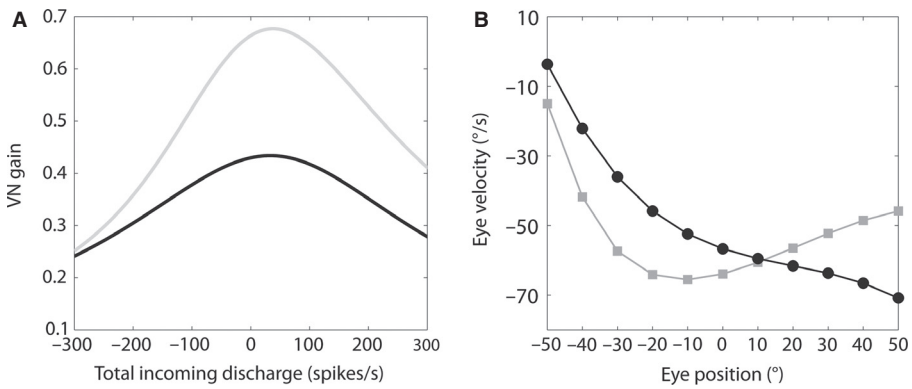

FIG. 9. The sigmoidal function of Fig. 5 (black curve) is modified to additionally reflect an increase in the sensitivity of the right VN caused by silencing of the left VN in acute left-side UVD. The resulting model response is shown in B. (A) The sensitivity function *g* for the two cases: black for the original sigmoidal shape and gray for the modified shape. For each of these cases the model was simulated with a rightward pulse of +60 spikes/s at different fixation points. (B) The resulting *P–V* plots. An increase in the sensitivity of the contralesional VN could result in an unstable integrator in the fast-phase direction (i.e. a positive slope for the *P–V* curve in the fast-phase direction).

During SN, the rate of change of slow-phase velocity with position depends on both eye position and the severity of the vestibular imbalance

The new hypothesis predicts that in acute UVD, VOR gain and integrator properties both become dependent not only on eye position, but also on the vestibular signal whose amplitude depends on the severity of the pathologic tonic imbalance.

With several sensory-motor signals converging onto it (e.g. head velocity and eye position), the VN constitutes the central processing stage of vestibular information. The medial VN is also involved in the temporal integration of horizontal eye velocity commands. Hence, a UVD-induced change in the population response of the VN would influence the manner in which the fused information is processed, while simultaneously affecting the NI properties. In the model, the proposed sigmoidal transfer function of the VN receives both the eye position and vestibular information. This means that the VN discharge would be a function of both these signals.

This dependence is shown in Fig. 8, where different *P–V* curves result from varying the input level. In other words, the intensity of the pathologic nystagmus influences how the slow-phase velocity changes with eye position. Furthermore, the figure shows that in all the *P–V* curves, velocity is not a linear function of position. For lower input amplitudes and eye positions close to straight ahead, the *P–V* plot could perhaps be approximated by a linear function, especially in the presence of noise in experimental data. But as the input amplitude increases (here: above 60 spikes/s), a saturation effect appears in the velocity in the fast-phase direction. This behavior is in agreement with the experimental findings of Hegemann *et al.* (2007)and Hegemann & Bockisch (2008) who reported that *P–V* plots from acute UVD patients were significantly nonlinear – in a sense that the rate of change of velocity with position declined in the fast-phase direction (i.e. a saturation effect).

Figure 8 also shows that by looking far enough to the slow-phase direction, the direction of the nystagmus could reverse. It should be noted, however, that the reversal of nystagmus direction by looking far to the ipsilesional side is also a prediction of Hess (1983) and Robinson *et al.* (1984) theory, which has also been experimentally verified by them. Hence, this observation alone cannot be used to favor the present model over previous theories.

Contribution of the right and left VN to the integration and its effect on P–V plots

The contribution of the right and left VN to the integration of eye commands is not yet fully known in humans. However, in the goldfish (with lateral eyes), it was shown that the integration of rightward eye positions is dominated mostly by the right VN–NPH complex and vice versa (Aksay *et al.*, 2007). Here we assumed that the same principle also applies to humans. The contribution of the right and left VN to the integration of eye velocity signals was explained with reference to the schematic in Fig. 4. In this figure, it is assumed that the right VN dominates integration of eye commands in the right half-plane and the left VN in the left half-plane. This means that the VN_R population transfer function has higher sensitivity for eye positions in the right half-plane and vice versa. Therefore, in acute left-side UVD when VN_L is mostly silenced, the overall VN transfer function becomes asymmetric around zero (straight ahead position), having higher sensitivity on the right side, as shown in Fig. 5, and the simulations in Figs 6–8 are the results of this assumption.

At the same time, silencing of the inhibitory commissural projections from VN_L to VN_R during acute left-side UVD increases the activity level of VN_R. If this increase in baseline activity also increases VN_R sensitivity to the input, then the overall sigmoidal function would be even more asymmetric around zero, as shown in Fig. 9A (gray curve). This increase in VN_R sensitivity leads to a positive slope for the resulting *P–V* plots when looking in the fast-phase direction (Fig. 9B, gray plot). A positive slope in the fast-phase direction would mean an unstable integrator. Indeed to help stabilize gaze, in addition to a hindering centripetal drift in the slow-phase direction, a centrifugal drift in the fast-phase direction is needed to counteract vestibular drift in both directions. Again, in the experiments of Hegemann & Bockisch (2008) in patients with acute UVD, the slope of the *P–V* plot was indeed positive in the fast-phase direction in several subjects. They suggested that the NI might have different time constants at different eye positions, enabling it to adapt to a UVD functionally: becoming leaky in the slow-phase direction and unstable in the fast-phase direction.

The new hypothesis with respect to existing literature

Previous hypotheses regarding the origin of AL (Doslak *et al.*, 1979; Hess, 1982; Robinson *et al.*, 1984) suggested that AL is the result of changes in either the NI or the VOR processing. In the model presented here, the UVD-induced change in the transfer function of the VOR interneurons simultaneously affects both the integrator and the VOR response. Moreover, unlike previous hypotheses, this new mechanism does not rely on extra triggering or guiding signals that would induce changes in the VOR or NI systems, nor on the use of lesion detection mechanisms: comparator networks or detection switches. Plus, this study shows that a single horizontal integrator that is dependent on eye position could produce the observed nonlinear *P–V* plots, without the need for multiple directional integrators as suggested by Crawford & Vilis (1993) and Hegemann *et al.* (2007).

The present hypothesis suggests that even though AL can help stabilize gaze in slow-phase direction, it is not necessarily an adaptation mechanism of the central nervous system. We propose that AL is not necessarily an intentional adaptive strategy, but an immediate consequence of UVD that results from a change in the response function of the secondary vestibular neurons.

Finally, the mechanism proposed here could also be responsible for the AL effects seen during vestibular nystagmus induced through caloric irrigations (Doslak *et al.*, 1982; Robinson *et al.*, 1984; Jeffcoat *et al.*, 2008). The persistent constant excitation/inhibition of the vestibular nerve during caloric tests could drive the ipsilateral VN units into saturation/cut-off, producing an asymmetry between the bilateral VN, and reducing the quasi-linear range of the central VOR neurons as was explained here. The ‘unnatural stimulation pattern’ that according to Robinson *et al.* (1984) is the triggering signal for AL, could in fact be the saturation of central VOR neurons caused by very low-frequency persistent stimulations of the vestibular nerve.

Acknowledgements

We thank Giovanni Bertolini for helpful discussions. This research was supported by the Swiss National Science Foundation (SNF) and les Fonds de Recherche du Québec–Nature et Technologies (FQRNT). The authors declare that they do not have any conflict of interest, financial or otherwise.

Abbreviations

AL, Alexander’s Law; FTN, flocculus target neurons; MN, motor nuclei; NI, neural integrator; NPH, nucleus prepositus hypoglossi; PJ, Purkinje neurons; PMT, paramedian tract neurons; SN, spontaneous nystagmus; UVD, unilateral vestibular deficit; VN, vestibular nuclei; VOR, vestibulo-ocular reflex.

References

Aksay, E., Olasagasti, I., Mensh, B.D., Baker, R., Goldman, M.S. & Tank, D.W. (2007) Functional dissection of circuitry in a neural integrator. *Nat. Neurosci.*, **10**, 494–504.

Alexander, G. (1912) Die Ohrenkrankheiten im Kindesalter. In: Pfaundler, M. & Schlossmann, A. (Eds), *Handbuch der Kinderheilkunde*. Vogel, Leipzig, pp. 84–96.

Anagnostou, E., Heimberger, J., Sklavos, S. & Anastasopoulos, D. (2011) Alexander's law during high acceleration head rotations in humans. *NeuroReport*, **22**, 239–243.

Büttner-Ennever, J.A., Horn, A.K. & Schmidtke, K. (1989) Cell groups of the medial longitudinal fasciculuc and paramedian tracts. *Rev. Neurol. (Paris)*, **145**, 533–539.

Chan, W. & Galiana, H.L. (2008) Modeling the nonlinear context-depedency of the neural integrator in the vestibulo-ocular reflex. *IEEE Trans. Biomed. Eng.*, **55**, 1946–1955.

Cheron, G., Escudero, M. & Godaux, E. (1996) Discharge properties of brain stem neurons projecting to the Flocculus in the alert cat. I. Medial vestibular nucleus. *J. Neurophysiol.*, **76**, 1759–1774.

Crawford, J.D. & Vilis, T. (1993) Modularity and parallel processing the oculomotor integrator. *Exp. Brain Res.*, **96**, 443–456.

Doslak, M.J., Dell' Osso, L.F. & Daroff, R.B. (1979) A model of Alexander's law of vestibular nystagmus. *Biol. Cybern.*, **34**, 181–186.

Doslak, M.J., Dell' Osso, L.F. & Daroff, R.B. (1982) Alexander's Law: a model and resulting study. *Ann. Otol. Rhinol. Laryngol.*, **91**, 316–322.

Eizenman, M., Cheng, P., Sharpe, J. & Frecker, R. (1990) End-point nystagmus and ocular drift: an experimental and theoretical study. *Vision. Res.*, **30**, 863–877.

Fukushima, K. & Kaneko, C. (1995) Vestibular integrators in the oculomotor system. *Neurosci. Res.*, **22**, 249–258.

Galiana, H.L. (1991) A nystagmus strategy to linearize the vestibulo-ocular reflex. *IEEE Trans. Biomed. Eng.*, **38**, 532–543.

Galiana, H.L. & Outerbridge, J.S. (1984) A bilateral model for central neural pathways in vestibuloocular reflex. *J. Neurophysiol.*, **51**, 210–241.

Galiana, H.L., Flohr, H. & Melvill Jones, G. (1984) A reevaluation of intervestibular nuclear coupling: its role in vestibular compensation. *J. Neurophysiol.*, **51**, 242–259.

Glasauer, S. (2003) Cerebellar contribution to saccades and gaze holding. *Ann. N.Y. Acad. Sci.*, **1004**, 206–219.

Goldman-Rakic, P.S. (1995) Cerebellar basis of working memory. *Neuron*, **14**, 477–485.

Hegemann, S. & Bockisch, C.J. (2008) Alexander's law and the oculomotor neural integrator: three-dimensional eye velocity in patients with an acute vestibular asymmetry. *J. Neurophysiol.*, **100**, 3105–3116.

Hegemann, S., Straumann, D. & Bockisch, C. (2007) Alexander's law in patients with acute vestibular tone assymmetry-Evidence for multiple horizontal neural integrators. *JARO*, **8**, 551–561.

Hess, K. (1982) Do peripheral-vestibular lesions in man affect the position integrator of the eyes? *Neurosci. Lett. [Suppl].*, **10**, 242–243.

Hess, K. (1983) Counterdrifting of the eyes following unilateral labyrinthine disorders. *Adv. Otorhinolaryngol.*, **30**, 46–49.

Huk, A.C. & Shadlen, M.N. (2005) Neural activity in macaque parietal cortex reflects temporal integration of visual motion signals during perceptual decision making. *J. Neurosci.*, **25**, 10420–10436.

Jeffcoat, B., Shelukhin, A., Fong, A., Mustain, W. & Zhou, W. (2008) Alexander's Law revisited. *J. Neurophysiol.*, **100**, 154–159.

Kaneko, C. (1997) Eye movement deficits after ibotenic acid lesions of the nucleus prepositus hypoglossi in monkeys. I. Saccades and fixation. *J. Neurophysiol.*, **78**, 1753–1768.

Lisberger, S.G. (2009) Internal models of eye movement in the floccular complex of the monkey cerebellum. *Neuroscience*, **162**, 763–776.

Lisberger, S.G., Pavelko, T.A. & Broussard, D.M. (1994) Responses during eye movements of brainstem neurons that receive monosynaptic inhibition from the flocculus and ventral paraflocculus in monkeys. *J. Neurophysiol.*, **72**, 909–927.

Nakamagoe, K., Iwamoto, Y. & Yoshida, K. (2000) Evidence for brainstem structures participating in oculomotor integration. *Science*, **288**, 857–859.

Robinson, D.A., Zee, D.S., Hain, T.C., Holmes, A. & Rosenberg, L.F. (1984) Alexander's Law: its behavior and origin in the human vestibulo-ocular reflex. *Ann. Neurol.*, **16**, 714–722.

Skavenski, A. & Robinson, D.A. (1973) Role of abducens neurons in vestibulooocular reflex. *J. Neurophysiol.*, **36**, 724–738.

Smith, P. & Curthoys, I. (1988a) Neuronal activity in the contralateral medial vestibular nucleus of the guinea pig following unilateral labyrinthectomy. *Brain Res.*, **444**, 295–307.

Smith, P. & Curthoys, I. (1988b) Neuronal activity in the ipsilateral medial vestibular nucleus of the guinea pig following unilateral labyrinthectomy. *Brain Res.*, **444**, 308–319.

Smith, P. & Curthoys, I. (1989) Mechanisms of recovery following unilateral labyrinthectomy: a review. *Brain Res. Rev.*, **14**, 155–180.

Taube, J.S. & Bassett, J.P. (2003) Persistent neural activity in head direction cells. *Cereb. Cortex*, **13**, 1162–1172.

Zee, D., Yamazaki, A., Butler, P. & Gücer, G. (1981) Effects of ablation of flocculus and paraflocculus on eye movements in primate. *J. Neurophysiol.*, **46**, 878–899.